WIND-TUNNEL STUDIES OF CERTAIN METEOROLOGICAL TOWER SITING CHARACTERISTICS AT THE JAMES A. FITZPATRICK NUCLEAR POWER STATION

Prepared by

Robert N. Meroney
Ronald L. Ewald
Seong Hee Shin
David E. Neff

Final Report
(November 1986 - January 1988)

Fluid Mechanics and Wind Engineering Program
Department of Civil Engineering
Colorado State University
Fort Collins, CO 80523

for

New York Power Authority
123 Main Street
White Plains, NY 11501

Contract No. 027277-86

CSU Contract No. 2-96920

February 1988

CER87-88RNM-RLE-SHS-DEN1

EXECUTIVE SUMMARY

WIND-TUNNEL STUDIES OF CERTAIN METEOROLOGICAL TOWER SITING CHARACTERISTICS AT THE JAMES A. FITZPATRICK NUCLEAR POWER STATION

A wind-tunnel measurement program was completed to evaluate the measurement errors at the main meteorological tower and backup meteorological tower at the James A. Fitzpatrick Nuclear Power Station. The effects of the Niagara Mohawk Power Corporation Nine Mile Unit 2 cooling tower on the main tower sensors, the effects of the Nine Mile Unit 2 cooling tower and the Fitzpatrick site structures on the backup tower, and the effect of the main meteorological tower's location on representativeness were estimated using fluid modeling techniques about a 1:750 scale model of the facility installed in the meteorological wind tunnels at Colorado State University. The effects of the main meteorological tower structure on its sensors were estimated using a 1:16 scale model of a typical section of the tower.

Measurement included deviations in wind speed, wind angle, turbulent intensity, and temperature for each of four tasks during neutral approach flow. Where appropriate, similar measurements during unstable and stable approach flows were also included. Measurements were also made to estimate the variations associated with the tunnel itself and to confirm the stationarity and homogeneity of the flow. No systematic variations were found to exist greater than the expected random instrumentation deviations.

Nuclear Regulatory Commission (NRC) draft guidelines suggest that for an instrumentation set like that found at the Nine Mile location, instrument errors must be less than ±0.5 mph for wind speed, ±5° for wind direction, ±0.12°F for mid- to low-level temperature differences, and ±0.28°F for upper- to low-level temperature differences. But since comparative measurements were of primary interest in this study, the absolute accuracy of a given laboratory instrument was not as important as errors in differential measurements, which are believed to be less than ±20 percent. Data were examined for their statistical significance, and estimates are provided of the influence of the systematic meteorological errors detected on the calculation of plume dispersion.

The major conclusions reached on the basis of these measurements are summarized below:

<u>Task I: Quantification of the Effect of the Site's Cooling Tower on Meteorological Sensors on the Main Meteorological Tower</u>

Measurements were performed at two wind speeds at the site of the main meteorological tower vis-a-vis the effect of the Niagara Mohawk cooling tower. During neutral flow conditions wind speed, turbulence and direction deviations were made with a single-film anemometer probe and a wedge-pressure probe. During stratified flow conditions X-film anemometer probes and a miniature thermocouple probe were used to determine deviations over the height of the main meteorological tower with and without the presence of the cooling tower. When the wind

blew directly from the cooling tower location to the main tower site it was concluded that:

> The wind tunnel data suggest that the cooling tower effects on the main meteorological tower may exceed the NRC guidelines during stratified conditions. This will occur when the main meteorological tower is directly downwind of the cooling tower during stable conditions. Local climatological data indicate that these conditions exist about 2 percent of the time on an annual basis.
>
> During neutral approach flows, the maximum perturbation of the wind speed and wind direction over the height of the main meteorological tower caused by the cooling tower were less than 12.1 percent of the approach stream and ±0.5° respectively while the average perturbation of wind speed was 6.6 percent and average perturbation of wind direction was ±0.25°. Turbulence levels changed as much as -23 percent at the 100 foot level of the tower, but varied by less than ±5 percent at other levels.
>
> During stable and unstable approach flows, the maximum perturbation of the wind speed and wind direction over the height of the main meteorological tower caused by the cooling tower were less than 19 percent of the free stream and 6.3° respectively while the average perturbation of wind speed was ±7.5 percent and average perturbation of wind direction was ±2°. Turbulence levels varied substantially over the tower height as the wake of the cooling tower deflected streamlines about the tower substantially. In the worst case turbulence levels increased by as much as 375 percent at upper tower levels during the high wind speed stable flow.

<u>Task II: Quantification of the Effect of the Meteorological Tower Structure on Sensor Measurements</u>

The main meteorological tower is a bulky rectangular lattice type structure with interior staircase. Measurements were made over a 1:16 scale model of a typical section of the tower at sensor locations on the boom location presently in use and for a proposed boom location. Measurements were most representative of the 100 ft level of the tower, but they can also be used to draw inferences about other tower levels. Deviations from approach flow conditions in neutrally stratified flow for 16 wind approach angles representing the principal wind directions were made with a single-film anemometer and a wedge-pressure probe. The measurements suggest that:

> The wind tunnel data suggest that the effects of the main meteorological tower on its wind sensors significantly exceed the NRC guidelines for winds from the NEE to ESE. Other deviations that are not as significant also occur in other affected sectors. Local climatological data indicate that the conditions that could cause the sensors to exceed the suggested acceptable errors exist about 20 percent of the time on an annual basis.
>
> At the current instrument location wind speed measurements may read up to 38 percent low, wind direction measurements may

deviate as much as ±5°, and turbulence intensities may increase by 0.11, when the winds blow from the sector between NEE and ESE. In all these measurements the maximum deviations occurred when the tower was directly upwind of the instrumentation. Even an instrument location directly upwind of the tower will see effects due to tower blockage and flow stagnation. For the sectors when the sensors were upwind of the tower (SSW through WNW) the maximum wind speed and wind direction deviations were -10 percent and ±2.5°, respectively. For the remaining sectors the maximum wind speed and wind direction deviations were +4 percent to -6 percent and ±4°, respectively.

Wind speed measurements at the proposed alternate instrument location may read up to 34 percent low while the wind direction and turbulent intensity levels remain about the same as those found for the current instrument locations. The proposed instrument location does not improve tower blockage related errors significantly. Even an instrument location directly upwind of the meteorological tower will see wind speed perturbations resulting in 10 percent low wind speeds due to tower blockage and flow stagnation.

Task III: Quantification of the Effect of the Nine Mile Unit 2 Cooling Tower and JAF Turbine, Service and Reactor Buildings on the Backup Meteorological Tower

The distance between the backup meteorological tower and the Nine Mile Unit 2 cooling tower does not meet NRC guidelines for distances to buildings. In addition, concern was expressed that the James A. Fitzpatrick (JAF) reactor buildings and new service building might influence the backup tower. Measurements of wind speed and wind direction with and without the cooling tower and buildings were made for neutral, stable and unstable approach flows. These measurements indicate that:

The wind tunnel data suggest that the effects of the JAF buildings on the backup meteorological tower exceed the NRC guidelines for acceptable errors. Local climatological data indicate that conditions that could cause the sensors to exceed the suggested acceptable errors exist about 28 percent of the time on an annual basis.

The JAF reactor structures caused maximum perturbations in wind speed and direction during neutral stratification of 20 percent and ±8°, respectively, and turbulence levels doubled from 0.12 to 0.24 (100 percent).

Tests made during neutral stratification with and without the new service building showed virtually no difference in wind speed and wind direction over those already detected due to the other JAF structures.

During neutral stratification the Nine Mile Unit 2 cooling tower does cause additional deviations at the 96 foot (29.3 m) measurement height of the backup tower instrumentation. The cooling tower perturbed wind speed by nearly 7 percent but only small wind angle deviations less than ±0.25°. Turbulence intensities decreased by as much as 15 percent.

During stable and unstable stratification the Nine Mile Unit 2 cooling tower produced perturbations in wind speed and wind direction at instrument height of as much as 15 percent and ±8°. During the high speed stable stratification case, turbulence levels at instrument height increased from 0.13 to 0.21 (64 percent), and for the low speed unstable case turbulence levels increased from 0.15 to 0.21 (37 percent). These changes were superimposed upon perturbations already produced by the presence of the JFK reactor complex.

Task IV: Quantification of the Effect of the Main Meteorological Tower's Location on the Representativeness of Measurements

The main meteorological tower is located on a point which has direct exposure to the lake when winds are from the WSW, W, WNW, and NW. For WSW and W wind directions the main buildings at Nine Mile Point Units 1 and 2 and JAF are indirectly exposed to the lake (i.e., they are 2000 to 5500 feet [1 to 2 kilometers] inland). Vertical profiles of wind speed, turbulence, and temperature were measured at a sequence of distances inland from a simulated coastline. Roughness and surface temperature were allowed to vary during simulations with neutral, stable, and unstable stratification approach flows. During the neutral stratification measurements, a small escarpment to simulate the shoreline beach was incorporated into the model. This escarpment was found to have a minimal influence at only the lowest (< 10 m) levels of the tower, so it was eliminated during the stable and unstable tests. The modeling suggests that:

The wind tunnel data suggest that the main tower meteorological data are not representative of conditions at the JAF and possibly the Nine Miles sites during on-shore winds (WSW to N). Local climatological data indicate that conditions where the measurements may not be representative occur about 43 percent of the time on an annual basis.

During neutral stratification the main meteorological tower location was subjected to wind profiles produced by the smooth lake surface; hence, wind speeds increased at a modest rate up the tower and turbulence intensities were relatively low. As one moved inland within the internal boundary layer caused by the change in roughness over the land associated with the forested rolling countryside, the velocity gradients increased substantially and turbulence levels increased dramatically. Deviations in wind speed at a 30 foot (10 m) height exceeded 30 percent, and turbulence levels increased from 0.15 to 0.25 over a 100 foot (30 m) height by the time one moved 5500 feet (2 kilometers) inland.

During unstable stratification the results were similar. Deviations at the 30 foot (10 m) height in wind speed and temperature were of the order of 12 percent at a 5500 foot (2 kilometers) inland distance. Turbulence intensities increase from 0.27 to 0.31 near the ground. Under low wind speed stable stratification conditions the stability suppressed the effect of the change in surface roughness; hence, little profile deviations occurred. But for high wind speed stable stratification conditions the surface roughness began to dominate below 60 feet (20 m), and 15 percent changes in wind speed along with an increase in ground level turbulence from 0.04 to 0.13 occurred. Also, mid- to low-level (100 ft to 30 ft) temperature differences typically changed by as much as 0.35°C for equivalent field winds of 8 mph.

Conclusions:

Based on this wind-tunnel measurement program it is likely that:

1. Due to the bulky nature of the main meteorological tower, errors in measurements of wind speed, wind direction, and turbulence probably exceed NRC accuracy guidelines for wind directions in the wind sectors between NEE and ESE. These conditions exist about 20 percent of the time on an annual basis.

2. The influence of the Nine Mile Point Unit 2 cooling tower on the main and backup meteorological towers could exceed NRC accuracy guidelines for isolated wind conditions. It is estimated that these conditions exist about 2 percent of the time for the main meteorological tower and about 20 percent of the time for the backup tower on an annual basis.

3. The influence of th James A. Fitzpatrick turbine reactor, and new service buildings on the backup meteorological tower could cause the wind sensors to exceed NRC instrument accuracy guidelines for wind directions in the wind sectors between SSW and W. These conditions exist about 28 percent of the time on an annual basis.

4. Because the main meteorological tower is closer to Lake Ontario than the buildings at JAF and Nine Mile Points Units 1 and 2 when winds are out of the WSW to N sectors, the influence of surface roughness and thermal heating modifies the flow field between the two locations. In this situation the measurements at the main tower may not accurately represent conditions at the generating stations. It is estimated that these conditions exist about 43 percent of the time on an annual basis.

Finally a sensitivity analysis of a simple generic Gaussian plume model suggest systematic measurements errors in wind speed, turbulence and temperature gradient will propagate through prediction models to produce errors in estimated concentrations.

TABLE OF CONTENTS

LIST OF TABLES

LIST OF FIGURES

LIST OF SYMBOLS

Symbol	Definition
z_o	Surface roughness length
L	Length
L_{mo}	Monin-Obukhov length
U,u	Mean velocity
E	Hot-wire output voltage
A,B,c	Hot-wire constants
k	Yaw factor
V	Total velocity vector approaching sensor array
T	Temperature
v	Lateral velocity
w_*	Convective velocity
u_*	Friction velocity
h	Inversion layer height
W,w	Vertical velocity
θ	Approach wind angle
$\Delta\theta$	Wind angle deviation
ΔT	Temperature difference between two heights
g	Gravitational acceleration
C	Observed concentration
Q	Source flow rate
h	Height
σ_y,σ_z	Standard deviation of the distribution of material in a continuous plume in the y and z directions
U	Velocity
$\sigma_\theta,\sigma_\phi$	Standard deviation of the distribution of material in a continuous plume in angular width
x,y,z	Carteisna coordinates

D	Characteristic width of the object

<u>Dimensionless Parameters</u>

V_R	Velocity ratio
$\bar{U},\bar{V}$	Normalized mean velocities
$(\bar{U})_c$	Fractional mean velocity change due to cooling tower
$(\Delta T)_c$	Fractional ΔT change due to cooling tower
TI	Turbulence intensity
$(TI)_c$	Fractional turbulence intensity change due to cooling tower
Ri	Bulk Richardson number

<u>Subscripts</u>

rms	Root-mean-square
m	Model
f	Field
a	Unperturbed values
e	Perturbed values
c	Change due to addition of cooling tower

<u>Superscripts</u>

$(\ )'$	Fluctuating part of a quantity
$(\overline{\ \ })$	Mean of a quantity

WIND-TUNNEL STUDIES OF CERTAIN METEOROLOGICAL TOWER SITING CHARACTERISTICS AT THE JAMES A. FITZPATRICK NUCLEAR POWER STATION

1.0 INTRODUCTION

The Nuclear Regulatory Commission requires that operating nuclear power stations maintain meteorological instrumentation capable of providing accurate atmospheric input information for emergency preparedness. Meteorological towers at the Nine Mile Point and James A. Fitzpatrick (JAF) Nuclear Power Plants in Oswego County, New York, near Lake Ontario provide key data for emergency preparedness and routine operations. For these purposes it is important that the generated data be accurate, reliably available, and representative of conditions at locations in the plants where release could take place. The Nuclear Regulatory Commission (NRC) requires that these instrumentations meet accuracy criteria; hence, they recommend certain siting standards. In the event these standards are not met, they encourage plant operators to establish the actual errors or bias based on laboratory or field measurements. This report summarizes the results of a wind-tunnel simulation of the reactor site along Lake Ontario to evaluate the influence of reactor buildings and cooling towers, meteorological tower location, and meteorological tower structure on data reliability.

Meteorological wind tunnels in the Fluid Dynamics and Diffusion Laboratory at Colorado State University were operated over scale models of the facilities to measure wind speed, wind direction, turbulence and temperature deviations resulting from site characteristics. Appendix A of this report reviews the scaling criteria which permits credible simulation of atmospheric flows. In Sections 2.0 and

3.0 details of the wind-tunnel facilities, models, test instrumentation and measurement techniques are described. An error analysis for each instrument examines the probable laboratory instrumentation errors and documents the variability and accuracy of the measurements. The four-task test program is summarized in Section 4.0, and a guide to attached appendices, tables and figures is provided. The implications of the measurements made during each task element are discussed in Section 5.0, and final conclusions and recommendations are provided in Section 6.0.

2.0 EXPERIMENTAL CONFIGURATION

These wind-engineering tests were performed in two different wind tunnels in the Fluid Dynamics and Diffusion Laboratory at Colorado State University. The two tunnels used were the Industrial Aerodynamics Wind Tunnel (Figure 1), and the Meteorological Wind Tunnel (Figure 2). Also, tests were performed on two different models. The first model was a 1:16 scale model of a section of the main meteorological tower and the second was a 1:750 site model of the test area.

2.1 Wind Tunnels

2.1.1 Industrial Aerodynamics Wind Tunnel (IWT)

This wind tunnel is a closed circuit facility driven by a 75 hp variable-pitch propeller. The test section is nominally 2 m square and 18 m long and is fed through a 4:1 ratio contracting section about 3 m long. The roof may be adjusted in height to maintain a zero pressure gradient along the test section. The mean velocity of the airflow can be adjusted continuously from 0.5 to 20 m/sec.

2.1.2 Meteorological Wind Tunnel (MWT)

This wind tunnel is especially designed to study atmospheric flow phenomena, and it incorporates special features such as an adjustable ceiling, a rotating turntable, temperature controlled boundary walls, and a long test section to permit adequate reproduction of micro-meteorological behavior. The test section is also nominally 2 m square but 25 m long, and is fed by a 9:1 ratio contracting section. Mean wind speeds of 0.1 to 40 m/sec (0.14 to 90 mi/hr) in the MWT can be obtained. Boundary-layer thickness up to 1 m can be developed "naturally" over the downstream 6 m of the MWT test section. Thermal stratification in the MWT is provided by the heating and cooling systems in the section passage and the test section floor. The flexible test section roof on the MWT is adjustable in height to permit the longitudinal pressure gradient to be set at zero.

For the stable case, a set of 12 Roll-bond aluminum panels were placed on the tunnel floor from 2 to 12 m. These panels were connected to the facility refrigeration system and cooled to approximately 0°C. From 12 m to the end of the test section, a permanently installed set of cooling panels was used to lower the aluminum floor temperature to a level of 0°C. The free stream temperature was raised to a level as prescribed by the bulk Richardson number.

For the unstable case, the 12 Roll-bond aluminum plates were placed in a stack upstream of the heated section of the floor to provide a layer of cold air above the heated floor and below the heated air above. See Figure 3 for exact orientation. The temperature of the plates was maintained at approximately 0°C and the surface temperature of the hot floor was approximately 110°C. This configuration provided for intense mixing near the ground.

2.2 <u>The Models</u>

Two different models were made for this study as shown in Figure 4. First a 1:16 scale model of a representative section of the main meteorological tower was made from plastic architectural modeling materials provided by Engineering Model Associates, Inc. This model represented a section of tower approximately 17 m (56 ft) high and included one instrumentation level near the middle (Figure 5). This model was used exclusively for the Task II measurements which were to determine the effects and errors that the tower itself caused on the instrumentation. Also, two different plastic boom arms were constructed to hold the laboratory velocity and direction measuring equipment. The first arm held the instruments in the same locations as the existing field boom, and the second arm held the instruments in a T-configuration to test some proposed locations. These exact locations are shown in Figure 6.

Since stratification does not tend to influence the production of aerodynamic turbulence associated with separation and flow over structural members the tower model was only examined in neutrally stratified flow. The turbulence produced by such structural members will contain most of their energy in eddy sizes associated with the size of beam and structural members. Thus in unstable flow, which involves energies at scales much larger than the tower structure, the tower turbulence will add to that of the background flow in the smaller scale range. Our experience for turbulence measurements behind structures in stable and unstable environments suggests that the background flow does not significantly change the structure before 5-8 characteristic structures sizes. In the case of the Primary tower this would suggest that tower turbulence will not decay or be significantly buried in background turbulence before 35 to 56 feet from the tower.

The second model consisted of 1:750 scale models of the site buildings and structures. Individual wooden models were made of the Nine Mile Point (NMP) Unit 1 and Unit 2 buildings, the James A. Fitzpatrick (JAF) building, and the JAF new service building. The cooling tower was made from styrofoam and was modeled to have an open area at the bottom as shown in Figure 7.

The total frontal area of the combined model structures produced about 2 percent shelter. This is less blockage than the 5 percent blockage frequently quoted as a desirable, but not absolute, upper limit during fluid modeling. The deviation of the flow due to the presence of the structures actually occurs in the atmosphere, and the measurements performed in the presence of the model buildings were performed in order to account for such effects.

2.3 Test Configuration

Task II, measurements of tower influences on instruments, were made entirely in the Industrial Aerodynamics Wind Tunnel. The 1:16 tower model was mounted on the turntable at the end of the test section such that approach winds from 0° to 360° could be tested. Since this part of the investigation was to determine effects caused by the tower structure, these tests were performed in a uniform but moderately turbulent approach flow instead of a boundary layer type approach flow. A TSI 1241 hot-film anemometer was used to measure velocity, and a United Sensor (No. W250) wedge type pitot probe was used to measure wind direction.

Tasks I and III, measurements of site effects on the main and backup meteorological tower locations; and Task IV, measurement of tower sitting effects (distance main tower is located away from lake shore) were conducted in both the Industrial Aerodynamics Wind Tunnel (IWT) and the Meteorological Wind Tunnel (MWT). All of the neutral wind conditions were completed in the IWT while all of the stable and unstable flow conditions were completed in the MWT. These tests were performed in a similar manner for each task.

Task I, measurements of the main meteorological tower site, and Task III, measurements at the backup tower site, were performed by placing the various 1:750 scale structures, in different combinations, in the wind tunnel as shown in Figure 8. For Task I the wind always came from 82° and for Task III the wind was from 241°. Upwind, and throughout the area, 1.3 cm high chains were placed across the wind tunnel every 30 cm to simulate the general terrain roughness of the site.

Smoke visualization in neutral, stable and unstable flow showed no tendency for the chain structure to produce a stagnant area at the surface or a raised jet over the chains. Indeed, the open structure of the chains probably produced a better wake profile than the alternative use of blocks, rocks, or other roughness elements. Many fluid modelers have used lateral strips or fences to produce the desired roughness in the past. Indeed, the famous experiments by Jensen and Franck in the 50's which first validated wind tunnel modeling used such fence structures.

It is unlikely that any heating of the chains produced significant changes in the unstable turbulence profiles. Energy due to heating of a surface is added at scales of the order of the inversion height not at the order of the size of the chains.

Task IV, measurements of the effect of different lengths of land fetch, were accomplished by measuring wind profiles at different distances from the lakeshore. The lake surface was represented by a smooth floor. For the appropriate distance upwind of the profile location, the land surface roughness was simulated by the chain arrays. This arrangement provided for a transition from lake to land surface and the subsequent varying length of land fetch, see Appendix F, Land/Lake Fetch Configurations. Also, for the neutral case tests in the IWT, a 4.6 m (15 ft) high escarpment was included. The escarpment was not included during the stable and unstable experiments since it was found during the neutral tests that any effect caused by the escarpment was small and confined to the lowest 9.1 m (30 ft) of elevation.

For all of the neutral wind data in the IWT, the various velocity profiles were measured with a TSI hot-film anemometer and the wind direction measurements were made with the United Sensor wedge probe at 10 m (30 ft), 30 m (100 ft), and 61 m (200 ft) elevations. For all of the stable and unstable wind conditions in the MWT, the velocity data was obtained with a two-film cross-wire TSI anemometer probe calibrated and compensated for temperature. Since this type of probe gives two distinct velocity components, it is possible to obtain wind angle variations directly. (The wedge probe would not operate correctly at the lower wind speeds used for the stable and unstable tests.) During the stable and unstable tests, temperature measurements were taken with a thermocouple mounted beside the velocity probe.

2.4 Approach Wind Conditions

Neutral flow conditions for Tasks I, III, and IV were run in the IWT at two free stream reference velocities of 2 1/2 mps (5.6 mph) and 5 mps (11.2 mph). Figure 9 shows that for neutral conditions the shape of the approach wind profiles is independent of wind speed. In Figure 10 the difference between approach winds which travel over long land (rough) fetches and long water (smooth) fetches can be seen. Land profiles were taken at the location of the NM cooling tower with the cooling tower removed. There was a chain roughness fetch of length 10 m upwind of the measurement location. Profiles to typify the lake surface were taken at the same location in the tunnel but with no chain roughness upwind at all. This difference is important since the primary meteorological tower is near the shoreline of

Lake Ontario. When the tower is nearer to the shoreline, for a particular wind direction, than the reactor complex, the wind velocities measured at the tower will be higher than if the tower were further inland. In Table 1 characteristic values for u_* (friction velocity) and z_o (surface roughness length) for these profiles are listed.

The stable and unstable flow conditions were run in the MWT at two different free stream reference velocities. The stable tests were performed at a low speed of approximately 0.70 mps (1.6 mph) and a high speed of 1.40 mps (3.2 mph), while the unstable tests were run at speeds of 0.50 mph (1.1 mph) and 0.95 mph (2.1 mph) respectively. These approach flow conditions are plotted in Figure 11--stable conditions, and Figure 12--unstable conditions. From Figures 11 and 12 it is seen that neither the stable nor the unstable approach profile shapes are independent of wind speed, unlike the neutral conditions which were velocity independent. Figure 11 indicates a peculiar wave-like variation in the vertical turbulence intensity profiles near 200 feet. This pattern did not reoccur in later measurements and seems to be a data anomally. The characteristic values for u_* and z_o for the stable and unstable cases are also listed in Table 1. The stable and unstable flows also are highly influenced by temperature. Approach flow temperature profiles for model conditions are shown in Figure 13.

As noted in Appendix A, section A.1, the simulated atmospheric stratification is usually related quantitatively to prototype conditions through the Monin-Obukhov length or the Richardson number. Golder (1972) prepared a figure which relates Pasquill-Gifford stability categories A through F to surface roughness, z_o, and Monin-Obukhov length, L. Once the Monin-Obukhov length is specified, the bulk Richardson number value can be calculated over a specific measurement height through equations for the dimensionless shear and temperature and the value of the relevant roughness length. The reference model velocity chosen can then be inserted into the definition of the Richardson number to calculate the desirable temperature variation over the specified model measurement height.

Unfortunately, this temperature difference can only be a goal sought while setting the wind-tunnel stratification conditions, because the temperature and velocity profiles are nonlinearly interactive! Once an operating condition is finally selected, the actual bulk Richardson number may be calculated using measured model velocity and temperature profiles. Relating these magnitudes to a specific Pasquill-Gifford category becomes the inverse of the earlier process. The report by Snyder (1981) summarizes the necessary equations and provides ranges of Richardson number for different Pasquill-Gifford categories.

The character of the temperature and velocity profiles during stable stratification deserves further comment. Stable atmospheric flows can occur with ground-level jets or elevated jets depending upon the nature of the winds just before the various layers are decoupled through stability. Many different atmospheric profiles can have the same bulk Richardson number, Monin-Obukhov length, or PG stability. We do not claim that the condition is unique, but it does represent a stable profile which might occur. If we started our facility with a different sequence of initial wall temperatures and subsequent velocity adjustments we could arrive at another "possible" profile. The atmosphere does the same thing.

The magnitudes of bulk Richardson number calculated for the model conditions studied herein are provided in Table 2. Note that the Pasquill-Gifford category specified is a function of the height of the parameter evaluation. For a 5 m to 10 m data range the Richardson numbers calculated suggest unstable and stable stratifications modeled were unstable Class A, moderately unstable Class B, and stable classes F and G. For a 10 m to 61 m data range the Richardson numbers calculated suggest unstable and stable stratifications modeled were unstable Class B, stable Class G, and stable Class F. Temperature profiles indicate there were elevated inversions present at about 120 m during the unstable cases.

During the unstable cases in particular there is some uncertainty in relating Pasquill-Gifford categories and the Monin-Obukhov stability length. Recent wisdom suggests that most of the unstable convective boundary layer is governed by the convective velocity, w_*, and the inversion layer height, h, but no data is now available which relates these parameters to Pasquill-Gifford categories. An alternative approach was suggested by Gifford (1976); he noted that σ_θ took on values at a 10 m height of 25, 20, 15, 10, 5 and 2.5° for Pasquill-Gifford categories, A, B, C, D, E, and F, respectively. Presuming a direct relationship between σ_θ and turbulence intensity, v'/U, then the Pasquill-Gifford categories simulated for the low speed unstable, high speed unstable, high speed stable, and low speed stable were C, C, D, and F, respectively. For this alternate method, the stability categories values are inconsistent with observations and Richardson number evaluations. The reason for this discrepancy is not apparent to the authors.

In summary, it is obvious from this discussion that assigning a Pasquill-Gifford stability category to a given flow condition is not an exact calculation. In reality, it is a somewhat tenuous and ambiguous exercise. However, it is also clear from this discussion that for these tests, two distinct unstable conditions and two distinct stable conditions were created.

3.0 INSTRUMENTATION AND DATA ACQUISITION

3.1 Flow Visualization

Making the airflow visible in the vicinity of the model is helpful in defining zones of separated flow, highly turbulent areas, wake regions, and other general flow characteristics. Titanium tetrachloride smoke or an oil smoke were released from sources near the model and around the test site to make the flow lines visible to the eye and to make it possible to obtain both still pictures and motion pictures of the tests. The still pictures were taken with a single lens reflex-35 mm camera and the motion pictures were taken with a Panasonic VHS videotape system.

3.2 Velocity Measurements

The range of velocities examined required the use of two different measurement systems. For Task II tests and the neutral flow conditions for Tasks I, III, and IV, mean velocities and local turbulence intensities were measured with a single hot-film Thermal Systems Inc. anemometer. For Task II, the probe was mounted with its axis vertical and supported at a fixed location relative to the 1:16 tower model. For the Task I, III, and IV measurements the probe was mounted with its axis horizontal and was supported from a vertical traverse which was positioned behind the model. Vertical profiles were taken with an automated traverse which stopped at regular intervals, close to but not exactly at the same height above the ground surface each time. The instrumentation used was a Thermo Systems constant temperature anemometer (Model 1050) with a 0.03 mm (0.001 in.) diameter platinum film sensing element 0.51 mm (0.020 in.) long. Output from the anemometer was fed to an on-line data acquisition system consisting of an IBM AT PC computer, disk unit, printer, plotter, and a Data Translation Inc. analog-to-digital card. The data was processed immediately into mean velocities, turbulence intensities, and corresponding heights and stored on the computer disk for printout or further analysis.

Single Hot-Film Probe Measurements

Calibration of the hot-wire anemometer was performed against a pitot tube mounted in the free stream flow of the wind tunnel. The calibration data were fit to a variable exponent King's Law relationship.

$$E^2 = A + BU^c$$

where E is the hot-wire output voltage, U the approach velocity and A, B, and c are coefficients selected to fit the data. The above relationship was used to determine the mean velocity at measurement points using the measured mean voltage data. The fluctuating velocity in the form U_{rms} (root-mean-square velocity) was obtained from

$$U_{rms} = \frac{2\ E\ E_{rms}}{B\ c\ U^{c-1}}$$

where E_{rms} is the root-mean-square voltage output from the anemometer. The turbulence intensity is then the ratio U_{rms}/U.

Errors in Single-Film Measurements

The calibration curve yielded hot-film anemometer velocities that were always within 2 percent of the measured pitot tube velocity. Typically a pitot tube oriented to within ±5° of the approach flow will measure velocities to within ±1 percent making it a very good calibration source. The accuracy of a single hot-film during the measurement of turbulent flow quantities is also dependent upon the flow regime being measured. During the present study the single-film probe was used in conditions of both mean wind shear and moderately high turbulence. Considering the accumulative effect, calibration pitot tube errors, calibration curve fit and flow regime, the model velocity time series should be accurate to within ±5 percent.

Cross-Film Probe Measurements

The second system used was a two-wire cross-film (TSI 1241) anemometer. This probe was used for velocity measurements at the lower speeds run during the stable and unstable conditions. The two-wire probe operates in a similar manner to the single-wire probe except that it has two wires which are positioned roughly 45° to the approaching flow. However, by using the sin and cos relationships of the two wires, two components of velocity can be extracted from the voltage outputs of the probe. Also, by including the measured temperature of an adjacent thermocouple, the hot-film results can be adjusted for temperature. Since this probe was used to measure lower velocities than the single-wire probe, it was calibrated against a mass flowmeter instead of a pitot tube. A brief description of this calibration standard follows.

Velocity Standard for Cross-Film Calibration

The velocity standard used in the present study consisted of a Matheson Model 8116-0154 mass flowmeter, a Yellowsprings thermistor, and a profile conditioning section designed and calibrated by the FDDL staff at CSU. The mass flowmeter measures mass flow rate independent of temperature at the exit conditions, and the profile conditioning section forms a flat velocity profile of very low turbulence at the position where the probe is located. Incorporating a measurement of the ambient atmospheric pressure and a small profile correction factor permits the calibration of velocity at the measurement station from 0.15-2.0 m/s ±5 percent. These error bounds were determined by comparison to TSI's 1125 velocity calibrator system.

Cross-Film Measurement Algorithm

During the calibration of the 1241 X-wire probe it was placed at the nozzle of the calibrator with the probe support axis parallel to air flow. In this position the angle between each sensor and the flow vector is 45°, thus the yaw angles for each sensor are 45°. The voltage from each anemometer channel was digitized for several velocities covering the range of interest. These voltage-velocity pairs (E_i, U_i; i = 1,2), at a fixed angle, were fit to the equation

$$E_{i,j}^2 = A_i + B_i'(U_j)^{c_i} \;;\quad i = 1,2;\; j = 1,n$$

where $$B_i' = B_i(\cos^2\phi_i + k^2\sin^2\phi_i)^{c_i/2}$$

ϕ_i = yaw angle between velocity vector and film i

k = yaw factor

n = number of calibration points

via a least squares fit with the secant method to find the best new estimate of exponent, c_i. Note that if the yaw factor, k, equals zero then a simple cosine law dependence of heat flux exists. To determine the yaw factor, k, the air velocity was set at a constant value, and the probe was rotated about its third axis so that voltage samples could be taken for a wide range of yaw angle variation on both films. These voltage-yaw angle pairs (E_i, ϕ_i; i = 1,2) were regressed to the equation

$$B_i' = (E_{i,j}^2 - A_i)/U^{c_i} = B_i(\cos^2\phi_{i,j} + k_i^2\sin^2\phi_{i,j})^{c_i/2}$$

where i = 1,2 and j = 1,n

via a least squares approach with the secant method to find the best new estimate for the yaw factor, k_i. A_i, B_i, c_i and k_i for both films are thus obtained, but for the reduction algorithm used, k_i must be equal for both films and not a function of velocity. Providing that both films have a similar aspect ratio, then both k_i values should be of similar magnitude, and forcing them equal does not introduce large errors. Once a value for k is specified, then a least squares fit will determine the optimal values for B_i. Once the value of k was determined for a specific probe, it was no longer necessary to do angle calibrations.

Given the calibration constants A_i, B_i, and c_i, then the equations

$$E_i^2 = A_i + B_i(V_{eff,i})^{c_i} \quad ; \quad i = 1,2;$$

where

$V_{eff,i} = V(\cos^2\phi_i + k^2\sin^2\phi_i)^{1/2}$; i = 1,2;

$V_{eff,i}$ = effective cooling velocity for film i; and

V = total velocity vector approaching sensor array are defined. To take measurements with this calibrated X-film probe, both anemometer signals and the temperature signal were digitized and stored on a disk file within an IBM AT computer. These voltage time series were converted to u and v (or w) velocity time series using the following algorithms proposedby Brunm, 1974

$$u = (V_{eff,1} + V_{eff,2})/[2(\cos^2\alpha + k^2\sin^2\alpha)^{1/2}],$$

$$v \text{ (or } w) = (V_{eff,1} - V_{eff,2})/[(\cos^2\alpha + k^2\sin^2\alpha)^{1/2})^{1/2} A \tan\alpha],$$

where $A = \cos^2\alpha(1 - k^2)/[\cos^2\alpha(1 - k^2) + k^2],$

$\alpha = 45°,$

$V_{eff,i} = [(E_i^2 - A_i^*)/B_i^*]^{1/c_i},$

$A_i^* = A_i\, T_{factor},$

$B_i^* = B_i\, T_{factor}$, and

$T_{factor} - (T_{sensor} - T_{environment})/(T_{sensor} - T_{calibration}).$

Errors in Cross-Film Measurements

The accuracy of X-film velocity measurements and associated reduction algorithms can be estimated by directing different known mean velocity vectors at the probe. Tests at calibration temperature determined that the mean velocity magnitude is generally within ±5 percent of the calibrators value. The error in angle calculations was approximately ±2° for angular deviations of 15° or less and somewhat larger than this for greater deviations. Considering the accumulative effect of calibrator, calibration curve fit and temperature correction errors, the model longitudinal velocity time series should be accurate to within ±10 percent. The lateral or vertical model velocity time series errors are greater than those of the longitudinal components, but should be accurate to within ±20 percent.

3.2.1 Conversion of Turbulence Intensity Measurements to Standard Deviations of Angle

Frequently atmospheric turbulence is characterized by the standard deviations of angular deviation of the wind measured by bivane sensors, σ_θ and σ_ϕ. These parameters may be directly related to standard deviations of the velocity deviations of the wind, u', v' and w', through simple formulae which relate the ratios of these quantities in typical atmospheres.

Although the magnitudes of turbulence intensities, u'/u_*, v'/u_* and w'/u_* are known to vary with roughness and stratification; their ratios appear to be somewhat better behaved. Thus, for neutral flow conditions, Snyder (1981) suggested that $w'/u' = \sigma_w/\sigma_u \simeq 0.5$ and $v'/u' = \sigma_v/\sigma_u \simeq 0.75$. For stratified conditions the work of Binkowski (1979) shows similarity between the variations of σ_v and σ_u such that $v'/u' = \sigma_v/\sigma_u \simeq 0.8$ over a wide range of stable and unstable stratification conditions. Haugen (1979) found similar behavior over a range of stratification conditions for the vertical component of turbulence such that $w'/u' = \sigma_w/\sigma_u \simeq 0.4$.

Given the above considerations and simple trigonometry it is simple to show that:

$$\sigma_\theta \simeq (\sigma_v/\sigma_u) * (\sigma_u/u) = 0.8\ u'/u, \text{ and}$$

$$\sigma_\phi \simeq (\sigma_w/\sigma_u) * (\sigma_u/u) = 0.5\ u'/u.$$

Thus, changes in angular deviation are directly proportional to changes in turbulence intensity; hence it is reasonable to state that:

$$\frac{[\sigma_\theta]_{\text{perturbed}}}{[\sigma_\theta]_{\text{unperturbed}}} = \frac{[u'/u]_{\text{perturbed}}}{[u'/u]_{\text{unperturbed}}}$$

Hence, deviations in turbulence intensity measured during fluid modeling tasks I through IV can be considered equivalent to deviations in angular standard deviations.

3.3 Angle Measurements

Approach wind angle measurements and deviations were measured two different ways. For the higher mean velocities used during the neutral flow conditions and the Task II measurements, a wedge type pitot probe was used. This probe is designed such that it measures a zero pressure difference when pointed directly into the flow and a positive or negative pressure difference when the flow comes from one side or the other. Since this pressure difference is not linear with angle the probe was rotated to find the zero location.

The second method for determining wind angle, θ, was by using the output of the cross-film velocity probe. Since two components of velocity were available (along-wind U and cross-wind V) the angle of the approaching flow could be computed from

$$\theta = \tan^{-1} \frac{V}{U} .$$

In both test situations, however, the change in measured approach wind angle due to site buildings or tower blockage from the true wind direction is reported as ($\Delta\theta$) for any location or height or condition. Delta θ is defined as follows:

$$\Delta\theta = \text{Wind direction}_{(\text{measured})} - \text{Wind direction}_{(\text{true})} .$$

Errors in Angular Measurement

Method 1, Wedge Probe: The errors associated with this probe and measurement technique were random errors. After a series of repeatability tests, this measurement system was determined to have a reliability of ±1.5°.

Method 2, Cross-Film Velocity Probe: Errors in this method of angle determination are mostly dependent on errors in the longitudinal and lateral components of velocity used to calculate the angle. Using only these velocity errors, angle deviations of as large as ±4° could be expected. However, random errors could also be encountered. Therefore, a series of repeatability checks were run and a total reliability of ±6° was established for this method.

3.4 Temperature Measurements and Errors

A copper-constant thermocouple with a bead diameter of 0.07 mm was mounted 2 mm to the side of the hot-film probes. An Omega Model DSS-199 digital thermometer connected to this thermocouple provided an analog signal directly proportional to temperature. This analog signal was digitized and recorded in an IBM AT computer. The absolute accuracy of the temperature measurement is stated by the manufacturer to be ±1.3°C. The ability of this, digital thermometer to measure temperature differences is better than this and is estimated to be ~ ±0.4°C. Because of Richardson number similarity between the model and the field (as discussed later in section 4.1), and depending on which flow stability is under consideration, a ± 0.4°C model deviation translates into the following field deviations in ΔT:

Mid to low level (100 to 30 feet) at 4 mph, $\Delta T \approx \pm 0.01°F$,

High to low level (200 to 30 feet) at 4 mph, $\Delta T \approx \pm 0.08°F$,

Mid to low level (100 to 30 feet) at 8 mph, $\Delta T \approx \pm 0.03°F$, and

High to low level (200 to 30 feet) at 8 mph, $\Delta T \approx \pm 0.30°F$.

4.0 TEST PROGRAM AND DATA EXPLANATIONS

4.1 Definition of Key Terms

Most of the data contained in this report are expressed in terms of normalized mean velocities ($\overline{U}$ or $\overline{V}$), local turbulence intensities (TI), wind angle deviations (delta theta or $\Delta\theta$), absolute temperature (T), or temperature difference (delta T or ΔT). Explanations of these terms follows:

Normalized Mean Velocity	- a measured local mean velocity divided by the simultaneous reference velocity measured at the 1500 foot elevation located in the free-stream of the wind flow.
Local Turbulence Intensity	- is the local standard deviation of velocity expressed as a percentage of the local mean velocity for either the longitudinal component U or the lateral component V.
Delta Theta ($\Delta\theta$)	- is the local deviation in measured approach wind angle from the true wind angle in degrees.
Temperature	- is the measured temperatures at points above the model in °C.
Delta Temperature (ΔT)	- is the difference in temperature between two elevations for a given profile location. In this report the lower or reference height is always selected as 10 meters or 30 feet.

An example listing with further explanation follows in Section 4.2.

For Task II an additional parameter called the velocity ratio (V_R) is specified. This is simply the ratio of the measured wind speed to the true approach wind speed. Therefore, a velocity ratio of 1.00 indicates no disturbance due to the primary tower; whereas ratios other than 1.00 indicate local velocity deficits or speed-ups of varying magnitude.

Finally, three quantities called the velocity change $(\bar{U})_c$, delta temperature change $(\Delta T)_c$, and the turbulence intensity change $(TI)_c$ are found in Table C1 (for Task I data) and Table E1 (for Task III data). Exact definitions for these quantities are found with the tables mentioned. As defined, they represent <u>fractional changes</u> in mean velocity, ΔT, and local turbulence intensity at a given elevation for either the primary or back-up meteorological tower location <u>caused by introducing the cooling tower</u>. Since these terms are all ratios they are independent of wind speed or the magnitude of field temperature gradients. For example (Table C3), during a flow which resembles the high speed unstable test the fractional change in velocity, $(\bar{U})_c$, at 200 feet equals -0.098, which means that the introduction of the cooling tower causes a 9.8 percent velocity reduction at the primary tower at 200 feet elevation. Conversely, during a flow approximated by the high speed neutral test the fractional change in velocity, $(\bar{U})_c$, at 200 feet equals +0.090, which means that for this case the introduction of the cooling tower causes a 9.0 percent velocity speed-up. This format gives a quick and simple way to check the effect of the cooling tower on the meteorological tower instrument locations. All other terms found in this report, along with their definitions, can be found in the list of symbols at the beginning of this report.

4.2. Sample Profile Listing

The following example profile listing with line and column explanations is hereby presented.

Sample Profile Listing

Profile Name	: NYS-3-B2	Review of Profile Conditions
Flow Condition	: Stable, High speed	
Task Number	: 3	
Configuration	: B	
Ref. Height	: 1500.0 ft	
Ref. Model Velocity	: 3.19 mph	

Column

(a)	(b)	(c)	(d)	(e)	(f)	(g)	(h)
Height (ft)	Velocity (Normalized)	Turb. Int. (%) u	v	del Theta (deg)	Model Temp (deg C)	Delta Temperature (Deg C) 4 mph Field	8 mph Field
30.0	.162	16.5	14.3	9.32	18.36	.00	.00
58.5	.201	19.0	18.7	10.31	21.87	.04	.16
97.7	.252	21.3	19.7	6.16	25.05	.07	.30
148.6	.347	19.3	16.8	1.36	28.95	.12	.47
196.3	.440	14.8	14.7	-1.73	31.92	15	.61
249.1	.503	12.3	13.2	-3.09	33.92	.17	.70
376.8	.615	9.3	11.3	-2.20	36.86	.21	.83
747.4	.869	3.2	4.4	.06	42.06	.27	1.06
1123.1	.928	3.8	4.8	.63	43.97	.29	1.15
1496.7	1.000	1.8	3.0	.47	45.84	.31	1.23

Row J → T@100-T@30 = .602*T@100-T@30 Undisturbed App. ie Change in del T = .05 .20

Row K → T@200-T@30 = .830*T@200-T@30 Undisturbed App. ie Change in del T = -.03 -.12

Column (a): Equivalent field height in feet.

Column (b): Local mean velocity normalized by the reference velocity at 1500 ft.

Column (c) and (d): Local turbulence intensity in % for both the U and V components.

Column (e): Delta Theta ($\Delta\theta$) - is the measured wind angle deviation of the flow from that of an undisturbed approach flow.

Column (f): The measured temperature during model testing.

Column (g) and (h): The computed ΔT in the field for two selected representative field velocities. For a given combination of ΔT and velocity in the model, an infinite number of possible field combinations exist. Therefore, it is necessary to select a field velocity and compute the ΔT's for that specific case. (See the following discussion of Richardson Number similarity for more detail.)

Row J = Mid to Low level (100 ft to 30 ft) ΔT expressed as a multiple of the Mid to Low level ΔT of the undisturbed approach flow conditions. A multiple of 1.000 would mean no change due to site conditions and multiples other than 1.000 would represent changes in ΔT due to site conditions. Once again, a velocity must be selected to compute ΔT, which has been done under column (g) and (h). In this example: -.05°C would be the change in ΔT at a field velocity of 4 mph caused by these site conditions.

Row K = High to Low level (200 ft to 30 ft) ΔT expressed as a multiple of the High to Low level ΔT of an undisturbed approach flow conditions.

Richardson Number Similarity between Model and Field

As discussed in Appendix A it is necessary to maintain Richardson number equality between the model and field conditions. The Richardson number is defined as:

$$R_i = \frac{g\ \Delta T\ L}{T\ U^2} \quad .$$

To maintain similarity between model and field

$$\left(\frac{g\ \Delta T\ L}{T\ U^2}\right)_{model} = \left(\frac{g\ \Delta T\ L}{T\ U^2}\right)_{field}$$

or $$\Delta T_{field} = \Delta T_{model} * \left(\frac{L_m}{L_f}\right) \left(\frac{U_f^2}{U_m^2}\right) \left(\frac{T_f}{T_m}\right) \quad .$$

Since T_f essentially equals T_m in terms of absolute temperature the equation becomes,

$$\Delta T_{field} = \Delta T_{model} * \left(\frac{1}{750}\right) \left(\frac{U_f^2}{U_m^2}\right) \quad . \qquad \text{Equation (A)}$$

Since U_f and U_m must be the field and model velocities at the same equivalent height we will arbitrarily select 200 feet (top of the primary meteorological tower) as a reference height. Also, we may select 4 mph and 8 mph as typical field velocities at the 200 foot level. Furthermore, the quantity $(1/750)(U_f^2/U_m^2)$ shall be called the ΔT multiplier factor (ΔT-MF) such that,

$$\Delta T_{field} = \Delta T_{model} * (\Delta T\text{-MF}) \quad .$$

Substituting the appropriate quantities into the equation produces the following table.

Model Flow Condition		Model Velocity @ 200 ft	ΔT-MF 4 mph	ΔT-MF 8 mph
Unstable:	Low Speed	37.84 cm/s = 0.846 mph	.0298	.1191
Unstable:	High Speed	56.07 cm/s = 1.254 mph	.0136	.0542
Stable:	Low Speed	20.11 cm/s = 0.450 mph	.1054	.4217
Stable:	High Speed	61.86 cm/s = 1.384 mph	.0111	.0446

These ΔT multiplier factors are used to convert the measured model ΔT's to equivalent field ΔT's in the data listings. It can be seen from these equations that ΔT in the field varies as the square of the field velocity increase or decrease. For example, if a high speed unstable condition developed at 12 mph instead of 4 or 8 mph the ΔT-MF for that condition would be .1221. Using equation A and the listed 200 ft model velocities in the table, a ΔT-MF factor could be calculated for any possible field situation.

4.3 Data Quality

Homogeneity

A few measurements were taken to one side of centerline (+ 375 feet prototype scale) during the setup of flow conditions for both the neutral and stratified flow situations. The profiles showed no variations greater than the expected random instrumentation deviations. Visualizations using smoke tracers during the various experiments gave no reason to believe there were tunnel size cork-screwing of the flow. In January of 1986 new triple pane insulated windows were installed in the Meteorological Wind Tunnel to reduce lateral heat transfer at side walls and eliminate any tendency to produce cells of motion of tunnel size. The elevated inversion present during the unstable flow also tended to constrain any tendency for large tunnel-size eddy development, since the aspect ratio of tunnel width to inversion height was about 6.

Stable flow situations have been considered dozens of times previously in the Meteorological Wind Tunnel. Many lateral variation checks showed no systematic or significant deviations; thus, check measurements of this type for this measurement series were limited. For the unstable flow situation Poreh and Cermak (1984) made lateral and longitudinal measurements to determine homogeneity. They used a similar method to that used in the current effort to produce the unstable flow. Consideration of temperature profiles at two downwind distances compared with lateral temperature measurements at plus/minus 0.4 m (equivalent to 1000 ft NYPA prototype distance) displayed no systematic deviations, and oral discussion with Dr. Poreh indicated no visualization evidence for cross-tunnel circulations.

A primary concern in this study was the presence or absence of streamline deviation at a meteorological tower due to the presence of cooling tower or reactor structures. Lateral wind vectoring was determined by comparing traverses of the wedge-type pitot probe or a X-film anemometer probe. Since the traverse itself had a systematic twist with height, the probes could not be used directly to evaluate the clean-tunnel flow condition. Fortunately, extremely careful crossfield measurements of the Meteorological Wind Tunnel cross-section were made by Veenhuizen and Meroney (1969) using laser transits and rotating hot-wire anemometry. Measurements in low wind speed neutral flows revealed maximum cross-flow components produced less than ±1.00° deviation from the tunnel centerline over the length of the tunnel. Thus, any streamline deviations about the meteorological towers which might occur in the absence of the cooling tower or reactor structures are extremely small compared to the perturbations introduced by the structures themselves.

Stationarity

All comparative measurements were made consecutively. There was normally never more than 45 minutes delay between measurements with and without cooling tower (typically, it took 30 minutes to take the profile and about 15 minutes to change model). This was true whether the flow was neutral, stable or unstable; however, several minutes between tunnel entry was always allowed for the flow to restabilize when doors were opened. In a number of cases profiles were repeated twice to assure the operator that no "opening the door" perturbations remained in the flow.

All stable low-speed profiles were taken on the same day.

All stable high-speed profiles were taken on the same day.

All unstable low-speed profiles were taken on the same day.

All unstable high-speed profiles were taken on the same day.

Repeatability

Repeat runs were taken for many of the test cases, but not all conditions. During the early phase of the testing comparisons were often made between these tests, but deviations were rarely more than that due to expected random errors discussed in the text. Also if the differences detected were due to random effects, one would expect less consistency in the results found. Velocity profiles do not deviate by more than 0.03 normalized velocity magnitude, turbulence profiles generally repeat within 0.02, but a few points may differ by as much as 0.03 to 0.035. Considering the expected accuracies of the instrumentation and the normal variability of a turbulence field, this is very very good.

All data reported in the figures and tables of this report are for specific runs and are not averages.

4.4 Guide to Data

This report consists of a main body and six appendices. Both a List of Figures and a List of Tables for the main body can be found at the beginning of this report. At the beginning of each Appendix a brief summary of its contents, data, and figures are provided. The appendices contain the following information:

Appendix A: Discussion of Fluid Modeling Criteria

Appendix B: Data listings for approach flow model conditions, and site meteorological data concerning the frequency of winds for different stability conditions

Appendix C: All Task I data and figures

Appendix D: All Task II data and figures

Appendix E: All Task III data and figures

Appendix F: All Task IV data and figures

5.0 DISCUSSION OF RESULTS

Each of the four measurement tasks are discussed separately in sections 5.2 through 5.5 provided below. Figures, tables and data for each task are summarized in separate Appendices C through F. First, however, in section 5.1 it is appropriate to consider the implication of propagation of measurement errors in wind speed, direction and turbulence into the predicted behavior of gas plumes released in the vicinity of the reactor buildings.

5.1 The Propagation of Measurement Errors into Dispersion Models

There are many possible analytic and numerical models available to predict puff or plume transport and diffusion downwind of a reactor complex. The propagation of errors in input meterological information through these models into final estimates of dispersion can be evaluated through parameter variation studies for each model. One can identify at least three sources of predictive error--model uncertainty, inherent uncertainties of atmospheric motion (random measurement uncertainties), and systematic measurement errors.

The deviations of the real atmosphere from simplifying model assumptions give rise to "model uncertainties". Simpson and Hanna (1981) predicted, for example, that elevated point sources in flat terrain with steady meteorological conditions and short averaging periods predict near source concentrations using a Gaussian plume model with an accuracy of 20 to 40 percent. Yet validation studies have shown that most models are inaccurate by a factor of 2 or greater. Model uncertainties are sometimes distinguished from the inherent uncertainties of the atmosphere resulting from natural random motions.

Alternatively, there are the effects of "measurement uncertainties" of the measured input data with which a model is supplied. Sensitivity studies frequently examine the influence of variations in model input on model output, but they are strictly speaking not uncertainty analyses in that they do not combine uncertainties into a final output uncertainty. The propagation of random errors and uncertainties into representative Gaussian dispersion models has been recently discussed by Freeman et al. (1986). They derived an error propagation formulae through a Taylor series expansion, and they validated their model using a Monte Carlo simulation. Their results show for a simple test case that uncertainties in wind direction are the prime contributors to total predictive uncertainty, and the uncertainty is large, equaling 76 percent to 38 percent at plume centerline as distances increase from 1.0 to 15.0 km and increasing dramatically to over 600 percent with lateral distance from the plume centerline. In most cases, however, the measurement uncertainties will be significantly less than model uncertainties. Nonetheless, measurement uncertainties might be considered the <u>minimum</u> uncertainty for a model.

The perturbations measured in this report are properly speaking systematic measurement errors arising from site conditions and structures not random errors. Thus a sensitivity analysis of the type described by McRae and Tilden (1980) might be used. But such a sensitivity analysis is generally very labor intensive and model specific; thus a more generic approach will be followed herein based on the familiar Gaussian plume formulae.

Error Propagation Formulae

Consider the classic Gaussian ground-level concentration plume formulae for continuous point source dispersion:

$$C/Q = \exp\left[-(h/\sigma_z)^2\right] / (\pi\sigma_y\sigma_z U),$$

where

$$\sigma_y = \sigma_\theta x^a,$$

and

$$\sigma_z = \sigma_\phi x^b.$$

Using the subscript "e" to represent perturbed values and the subscript "a" to represent the unperturbed values, then the ratio of concentrations predicted using systematically flawed input meteorological data to concentrations using the actual flow conditions would be:

$$[C_e/C_a] = [\sigma_\theta\sigma_\phi U]_a/[\sigma_\theta\sigma_\phi U]_e{*}E$$

where E is a nonlinear function of height, downwind distance, and perturbed and unperturbed angular standard deviations of the order of magnitude of 1.0. E equals 1.0 for ground-level sources. But as noted earlier in section 3.2, measured deviations in turbulence intensity over the models can be related to deviations in standard deviation of wind direction; thus,

$$[C_e/C_a] = [U_a/U_e] * [(u'/U)_a/(u'/U)_e]^2,$$

or

$$[C_e/C_a] = [(1 + \Delta\{U\}) * (1 + \Delta\{u'/U\})^2]^{-1}.$$

Thus, predicted errors in concentration vary inversely with the magnitude of the velocity perturbation ratio and inversely with the square of the magnitude of the turbulence perturbation ratio. Figure 14 displays the behavior of the function for velocity deviation ratios from 0.5 to 1.5 (ΔU from -0.5 to +0.5) and turbulence deviation ratios from 0.9 to 2.0 ($\Delta\{u'/U\}$ from -0.1 to +1.0). Typical systematic errors detected during the current measurement program were velocity perturbations ranging from -0.4 to +0.2 and turbulence perturbations ranging from 0 to +3.7. But, since the errors which result in velocity defect and turbulence excess occur together, there is some tendency for self-correction, and final errors which propagate into concentration estimates may only result in concentration ratios from 0.1 to 1.5.

5.2 Task I: Quantification of the Effect of the Site's Cooling Tower on Meteorological Sensors on the Primary Meteorological Tower

Measurements were performed at two wind speeds at the site of the primary meteorological tower vis-a-vis the effect of the Niagra Mohawk cooling tower for a wind orientation of 82°. Wind speed, angle, turbulance and temperature deviations were measured, and the results are summarized in Appendix C.

During neutral stratification, perturbations in wind speed and wind direction were less than 12.1 percent of free stream and ±0.50°, respectively. Turbulence levels decreased from 0.23 to 0.18 percent. Thus, the cooling tower did not significantly affect the shape of the profiles measured over the height of the tower (Figure C2). This result is consistent with the measurements of Kothari et al. (1979), which show that building wake effects in neutral flow may not persist as long as in stable flow and nearly disappear by x/H values near

10.0. Hence, no corrections to primary meteorological tower measurements associated with the cooling tower are necessary.

During the high speed stable stratification conditions, the cooling tower wake was evident at the primary meteorological tower site. At the lower wind speed (stronger stable stratification) the cooling tower wake appeared to effectively disappear before the meteorological tower site was reached (Figure C3). Apparently both mechanical turbulence and vortex wake effects were dampened by the stratification. However, at the higher wind speed, stable stratification condition perturbations of as much as 19 percent in wind speed and ±6.3° in wind direction occurred (Figure C4). Turbulence levels changed from magnitudes of 0.05 to 0.15. These perturbations are due to a combination of mechanical turbulence and secondary flow introduced by the upstream cooling tower, which appear to persist under the intermediate stratification condition. Again, this is consistent with the earlier measurements of Kothari et al. (1979), who found significant perturbations in velocity, turbulence, and temperature at distances as large as x/H equal to 60!

During unstable stratification conditions, the cooling tower affected the overall wind profiles slightly. For the lower wind speed unstable stratification conditions, insertion of the cooling tower caused velocity defects of about 8 percent (Figure C5); whereas at the higher speed velocity defects of 12 percent were detected (Figure C6). Turbulence intensity levels were between 0.15 to 0.30. Wind angle deviations were generally below 5°, except for a few readings between 10° at heights above 60 m (200 ft) at the lower wind speed.

Although the perturbations detected for the situation when the primary tower is directly in the wake of the cooling tower are significant, they will occur for only a very narrow wind direction segment. According to the measurements of Hansen and Cermak (1975) and Kothari et al. (1979), perturbations in the wake of structures embedded in a deep turbulent boundary layer reduce to less than 2 percent at lateral distances of ±D, where D is a characteristic width of the object. Thus, presuming an average diameter of the cooling tower of 100 m (300 ft) and a separation distance to the primary tower of 1100 m (3600 ft), no significant wind perturbations will be present at the primary tower due to the cooling tower outside the wind sector between 77° and 87°. Nine Mile Point climatological data suggest that winds persist in the easterly sector less than 4 percent of the time; thus winds in the critical sector will occur less than 2 percent of the time. Breaking the wind frequencies down by stability gives way to even a smaller chance that for a given stability condition, wind will come from the 77° to 87° sector. Using the wind frequency data found in Appendix B, the following is found for the 77° to 87° critical wind sector:

Unstable conditions (A,B and C) occur less than .15% of the time,

Neutral conditions (D) occur less than .5% of the time, and

Stable conditions (E,F and G) occur less than 1.2% of the time.

(Note: Frequencies for the critical 10° sector are taken as one-half of the frequencies of the 22 1/2° easterly sector as listed.)

During both the stable and unstable conditions, ΔT model measurements were taken and converted to equivalent field ΔTs of 4 mph and 8 mph. These ΔTs for different site configurations were then compared to the ΔT at each height for an undisturbed approach flow condition (no buildings or structures) to see how ΔT changed due to the presence of site structures. This change in ΔT is expressed on each listing as both change in ΔT for the 100 to 30 ft levels for both 4 mph and 8 mph. Thus, a change in ΔT of 0.00 means that the particular site configuration did not affect the temperature gradient.

For all of the stable and unstable tests of Task I, these ΔT changes were small (-.16°C being the largest) except for one case, that being the stable-low speed-Configuration B test. Here, the ΔT changes were 1.00°C and .62°C at 8 mph for the mid- to low-level and high- to low-level changes, respectively.

Upon closer inspection of this data set, it was found that these large ΔT changes arise because the measured model temperature at the 30 ft elevation was about 2.0 to 2.5°C lower than might be expected after reviewing all of the other test data. Hence, this data point is probably suspect. Extrapolation of the equivalent 30 ft elevation temperature from other data points brings the computed ΔT changes at 8 mph to +.14°C and -.26°C, respectively. These numbers are more in line with those of the other test runs.

Table C3, Appendix C, has been constructed to summarize the fractional changes in mean velocity, temperature and turbulence caused by the Niagra Mohawk cooling tower for different anticipated field conditions when the wind blows directly from the cooling tower toward the meteoro-logical tower.

Consider the following example of low wake perturbation effects on meteorological tower instruments affect predicted concentrations. During unstable high speed conditions for Task I, $(\bar{U}_c)$ = -.098 and $(TI)_c$ = .213 at 200 ft elevation (from Table C3). Figure 14 (Error Propagation Curves) is useful to analyze this situation. By plotting $(\bar{U})_c$ on the Del U axis and $(TI)_c$ on the Del (u'/u) axis point A is established. Reading back to the C_e/C_a axis the perturbed concentration reading will be approximately 70 percent of the actual or expected ground level concentration reading. This example shows how a combination of errors or data perturbations can be translated into a concentration deviation. (Note: Figure 14 is not limited to analysis of $(\overline{U})_c$ and $(TI)_c$ but is applicable for many sources of data deviations.) Unfortunately, it is unlikely that a simple multiplicative correction factor would properly correct average wind speed, direction, turbulence or temperature measurements for the wake effect of the cooling tower. Although instantaneous values of these quantities might be corrected for wake effects, 15 min, 30 min, or hourly averages usually contain wind vectors which arrive from several wind sectors. The percentage of time the wind spends in each quadrant is a function of an angular probability function which will vary with wind direction and stability. Hence, a correction factor for averaged data based on the extremely nonhomogeneous effect of the cooling tower wake would be inappropriate.

5.3 Task II: Quantification of the Effect of the Meteorological Tower Structure on Sensor Measurements

Tests were performed for both the current instrument locations and new locations on a proposed boom (Figure 6) during neutral conditions. The initial tests were computed at three wind speeds for four different approach wind directions (67.5°, 90°, 112.5°, and 270°). These data are summarized in Table D1 for the current boom position, and Table D2 for the proposed boom position. Figures D1, D2 and D3 express the data in graphical form. The data indicate that the effects caused by the structure on the instrumentation is essentially independent of wind speed.

A second group of data--Table D3 for the current boom position and Table D4 for the proposed boom position, along with Figures D4, D5 and D6--demonstrate the effects of the tower structure on the instrumentation for a full 360° are of approach wind conditions. From this data, two distinct areas of disturbance can be seen. First, in the sector of winds from NNE to ESE, an area of large velocity defect and large turbulence increase is observed. Although the current and proposed boom locations vary somewhat, they both show velocity defects through this sector of as much as 35 to 38 percent, and turbulence levels that increase from a background level of about 1 or 2 percent to levels around 7 to 12 percent. As discussed earlier, changes in turbulence relate directly to changes in σ_θ; therefore, σ_θ changes can be on the order of factors from 3 to 12 times too high. Wind from this sector (NNE to ESE) occurs approximately 20 percent of the time (see Appendix B).

The second disturbance region is found in the sector of winds from S to W. In this region a slight slowdown in the mean velocity of the order of 2 to 10 percent is observed, because as the flow approaches the tower from upwind it begins to slow down or stagnate before it is pushed out around the sides of the tower. This same effect causes a slight speedup of mean velocity at the instrument locations for SE and NW winds of about 3 percent as the wind moves out and around the tower. However, for these wind directions there is no measurable affect of the tower on the turbulence. An upwind set of instrumentation would eliminate turbulence errors and reduce velocity errors from the 35 percent range to less than 10 percent.

The third quantity measured during these tests was the deviation of measured wind angle from the true wind angle ($\Delta\theta$). Both the current and proposed boom locations did see some small deviations in measured wind angle but these deviations were never more than ±4.11° (which is within the NRC guidelines of ±5°); therefore, wind angle deviations for Task II are considered to be minor and insignificant.

To adjust for the tower perturbations measured during Task II it is possible to construct a tabular correction function for mean velocities, turbulence, and wind direction, all of which could be related to the measured wind direction. Unfortunately, unless the field data were to be reduced and corrected on an instantaneous basis, this tabular correction function would not work very well. Since field data averaged over 60, 30 or even 15 minutes contains an unknown distribution of wind values and wind velocities, applying a function of this type to the average would provide questionable improvement.

Although the wind-tunnel tests for Task II were all performed under neutral conditions, the above discussion should apply equally well to both stable and unstable conditions. This would be true for two reasons. First, the phenomenon is strictly a mechanically induced effect of the tower and its members; and secondly, the distances involved (12 to 14 ft out from the tower) are too short for stability conditions to have any noticeable impact. In other words, it does not matter how a velocity or turbulence is generated before it reaches the tower, but once it impinges on the tower, the effect of the tower locally will be predictable.

5.4 Task III: Quantification of the Effect of the Cooling Tower and Other Site Structures on the Back-Up Meteorological Tower Measurements

The data for the tests conducted at the back-up meteorological tower site are found in Appendix E. This data is very similar in nature to the data of Task I with profiles of mean velocity, turbulence, and ΔT measured. All data was obtained for an approach wind direction of 241°. However, since the back-up tower only has instruments at the 96 ft elevation, this discussion will concentrate on measurements at the 100 ft height. If full profile data is desired, it is available in the Appendix.

For the neutral flow situation at the 96 ft level, a 20 percent velocity reduction exists relative to the undisturbed approach flow (no site structures in place) for Configuration A (site structures in place - no cooling tower). This same trend is noticed for the stable and unstable wind conditions for Configuration A with velocity reductions of 7 to 18 percent. The JAF reactor building is very close to and directly upstream of the back-up tower location. Configuration A data shows that the JAF building itself (without the new service building) can cause as much as 20 percent mean velocity measurement errors.

Returning to the neutral flow discussion, it is found that insertion of the cooling tower (Config. B) and subsequently the new service building (Config. C) does cause some small changes in velocity and turbulence relative to Configuration A (see Figure E1), especially near the ground. This result shows that the influence of the new service building and cooling tower on the back-up tower instruments is secondary compared to the influence of the JAF building itself. For this reason, the subsequent stable and unstable tests were only performed for Configurations A and B. Configuration C tests, with the new service building in place, were omitted in favor of performing more runs during the Task IV testing phase. The influence of the JAF building will be noticeable over a wide range of wind directions, roughly SSW to W. These winds occur approximately 28 percent of the time; therefore, because of its proximity to the JAF building, the back-up tower location will be exposed to this disturbed flow a good portion of the time.

During the stable and unstable tests, ΔT measurements were taken and they are available in the data listings, but no discussion will follow since no temperature measurements are taken on the back-up tower.

For stable conditions the addition of the cooling tower caused virtually no changes in the measured profile at the lower speed (Figure E2). However, at the higher speed velocity defects on the order of 10 to 30 percent in the lower 60 m (200 ft) occur along with increases in the turbulence levels. Turbulence intensity levels increase from around the 0.05 to 0.10 level to the 0.12 to 0.22 level. These types of increases in turbulence intensity correspond to increases in σ_θ of 2.0 to 3.0 times.

For the unstable conditions some difference in profile shapes were seen for both wind speeds when the cooling tower was introduced. At the lower speed (Figure E4), velocity defects of 4 to 10 percent were observed (6 percent at 96 ft). At the higher speed, velocity defects of 9 to 15 percent were noted above the 30 m (100 ft) elevation (9 percent at 100 ft). For both cases, turbulence levels increased noticeably. Generally, turbulence intensities, and therefore σ_θ, increased by a factor on the order of 1.3 to 1.6.

Wind angle deviations at the 96 (100) ft elevation were all within ±8°. However, looking at other elevations gives maximum wind angle deviations of -5.83° to +10.37°. Large angle deviations occur with both the cooling tower in and out, therefore any deviations from the true wind angle are not necessarily caused by the cooling tower, but by other site structures upwind, namely the JAF buildinig.

Table E3, Appendix E, has been constructed to summarize the fractional changes in mean velocity, temperature and turbulence caused by the Niagara Mohawk cooling tower for different anticipated field conditions, when the wind blows directly from the cooling tower toward the meteorological tower.

As for Task I, it is unlikely that a systematic simple correction function would properly correct the data at the back-up tower site. The correction would need to be applied to instantaneous data, whereas the field data are 15, 30 or even 60 min averages; in addition the distribution of approach wind directions and speeds within the averaging period would be unknown. The errors due to the cooling tower wake discussed in this section might be expected to occur with the following frequencies based on the average of SW and WSW wind data found in Appendix B:

Unstable conditions (A,B and C) occur less than 0.9% of the time,

Neutral conditions (D) occur less than 3.1% of the time, and

Stable conditions (E,F and G) occur less than 3.9% of the time.

5.5 Task IV: Quantification of the Effect of Primary Meteorological Tower's Proximity to Lake Shore on the Representativeness of Measurements

The primary meteorological tower is very close to the shoreline of Lake Ontario. This close proximity to the shoreline causes the wind data at the tower location to be somewhat different from that the power plants would see for selected wind directions. The wind directions where this problem arises are in the sector from SW to NE. An estimate of how the land fetch lengths for the primary meteorological tower and power plant sites differ for each wind direction is given in Table E3, Appendix E. Average wind frequencies for all conditions are also shown. Since these winds occur 55 percent of the time and that the primary meteorological tower is much too close to the shoreline to be representative of the winds over the power plant site itself, the following discussion of fetch related errors is quite pertinent. All of the data and figures for these Task IV tests are found in Appendix F.

During neutral conditions, as the distance inland was increased, changes in both mean velocity and turbulence intensity were seen (Figure F2). Mean velocity measurements decreased by as much as 35 percent near the ground (10 m and below) and turbulence intensity levels rose from around 0.15 to 0.25 (which implies a change in σ_θ of 1.67 times). At the 10 m (30 ft), 30 m (100 ft), and 61 m (200 ft) elevations where the field instruments are located, large differences in both mean velocity and turbulence do indeed exist.

For stable conditions essentially no change in the mean velocity profiles was observed at either speed (Figures F3 and F4). The turbulence was also unaffected except at the 10 m and 20 m (30 ft and 60 ft) elevations for the higher speed case. This is consistent with what might be expected in a stable flow condition. During stable conditions the flow is dominated by the thermal gradients; hence, the mechanical turbulence generated by the surface roughness is suppressed very quickly and does not carry downstream more than a few roughness heights. Turbulence differences are only observed at 10 m and 20 m for the high speed cases (Figure F4). At the higher speeds, the surface roughness generated turbulence will carry a little farther downwind before it is suppressed; therefore, one observes these deviations at 10 m and 20 m, but not at 30 m (100 ft).

For unstable conditions small decreases in mean velocity were measured for both wind speeds (Figures F5 and F6). These velocity defects were generally on the order of 10 to 15 percent and were observed below the 46 m (150 ft) elevation. Increases in turbulence intensity were also observed throughout the lower 76 m (250 ft) of the profiles. Generally, the turbulence intensity levels increased by less than 0.07 at each individual elevation.

The growth of the atmospheric boundary layers over nonhomogeneous terrain is considered in depth by Hunt and Simpson (1982) and Plate (1971). When the surface roughness changes on a line at say $x = 0$, the change in air flow in neutral conditions and within about a kilometer of the change in roughness can be characterized by the rates of the downstream to upstream roughness, (z_{02}/z_{01}). The main effect of the change in roughness (i) a sudden increase in surface stress, U_*^2, (ii) a reduction in wind speed within an internal boundary layer regime, (iii) a growth in height of a region near the wall influenced by the roughness change, and (iv) turbulence variances increase proportional to the increases in shear stress. Simplified algorithms are proposed suitable for prediction of wind speed at various heights and downwind distances.

The influence of changes of surface temperature on characteristics of the surface layer are not yet well understood. In near neutral situations, nonhomogeneous in temperature are expected to affect local values of z/L_{mo} where L_{mo} is the Monin-Obukhov stability length. Algorithms have not yet been prepared which reliably incorporate the joint effects of roughness and temperature changes on the structure of a surface layer.

Thus in absence of analytic or empirical guidance in the area of complex nonhomogeneous surface changes one must rely on empirical data. The range of conditions studied in this report are too limited to facilitate construction of such an algorithm. A program of measurements during which thermal stability is varied in small increments could be appropriate.

6.0 CONCLUSIONS

A sensitivity analysis suggests systematic measurement errors in wind speed, turbulence and temperature gradient will propagate through prediction models to produce substantial errors in estimated concentrations. Since velocity deficits as large as -0.4 and turbulence excess may increase as much as 3.7 times, then multiplicative errors in concentration from 0.1 to 1.5 may occur. Based on this wind-tunnel measurement program, it is likely that:

1. Due to the bulky nature of the main meteorological tower, measurements of wind speed, wind direction, and turbulence probably exceed NRC accuracy guidelines for wind directions in the wind sectors between NNE and ESE. These conditions exist about 20 percent of the time on an annual basis.
2. The influence of the Nine Mile Point Unit 2 cooling tower on the main and backup meteorological towers could exceed NRC accuracy guidelines for isolated wind conditions. It is estimated that these conditions exist about 2 percent of the time for the main meteorological tower and about 20 percent of the time for the backup tower on an annual basis.
3. The influence of the James A. Fitzpatrick turbine reactor, and new service buildings on the backup meteorological tower could cause the wind sensors to exceed NRC instrument accuracy guidelines for winds directions in the wind sectors between SSW and W. These conditions exist about 28 percent of the time on an annual basis.
4. Because the main meteorological tower is closer to Lake Ontario than the buildings at JAF and Nine Mile Points Units 1 and 2 when winds are out of the WSW to N sectors, the

influence of surface roughness and thermal heating modifies the flow field between the two locations. In this situation the measurements at the main tower may not accurately represent conditions at the generating stations. It is estimated that these conditions exist about 43 percent of the time on an annual basis.

REFERENCES

Binkowski, F. S., 1979, "A Semi-Emperical Theory for Turbulence in the Atmospheric Surface Layer," Atmos. Envir., Vol. 13, No. 2, pp. 247-253.

Freeman, D. L., Egami, R. T., Robinson, N. F. and Watson, J. G., 1986, "A Method for Propagating Measurement Uncertainties through Dispersion Models," J. of the Air Pollution Control Association, Vol. 36, No. 3, pp. 246-253.

Gifford, F. A., Jr., 1975, "Turbulent Diffusion Typing Schemes: A Review," Enviromental Research Laboratories, ATDL Report No. 75/2, or, 1976, Nuclear Safety, 17, No. 1, pp. 68-86.

Golder, D., 1972, "Relations Among Stability Parameters in the Surface Layer," Boundary-Layer Meteorol., Vol. 3, pp. 56ff.

Hansen, A. C. and Cermak, J. E., 1975, "Vortex-Containing Wakes of Surface Obstacles," FDDL Report CER75-76ACH-JEC16, Colorado State University, Fort Collins, Colorado.

Haugen, D. A., ed., 1973, "Workshop on Micrometeorology," American Meteorological Society, Boston, 392 pp.

Hunt, J. C. R. and Simpson, J. E., 1982, "Atmospheric Boundary Layers over Non-homogeneous Terrain," Engineering Meteorology (ed. E. Plate), Elsevier, New York, Ch. 7, pp. 269-318.

Kothari, K. M., Peterka, J. A. and Meroney, R. N., 1979, "Stably Stratified Building Wakes," Fluid Dynamics and Diffusion Laboratory, Colorado State University, Fort Collins, Colorado, CER78-79KMK-JAP-RNM65.

McRae, G. J. and Tilden, J. W., 1980, "A Sensitivity and Uncertainty Analysis of Urban Scale Air Pollution Models--Preliminary Steps," in Second Joint Conference on Applications of Air Pollution Meteorology, American Meteorological Society, Boston, MA.

Plate, E. J., 1971, "Aerodynamic Characteristics of Atmospheric Boundary Layers," US Atomic Energy Commission, TID-25465, 190 pp.

Poreh, M. and Cermak, J. E., 1984, "Wind Tunnel Simulation of Diffusion in a Convective Boundary Layer," Boundary Layer Meteorology, Vol. 30, pp. 431-455.

Simpson, R. W. and Hanna, S. R., 1981, "A Review of Deterministic Urban Air Quality Models for Inert Gases," NOAA-TM-ERL-ARL-106, Silver spring, MD.

Snyder, W. HY., 1981, "Guideline for Fluid Modeling of Atmospheric Diffusion," United States Environmental Protection Agency Report EPA-600/8-81-009, 185 pp.

Veenhuizen, S. D. and Meroney, R. N., 1969, "Secondary Flow in a Boundary Layer," Project THEMIS Report No. 3, CER68-69DSV-RNM28, (also Paper 72WA/FE34, ASME Winter Annual Meeting, 1972).

TABLES

Table 1. Approach Flow Characteristics

Approach Flow Conditions during
Wind-Tunnel Tests over NYPA Model
Scale: 1:750

Flow Condition	Z_o (cm)	U_*/U_{10}	(T_*) model (°C)	(L_{mo})field (m)
Neutral over Land	50	0.140	0	∞
Neutral over Lake	2	0.066	0	∞
Stable, Low Speed	50	0.072	3.6	1.15
Stable, High Speed	50	0.203	9.5	10.5
Unstable, Low Speed	50	0.055	-6.6	-1.4
Unstable, High Speed	50	0.071	-5.2	-4.5

Table 2. Stability Classifications

MEASURED MODEL/PROTOTYPE CONDITIONS FOR STRATIFIED FLOWS FOR NYPA
WIND-TUNNEL STUDY MEASUREMENTS MADE AT METEOROLOGICAL TOWER LOCATION
Length Scale Ratio: 1:750

MODEL CONDITIONS						STABILITY CLASSIFICATIONS			
CONDITION	HEIGHT Model (cm)	HEIGHT Field (m)	VELOCITY (cm/sec)	TEMPERATURE (°C)	RiB (model)	RiB Range Field Measurements**	Pasquill-Gifford Category**	RiB Range Field Measurements***	Pasquill-Gifford Category***
Unstable Low Speed	0.610	4.57	33.51	56.00	-0.0421$^{\Delta}$	B: -.039 to -.009	A		
	1.219	9.14	35.13	41.72		C: -.009 to -.001	inversion	B: -.188 to -.046	B
	4.063	30.47	38.55	36.66		D: -.001 to +.002		C: -.046 to -.008	inversion
	8.129	60.97	37.81	36.68	-0.0894$^{\Delta\Delta}$			D: -.008 to +.014	
	60.960	457.20	48.57	45.92					
Unstable High Speed	0.610	4.57	38.96	54.00	-0.0218$^{\Delta}$	B: -.039 to -.009	B		
	1.219	9.14	43.15	42.92		C: -.009 to -.001	inversion	B: -.188 to -.046	B
	4.063	30.47	52.21	37.41		D: -.001 to +.002		C: -.046 to -.008	inversion
	8.129	60.97	56.05	35.40	-0.0605$^{\Delta\Delta}$			D: -.008 to +.014	
	60.960	457.20	95.03	47.90					
Stable Low Speed	0.610	4.57	14.89	2.30	0.0512$^{\Delta}$	D: -.001 to +.002	G		
	1.219	9.14	15.96	5.30		E: +.002 to +.012		D: -.008 to +.014	G
	4.063	30.47	18.83	13.10		F: +.012 to +.047		E: +.014 to +.059	
	8.129	60.97	20.08	20.83	1.1043$^{\Delta\Delta}$	G: +.047 AND ABOVE		F: +.059 to +.129	
	60.960	457.20	74.47	40.67				G: +.129 AND ABOVE	
Stable High Speed	0.610	4.57	13.81	7.10	0.0454$^{\Delta}$	D: -.001 to +.002	F		
	1.219	9.14	22.70	12.58		E: +.002 to +.012		D: -.008 to +.014	F
	4.063	30.47	49.71	23.69		F: +.012 to +.047		E: +.014 to +.059	
	8.129	60.97	61.89	28.92	0.1192$^{\Delta\Delta}$			F: +.059 to +.129	
	60.960	457.20	138.07	45.57					

Δ 5-10 m interval
$\Delta\Delta$ 10-61 m interval

** For assumed heights of H = 10 m and B = 5 m, Z_o = 50 cm
*** For assumed heights of H = 61 m and B = 10 m, Z_o = 50 cm

FIGURES

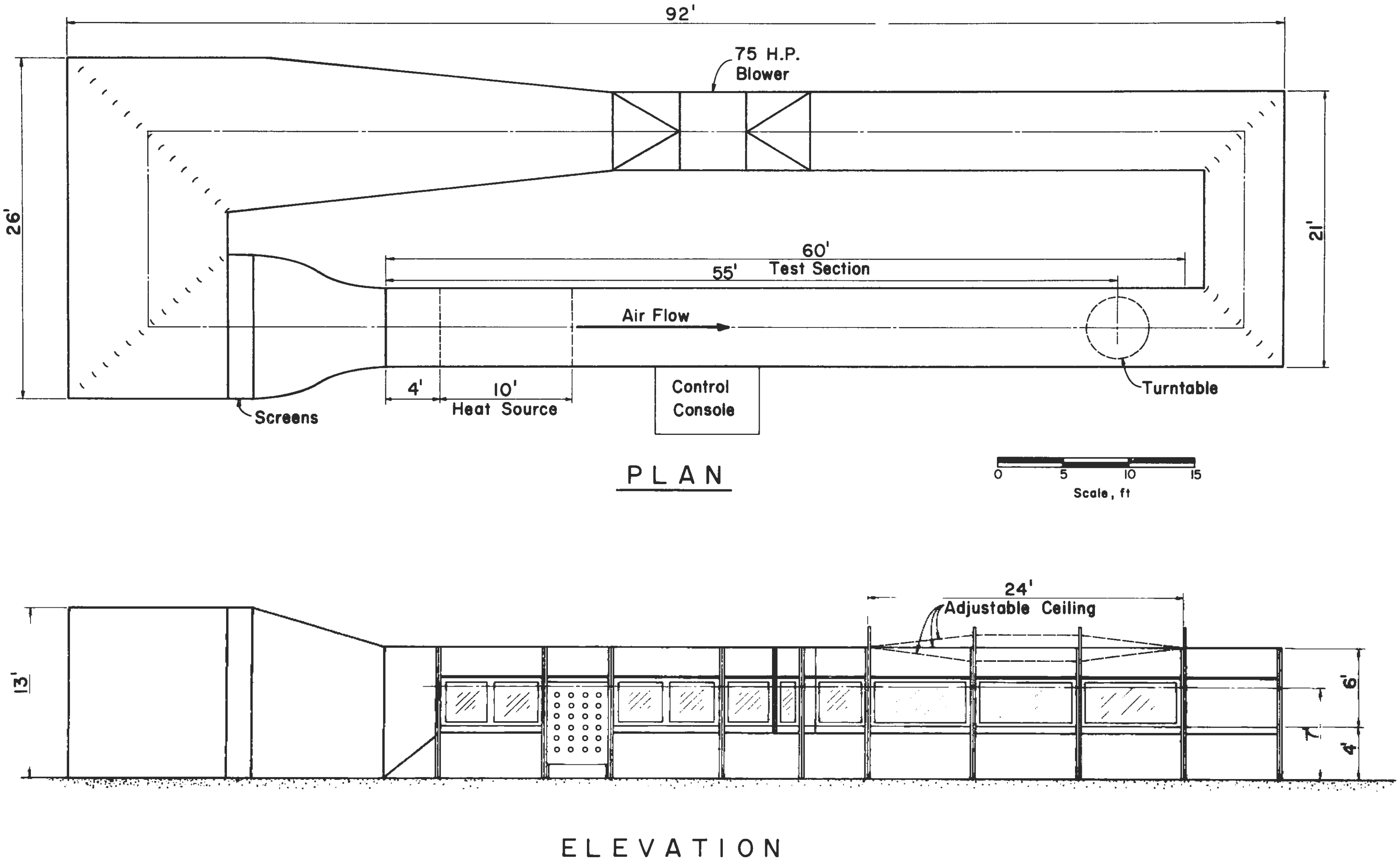

Figure 1. INDUSTRIAL AERODYNAMICS WIND TUNNEL
FLUID DYNAMICS & DIFFUSION LABORATORY
COLORADO STATE UNIVERSITY

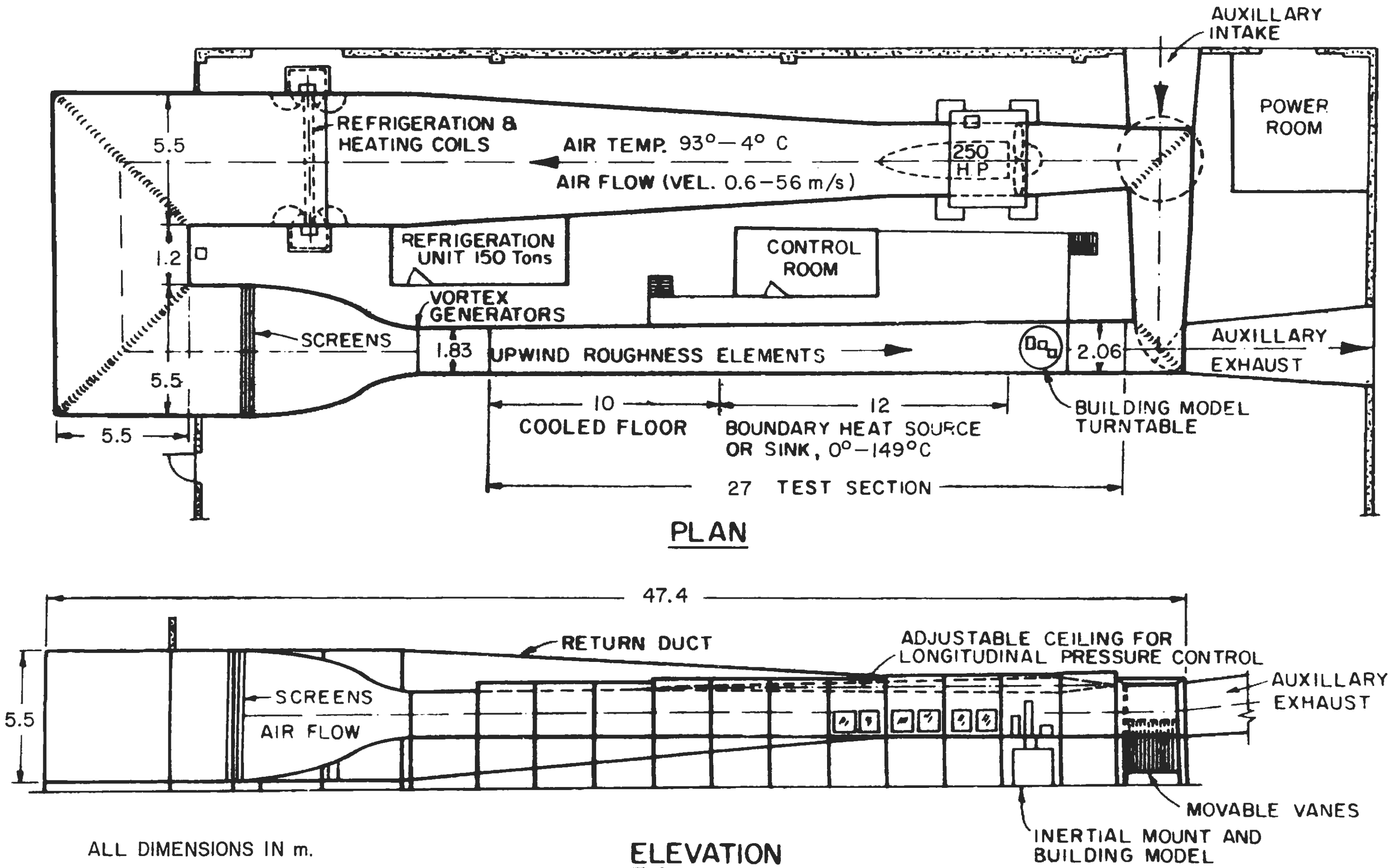

Figure 2. METEOROLOGICAL WIND TUNNEL (Completed in 1963)
FLUID DYNAMICS & DIFFUSION LABORATORY
COLORADO STATE UNIVERSITY

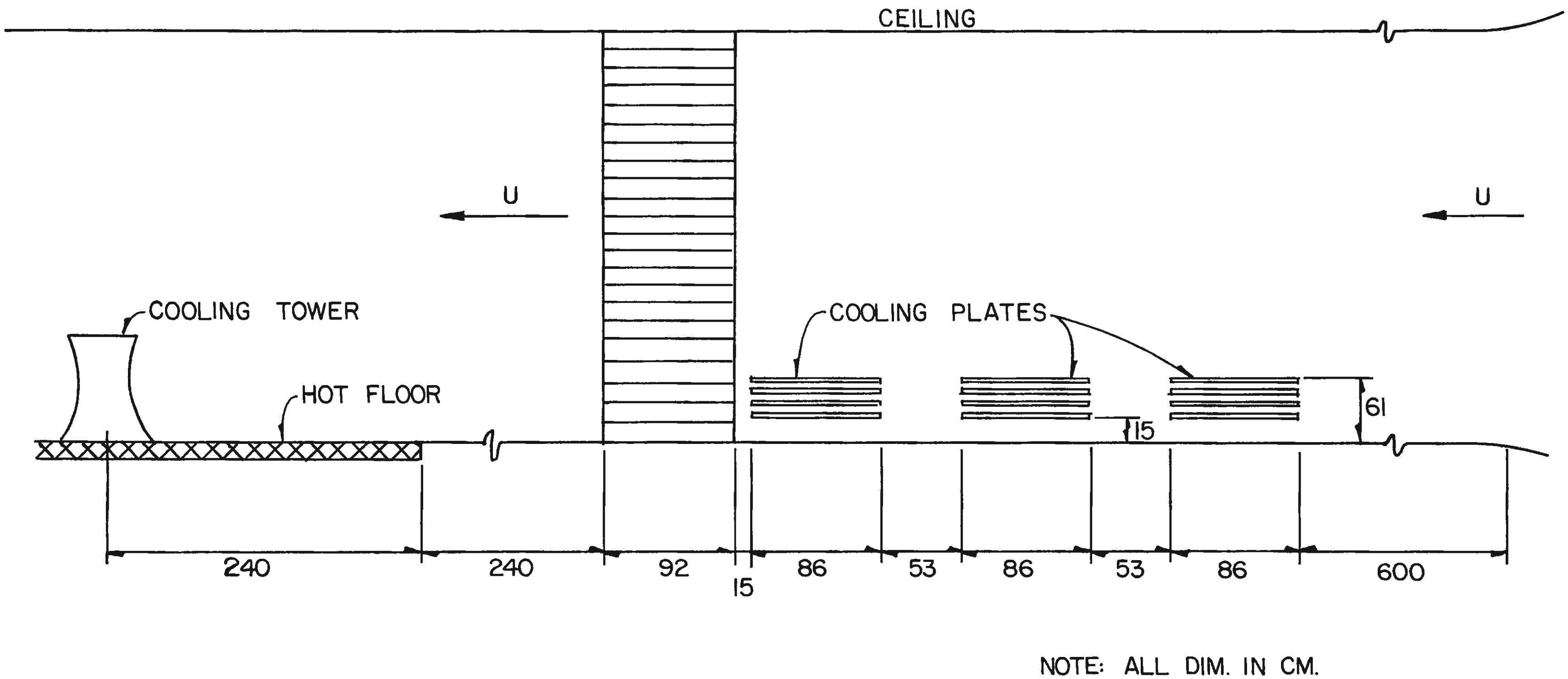

Figure 3. Unstable Flow Cooling Plate Configurations

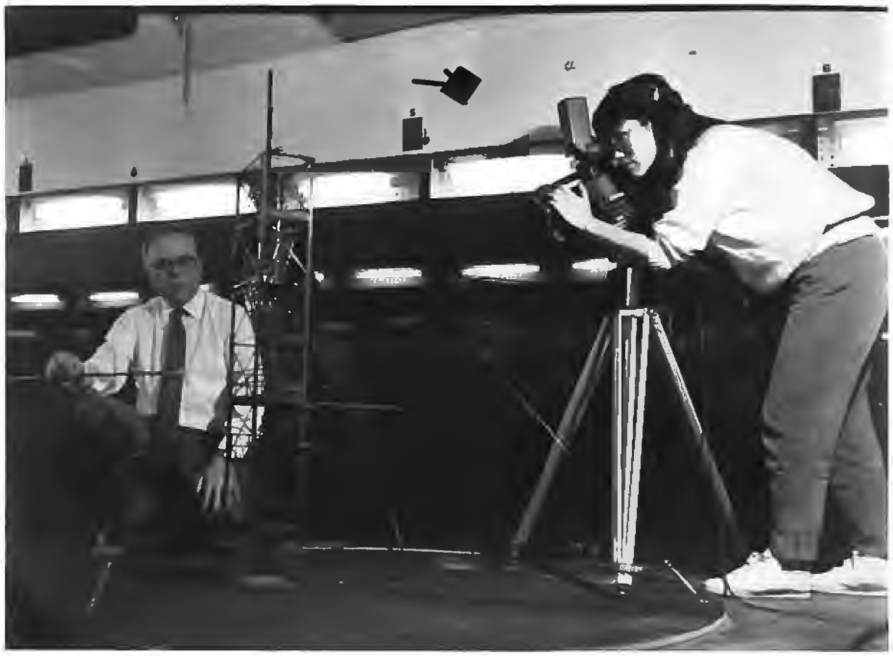

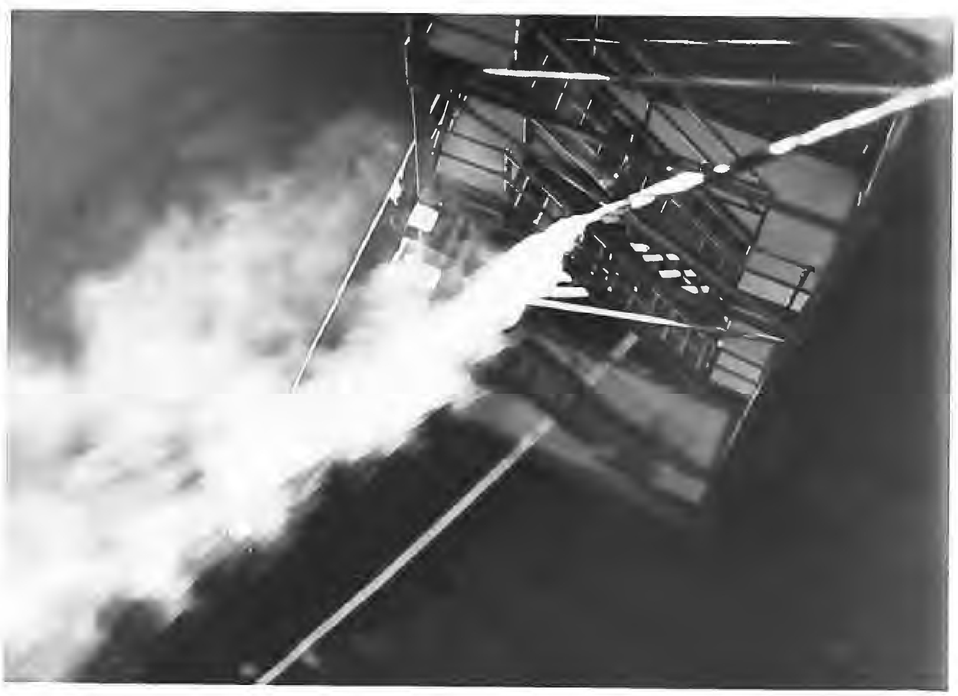

Figure 4a. Pictures of 1:16 Scale Primary Meteorological Tower Model

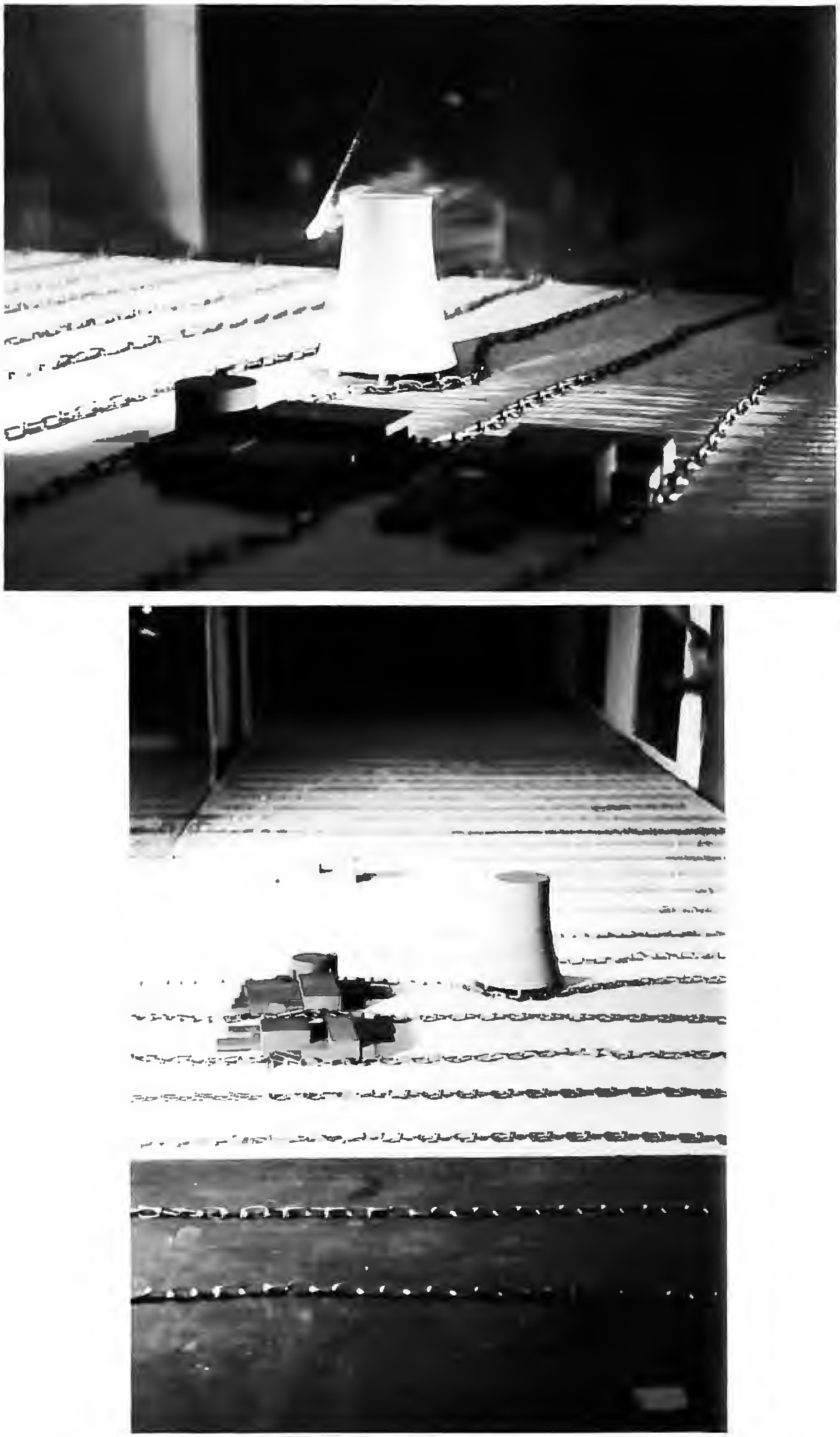

Figure 4b. Pictures of 1:750 Scale Site Model

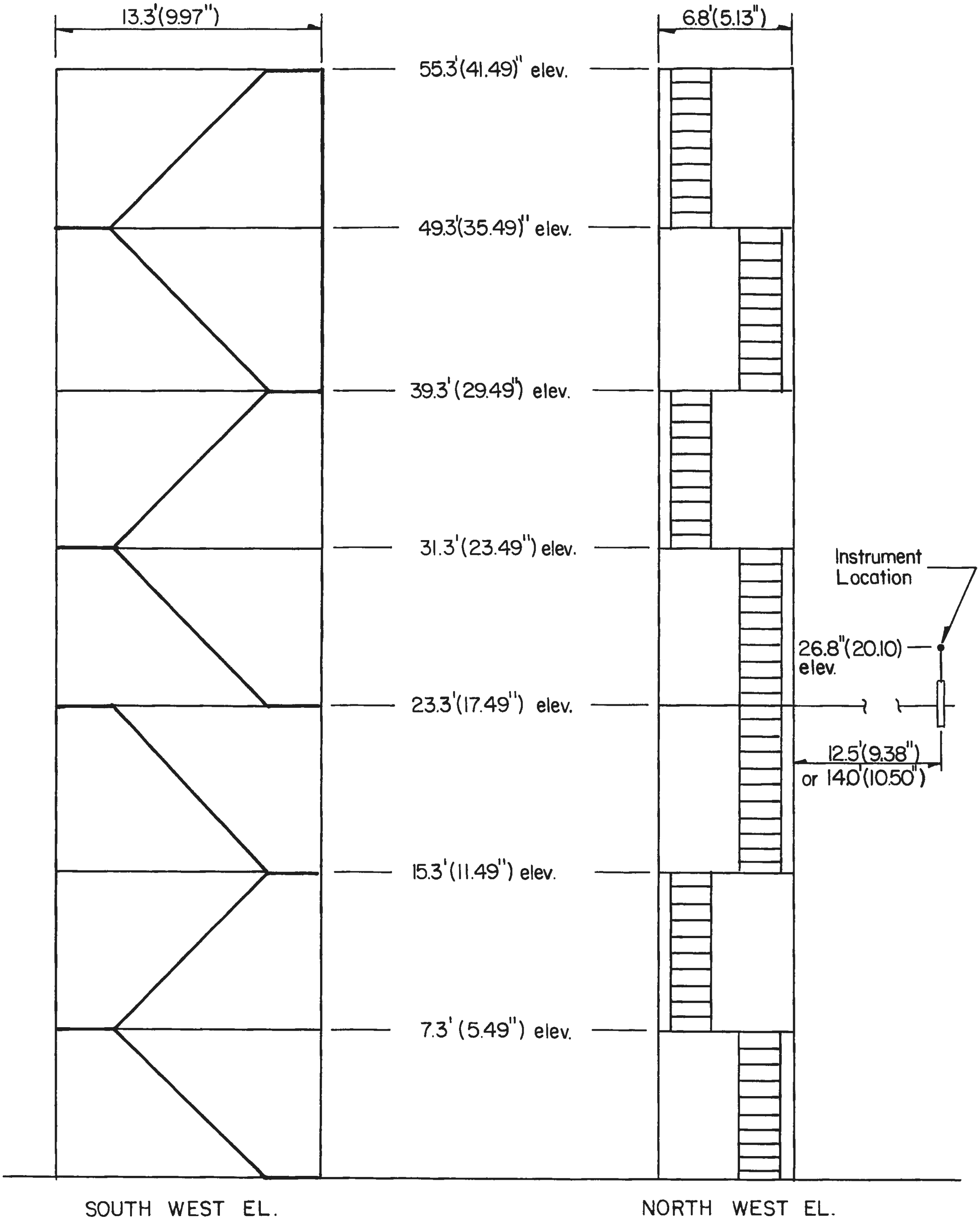

Figure 5a. Primary Meteorological Tower Model, Dimension Drawings

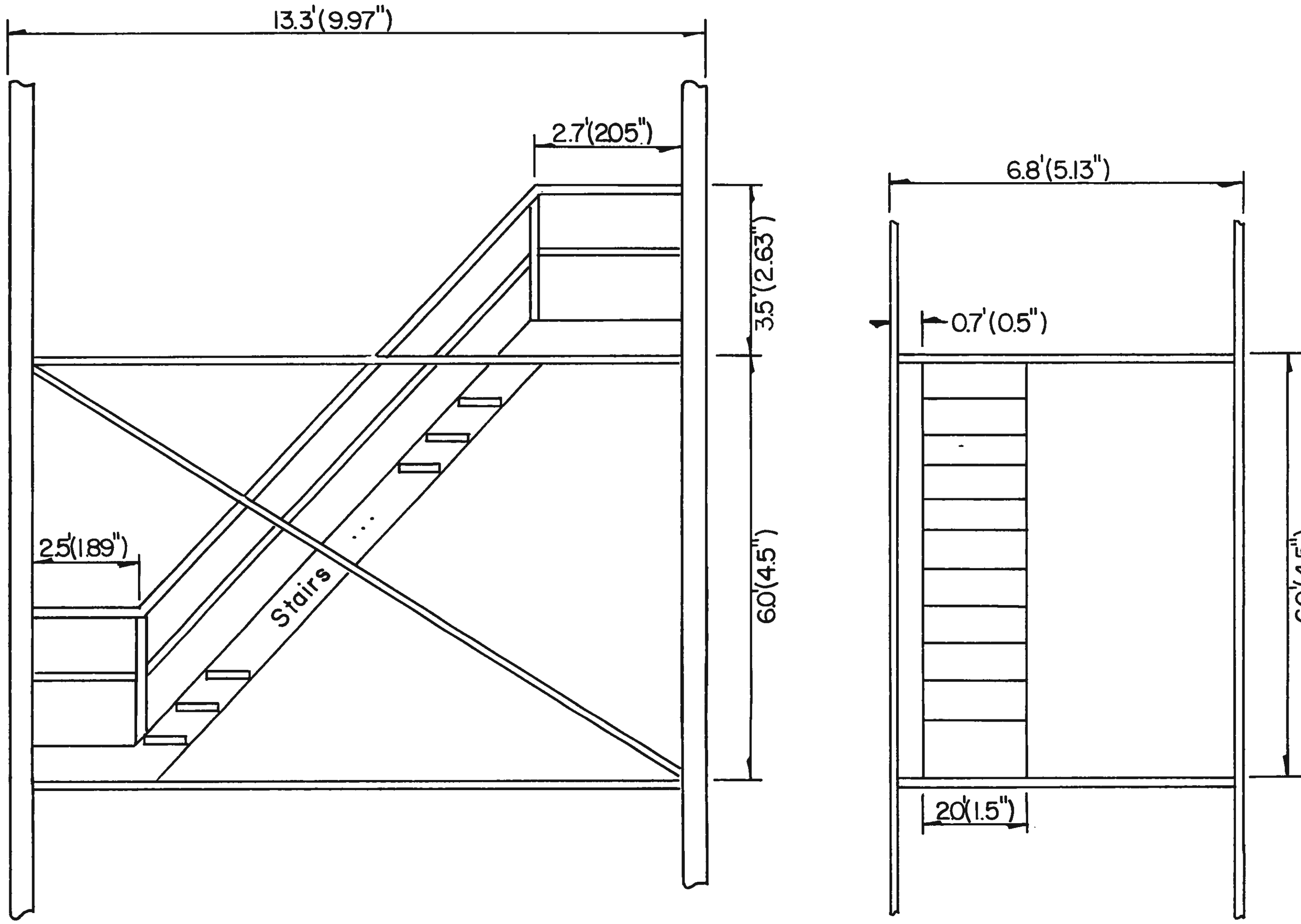

Figure 5b. Primary Meteorological Tower Model, Dimension Drawings

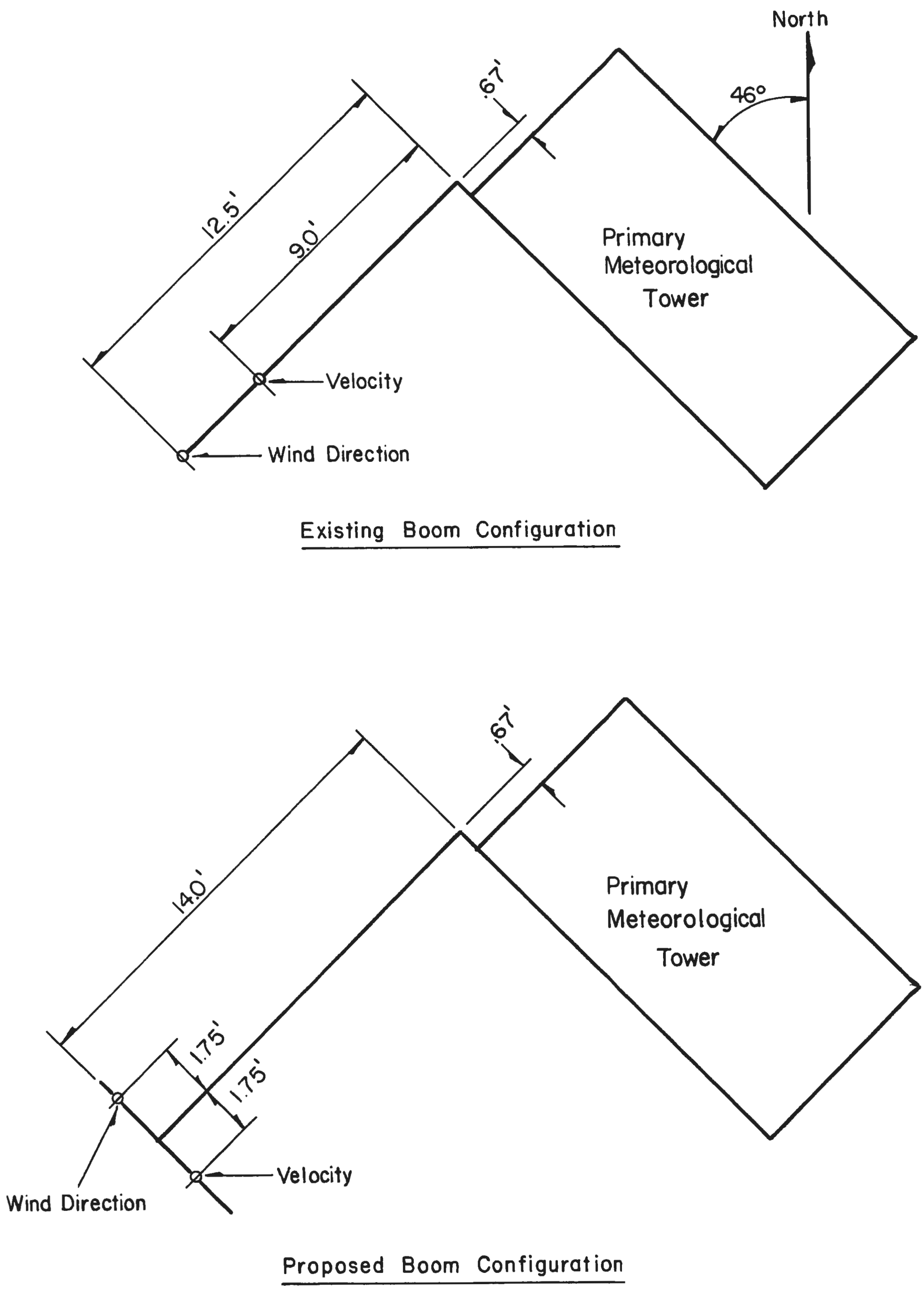

Figure 6. Existing and Proposed Instrument Boom Locations

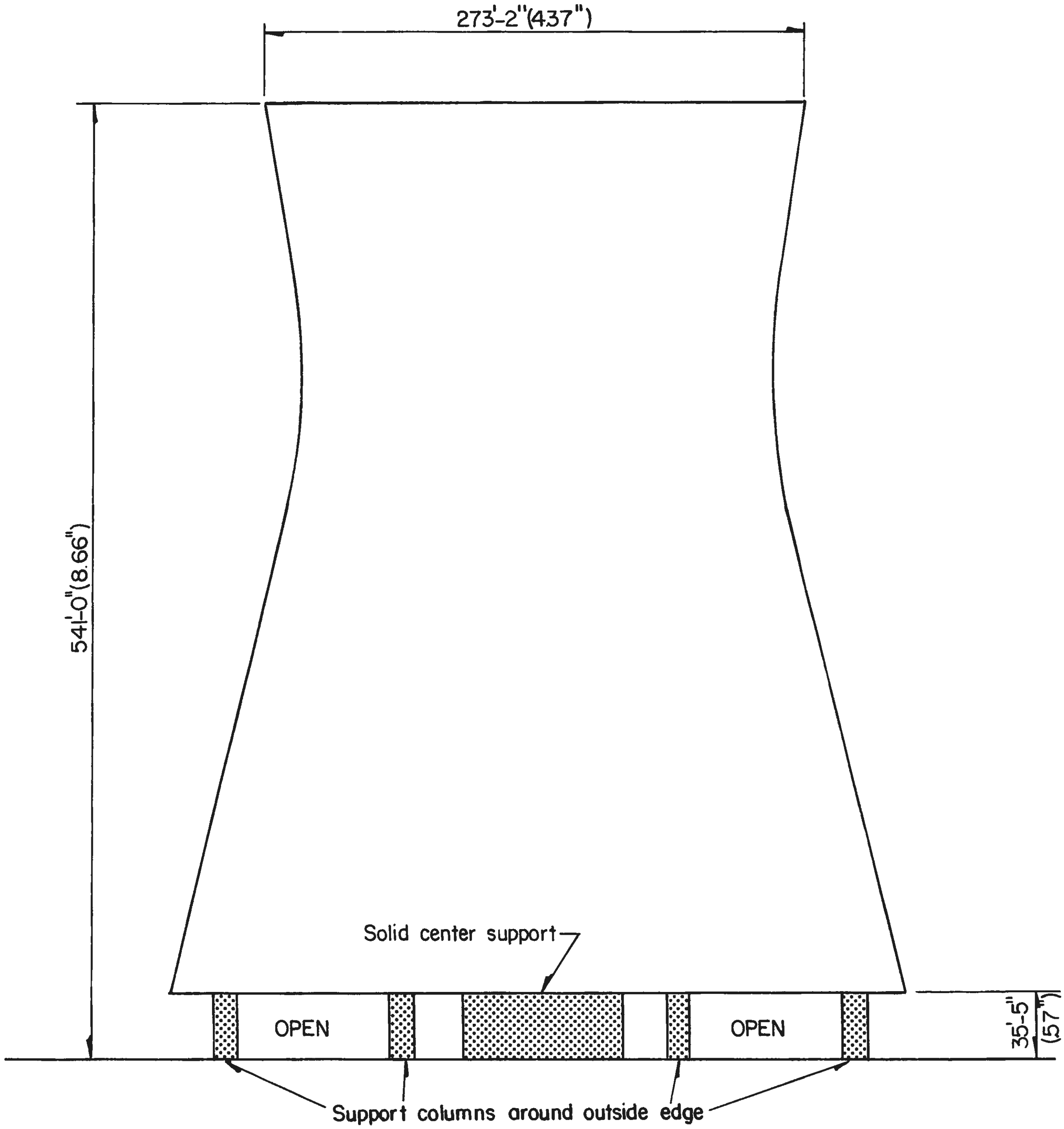

Figure 7. Cooling Tower Dimensions

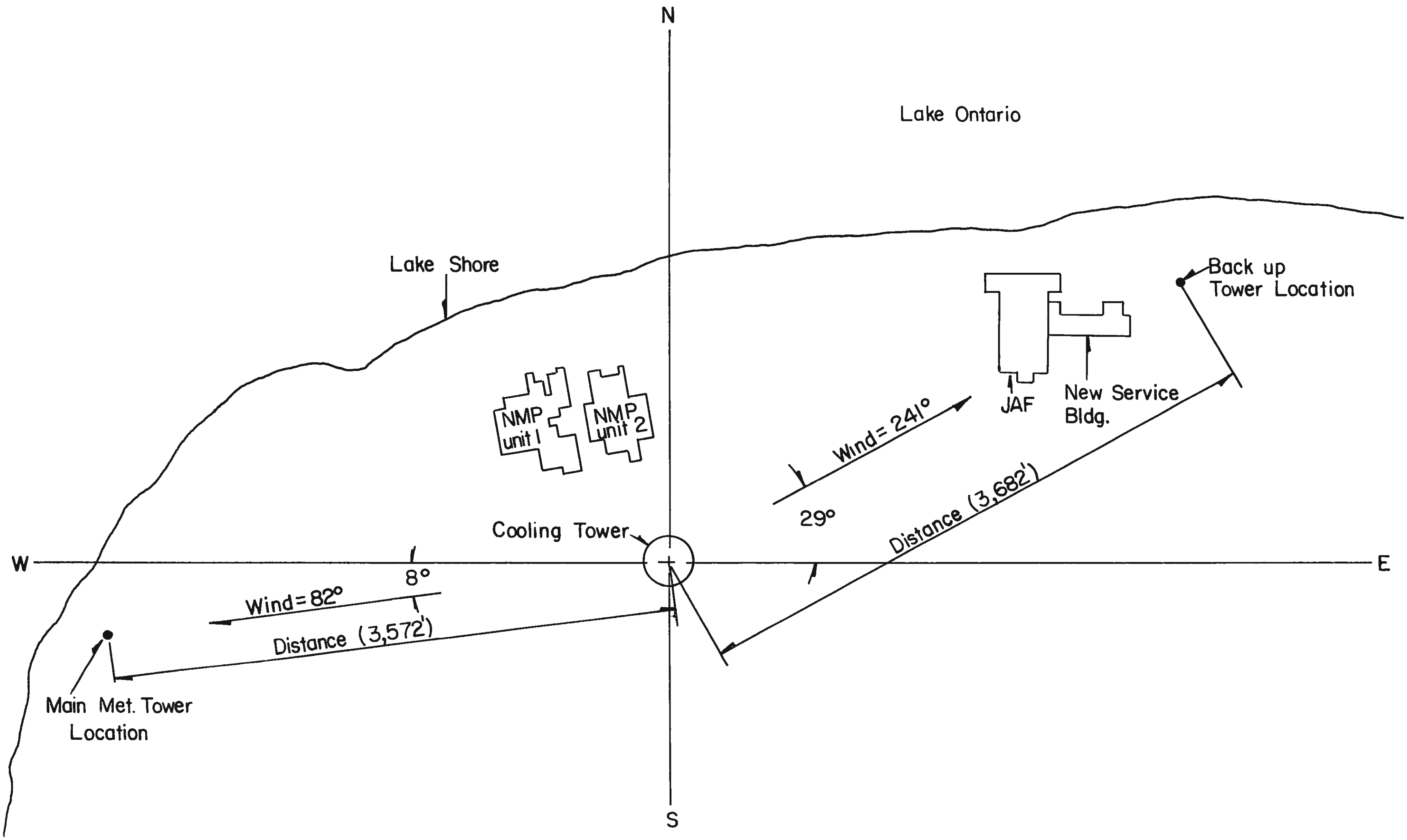

Figure 8. Site Map and Structure Locations

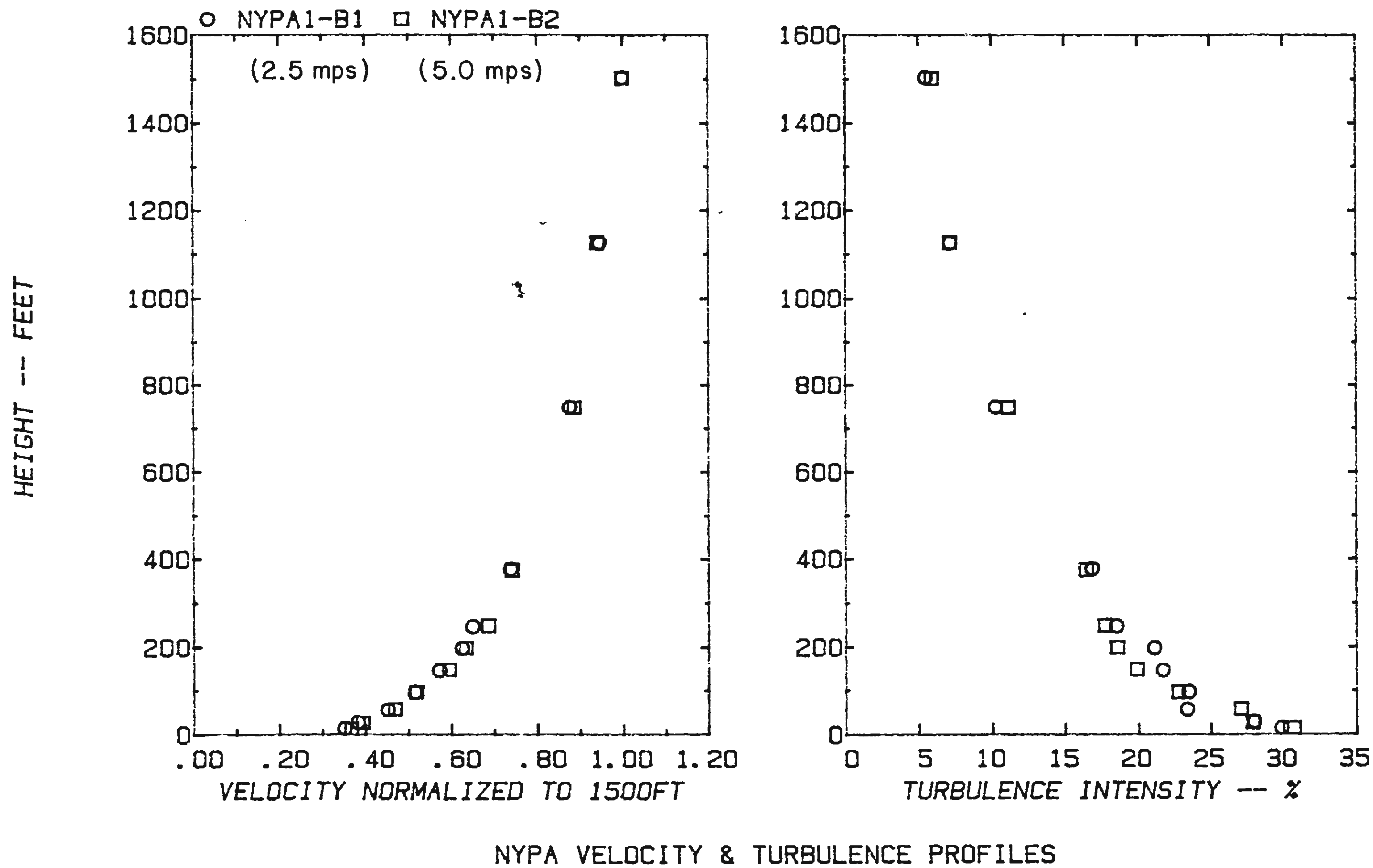

Figure 9. Velocity Independence for Neutral Flow

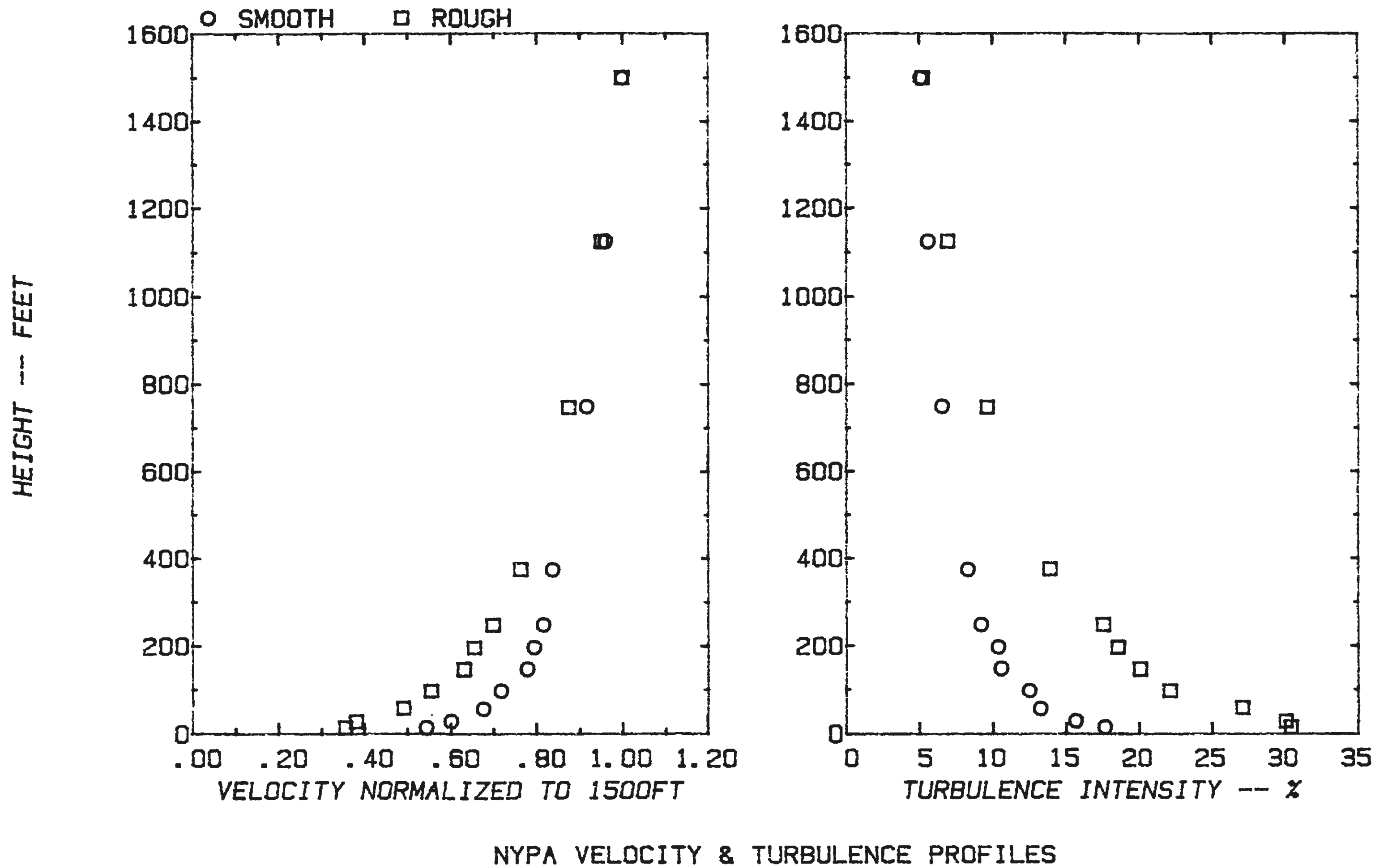

Figure 10. Land and Lake Approach Profiles for Neutral Conditions

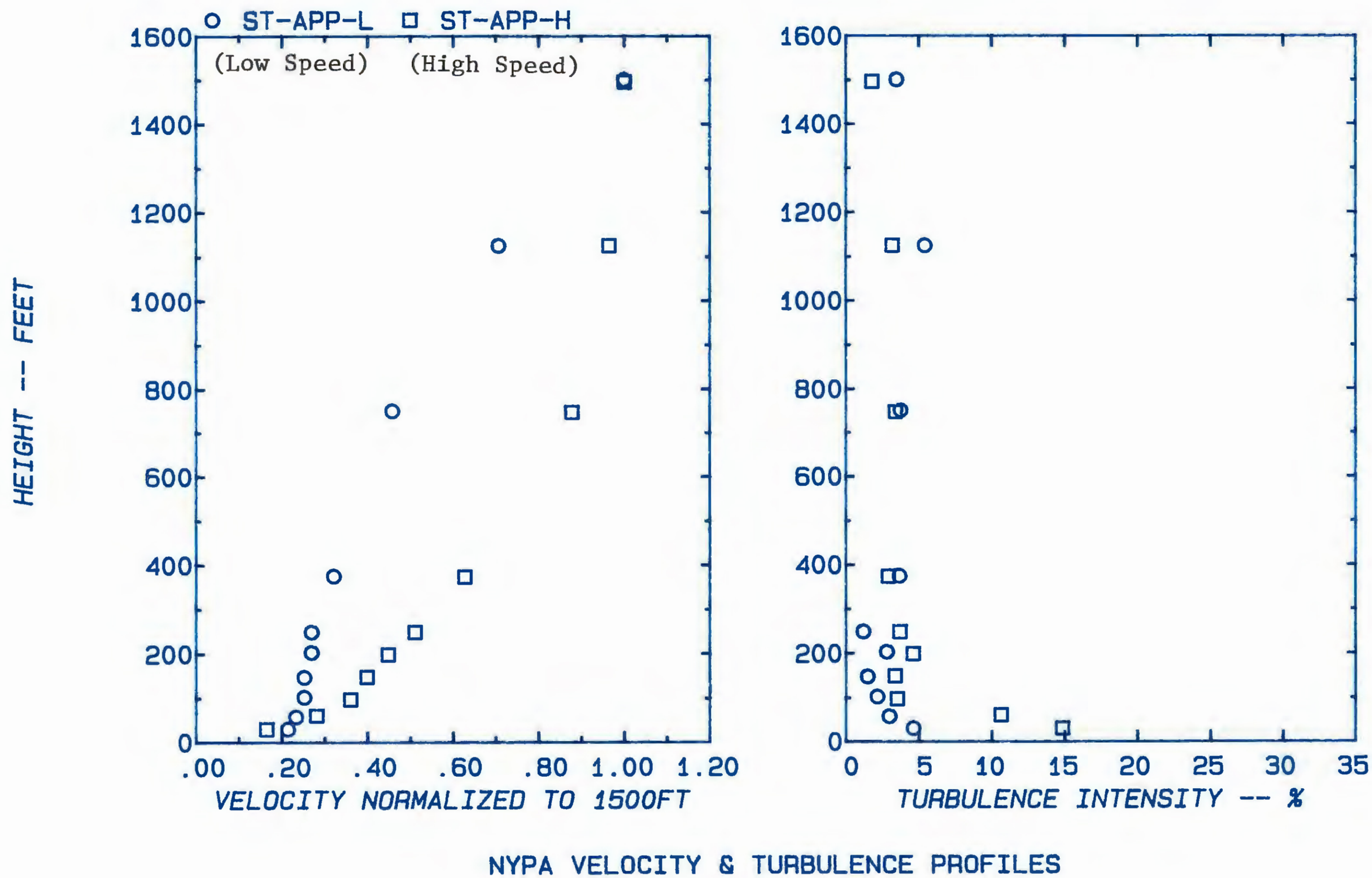

Figure 11. Stable Approach Flow Conditions

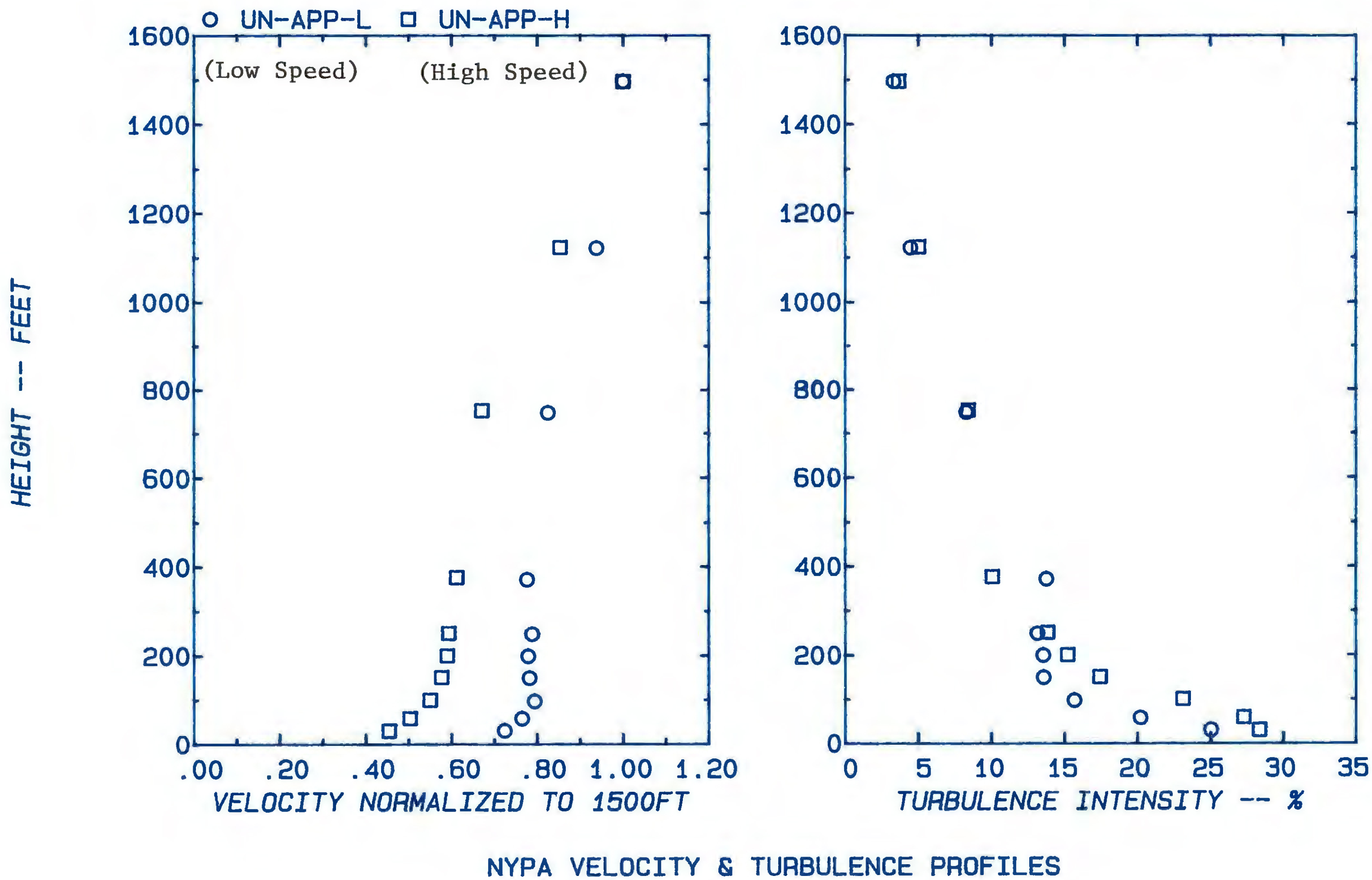

Figure 12. Unstable Approach Flow Conditions

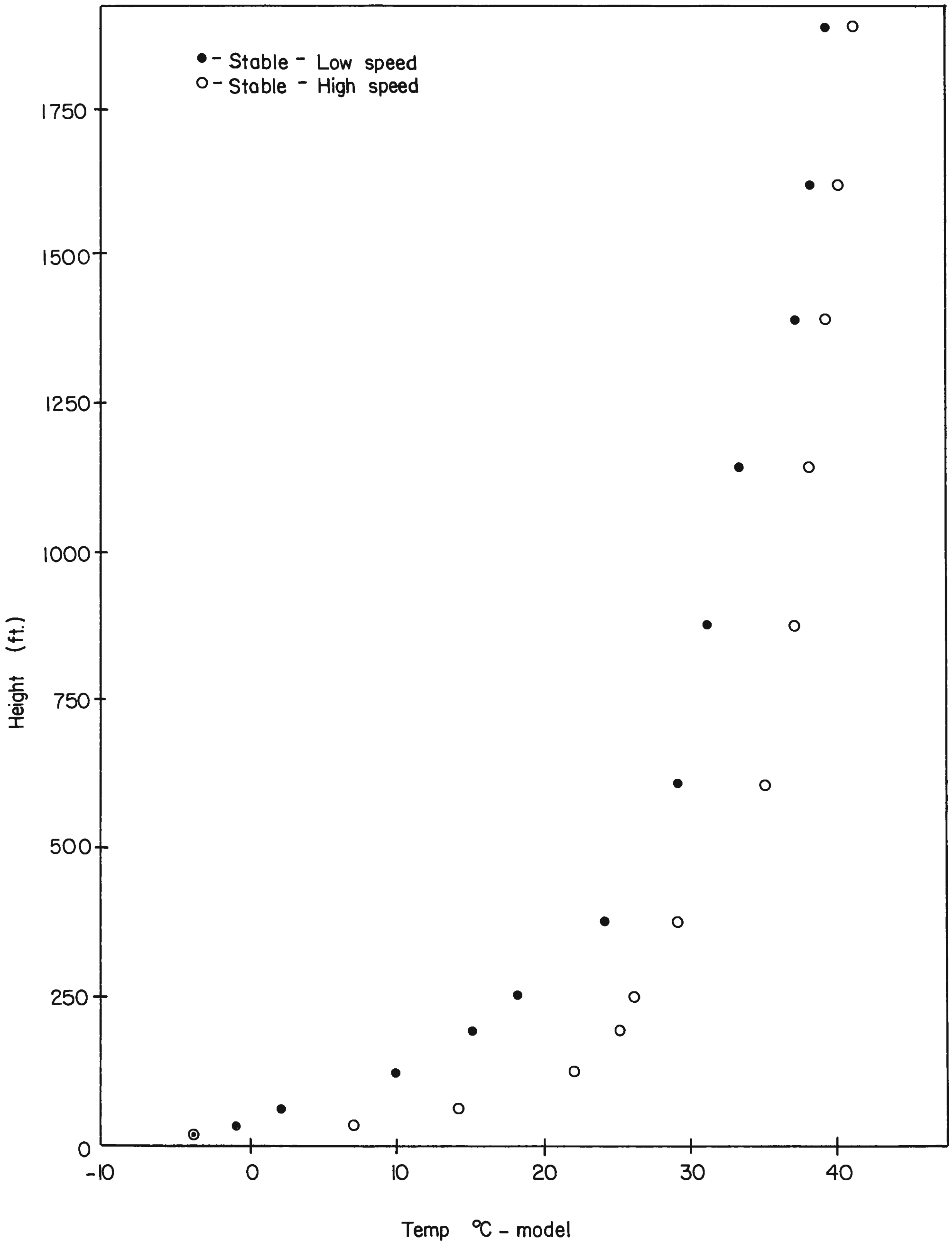

Figure 13a. Stable Approach Flow Temperature Profiles

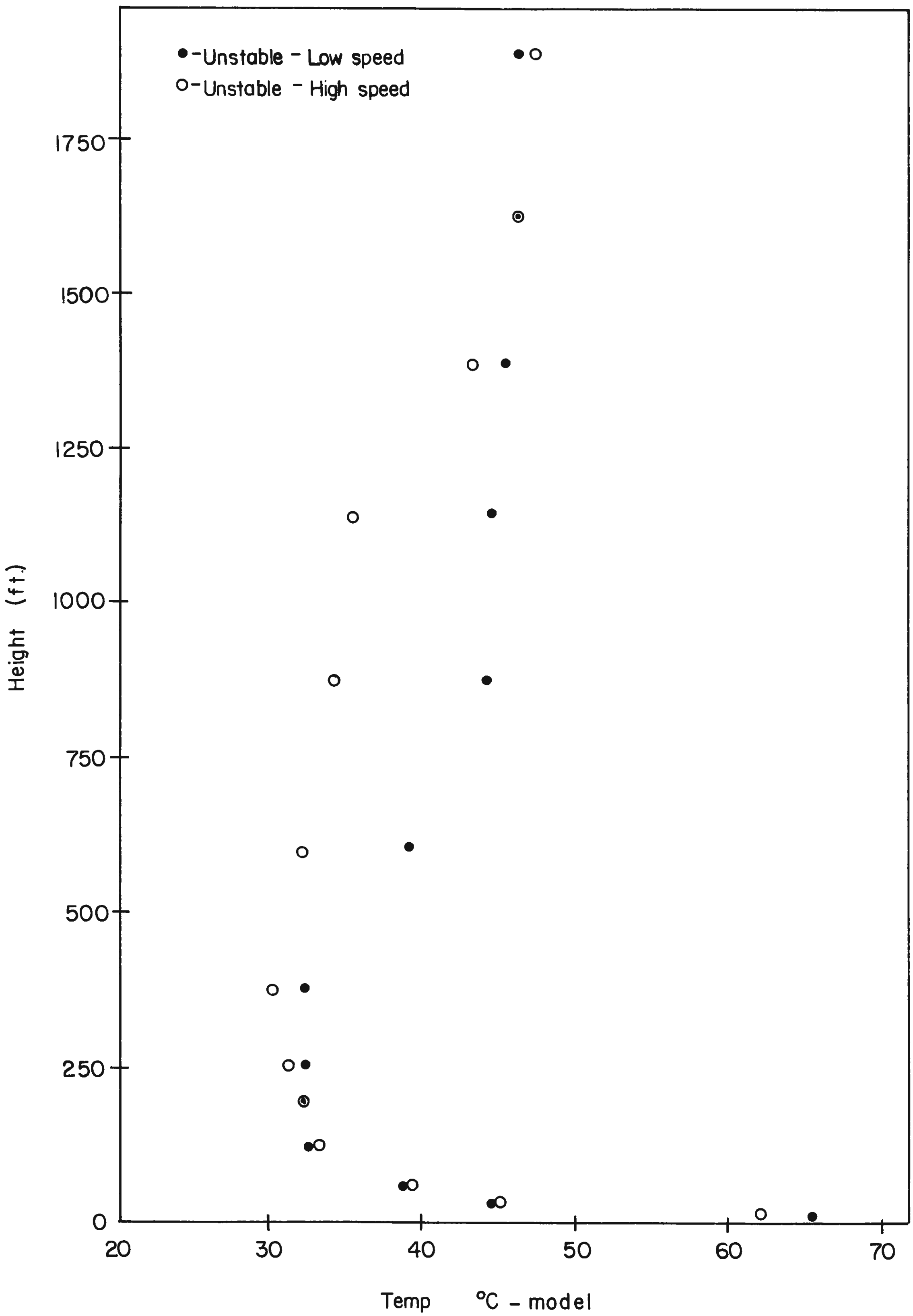

Figure 13b. Unstable Approach Flow Temperature Profiles

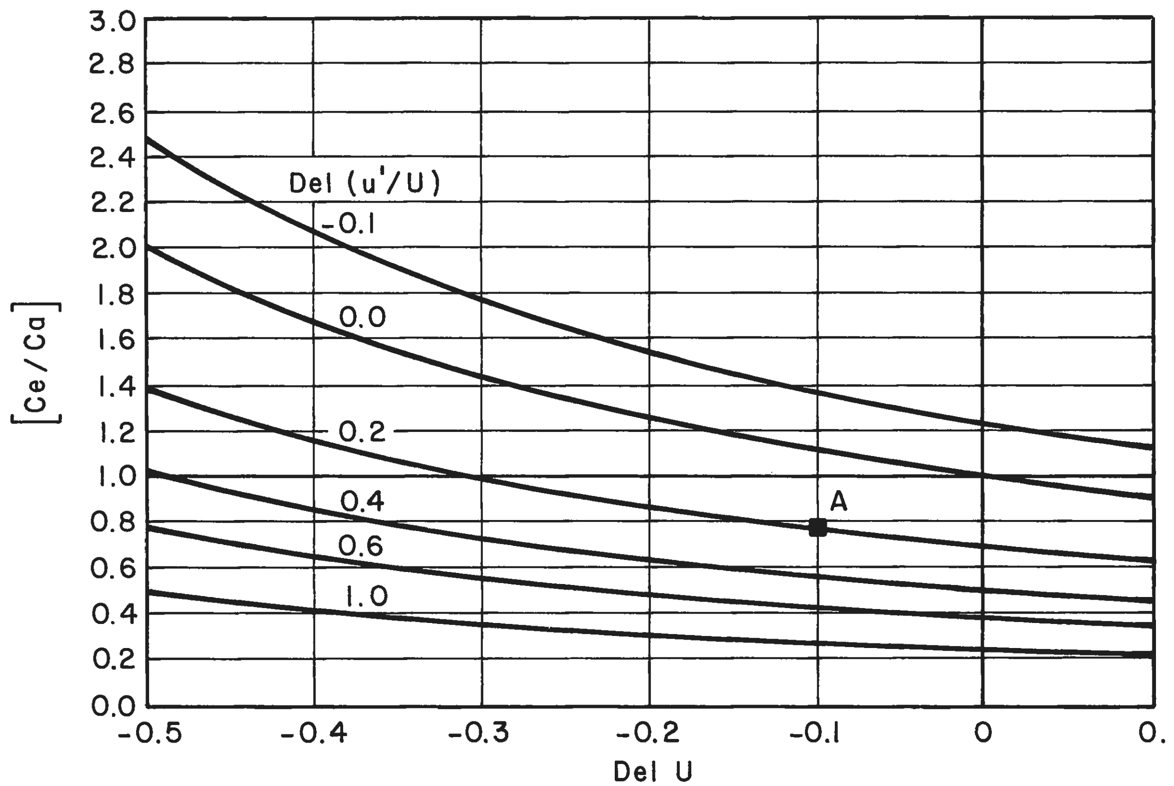

Point A: Represents Changes Caused by Cooling Tower for Task I, Unstable - High Speed Conditions, at 200 ft Elevation

$(\bar{u})_c = -0.098$, $(TI)_c = +0.213$ (From Table C3)

$\therefore$ Ce / Ca $\approx$ 0.78

Figure 14. Error Propagation Curves

APPENDIX A

Fluid Modeling Criteria

TABLE OF CONTENTS

LIST OF SYMBOLS

Symbol	Definition
U, u	Mean velocity
L	Length
ν	Kinematic viscosity
g	Gravitational acceleration
ΔT	Temperature difference across some reference layer
T	Temperature
Ω	Angular velocity of earth -0.726×10^{-4} (radians/sec)
λ	Thermal conductivity
ρ	Density
C_p	Specific heat capacity at constant pressure
u_*	Friction velocity
z_o	Surface roughness parameter
Γ_d	Dry adiabatic potential temperature lapse rate
Γ	Actual adiabatic potential temperature lapse rate
z	General vertical coordinate
k	Thermal conductivity
L_{mo}	Monin-Obukhov length
C_f	Friction coefficient
DU_{mx}	Maximum mean velocity deficit created by the obstacle
h	Height of the obstacle
s	Distance downstream of the obstacle
A	Constant dependent upon the obstacle shape, orientation, boundary layer thickness, etc.
R	Characteristic obstacle radius of curvature

Subscripts

r	Reference conditions
m	Model
p	Prototype

Superscripts

$(\ )'$	Fluctuating part of a quantity
$(\dot{\ })$	Quantity per unit time

Dimensionless Parameters

Re	Reynolds number
Ri	Bulk Richardson number
Ro	Rossby number
Pr	Prandtl number
Ec	Eckert number
Ma	Mach number
B	Bowen ratio

A.0 INTRODUCTION

To obtain a predictive model for a specific plume dispersion problem, one must quantify the pertinent physical variables and parameters into a logical expression that determines their interrelationships. This task is achieved implicitly for processes occurring in the atmospheric boundary layer by the formulation of the equations of conservation of mass, momentum and energy. These equations with site and source conditions and associated constituitive relations are highly descriptive of the actual physical interrelationship of the various independent variables (release size or release rate, space and time) and dependent variables (velocity, temperature, pressure, density, etc.).

These generalized conservation statements subjected to the typical boundary conditions of atmospheric flow are too complex to be solved by present analytical or numerical techniques. It is also unlikely that one could create a physical model for which exact similarity exists for all the dependent variables over all the scales of motion present in the atmosphere. Thus, one must resort to various degrees of approximation to obtain a predictive model. At present, purely analytical or numerical solutions of boundary layer, wake, and plume dispersion are unavailable because of the classical problem of turbulent closure (Hinze, 1975). Boundary layer wind tunnels are capable of physically modeling fluid processes in the atmosphere under certain restrictions. These restrictions are discussed in the next few sections.

A.1 Fluid Modeling of the Atmospheric Boundary Layer

Successful modeling of some of the more complex atmospheric surface layer phenomena in a wind tunnel has only been accomplished in the last fifteen years. Although guidelines for modeling flow over complex terrain are essentially similar to those for modeling hydraulic flows or flow around buildings, a few unique features are different. Irregular terrain may alter atmospheric airflow characteristics in a number of different ways. These effects can generally be grouped into those due to inertial-viscous interactions associated with a thick neutrally stratified shear layer and to thermally induced interactions associated with stratification or surface heating (Meroney, 1980).

Performance of Prior Fluid Modeling Experiments:

Meroney et al. (1978) summarized experimental data available from field and laboratory studies for neutral airflow over hills, ridges, and escarpments. Wind-tunnel model measurements were performed to study the influence of topography profile, surface roughness and stratification on the suitability of various combinations of these variables. Detailed tables of velocity, turbulence intensity, pressure, spectra, etc., were prepared to guide numerical model design and experimental rule of thumb restrictions. Cases included hill slopes from 1:2 to 1:20, neutral and stratified flows, two- and three-dimensional symmetric ridges, six alternate hill and escarpment shapes, and a variety of windward versus leeward slope combinations to evaluate ridge separation characteristics. The laboratory data were validated by comparison with field measurements for flow in the Rakaia Gorge, New Zealand, and over Kahuku Point, Oahu, Hawaii, (Meroney et al., 1978; Chien, Meroney and Sandborn, 1979).

The Rakaia Gorge field study documented 10-minute wind speed and direction information at 27 sites during stationary conditions on two spring days selected for strong adiabatic down-valley wind flow. The

Kahuku Point field study documented 24-hour average wind speed, turbulence, and direction at 32 sites during strong fall trade wind conditions. In the Rakaia Gorge and the Kahuku Point cases, measurements were compared point to point, scatter diagrams constructed, and sample correlation coefficients calculated. If simulation is good, there must be a high linear causal relationship between measurements in the field and laboratory. The best estimation of the population correlation is the sample correlation coefficients. Wind speed and directions were found to correlate with field data at levels from 0.7 to 0.80. Rank correlation of the respective wind sites exceeded 0.95. Holmes et al. (1979) reported a comparison of field and laboratory measurements of maximum gust velocities over Castle Hill (286 m) near Townsville, Australia. Linear correlation coefficients ranged from 0.68 to 0.78. Recently, Neal (1983) examined field and model results for the Gebbies Pass area of Bank's Penninsula, New Zealand, and he obtained sample and rank correlations exceeding 0.75 and 0.95, respectively.

Local heating and cooling of coastline or hill surfaces are the driving mechanisms for sea-land breezes, and anabatic and katabatic winds which may inhibit or enhance airflow over the land surface. Early laboratory work includes simulations of urban heat islands by Yamada and Meroney (1971) and Sethuraman and Cermak (1974), simulation of flow and dispersion at shoreline sites by Meroney et al. (1975a), and simulation of dispersion effects of heat rejected from large industrial complexes by Meroney et al. (1975b).

Meroney et al. (1975a) pioneered the use of the wind tunnel as a prediction tool for shoreline air pollution fumigation. They simulated the behavior of plumes emitted from a shoreline fossil fuel power plant near Lake Erie, Ohio. By alternately cooling and heating the test section floor, the shoreline turbulent internal boundary layer (TIBL) was reproduced. The growth rate of the TIBL agreed with empirical formulae developed from field data taken at lake and coastal shoreline sites.

Recently Briatore, Elisei and Longhetto (1980) reported a comparison between local air circulations found over a complex coastal site and a hydraulic stratified laboratory model. The La Spezia gulf area analyzed in Italy included shoreline hill barriers and a region 11 km in diameter at a scale of 1:8000. Sea breezes flows were produced by salt solutions injected at the flume bottom. The hydraulic model reproduced complicated secondary circulations seen over the bay, identified correctly regions of maximum velocity, and the progression of the sea breeze under stationary and transient inversion conditions. Briatore et al. conclude that the physical modeling technique could reliably be used in planning studies for complex sites, "thus avoiding more expensive and time consuming field observations or making these last more simple and reduced."

Meroney (1980) compared three model/field investigatios of flow over complex terrain, suggested performance envelopes for realizable modeling in complex terrain, and discussed recent laboratory studies which provide data for valley drainage flow situations. Not all of the model/field comparison experiments performed in the past were successful. Many early studies had model approach flow velocity exponents near zero, were modeled as neutral flows when the field observed strong stratification effects, or simulated unrealistic boundary layer depths, integral scales, or turbulence intensities which did not match their atmospheric counterpart. But few studies claimed unreasonable correlation, and some were strongly self-critical. Nonetheless, most studies accomplished their prestated limited objectives. It would appear that the simulation wisdom developed in the last few years is appropriate for physical modeling of flow over complex terrain when appropriate care is taken to simulate the approach flow conditions and to maintain simulation parameters equal between model and prototype.

Simulation Criteria:

The atmospheric boundary layer is that portion of the atmosphere extending from ground level to a height of approximately 1000 meters within which the major exchanges of mass, momentum, and heat occur. This region of the atmosphere is described mathematically by statements of conservation of mass, momentum and energy (Cermak, 1975). The mathematical requirements for rigid laboratory-atmospheric-flow similarity may be obtained by fractional analysis of these governing equations (Kline, 1965). This methodology is accomplished by scaling the pertinent dependent and independent variables and then casting the equations into dimensionless form by dividing by one of the coefficients (the inertial terms in this case). Performing these operations on such dimensional equations yields dimensionless parameters commonly known as:

Reynolds number	$Re = (UL/\nu)_r$	$= \dfrac{\text{Inertial Force}}{\text{Viscous Force}}$
Bulk Richardson number	$Ri = (Lg(\Delta T/T)/U^2]_r$	$= \dfrac{\text{Gravitational Force}}{\text{Inertial Force}}$
Rossby number	$Ro = (U/L\Omega)_r$	$= \dfrac{\text{Inertial Force}}{\text{Coriolis Force}}$
Prandtl number	$Pr = [\nu/\lambda/\rho C_p)]_r$	$= \dfrac{\text{Viscous Diffusivity}}{\text{Thermal Diffusivity}}$

Eckert number $\quad Ec = [U^2/C_p(\Delta T)]_r$

For exact similarity between different flows which are described by the same set of equations, each of these dimensionless parameters must be equal for both flow systems. In addition to this requirement, there must be similarity between the surface-boundary conditions and the approach flow wind field.

Surface-boundary condition similarity requires equivalence of the following features:

a. Surface-roughness distributions,

b. Topographic relief, and

c. Surface-temperature distribution.

If all the foregoing requirements are met simultaneously, all atmospheric scales of motion ranging from micro to mesoscale could be simulated within the same flow field. However, all of the requirements cannot be satisfied simultaneously by existing laboratory facilities; thus, a partial or approximate simulation must be used. This limitation requires that atmospheric simulation of the wind flow over the reaction site area must be designed to simulate most accurately those scales of motion which are of greatest significance for mean velocity, turbulence, and thermal profiles over complex terrain.

Partial Simulation of the Atmospheric Boundary Layer

For the case of the interactions between buildings and structures near a lakeshore and the atmospheric boundary layer, several of the aforementioned parameters are unnecessarily restrictive and may be relaxed without causing a significant effect on the resultant concentration field. The Rossby number magnitude, Ro, controls the extent to which the mean wind direction changes with height. The effect of Coriolis-force-driven lateral wind shear on wind flow is only significant when the tower and building height are of the same order of magnitude as the boundary layer height. The Eckert number (in air $Ec = 0.4\ Ma^2\ (T_r/\Delta T_r)$, where Ma is the Mach number) is the ratio of energy dissipation to the convection of energy. In both the atmosphere and the laboratory flow, the wind velocities and temperature differences are such that the Eckert number is very small; hence, it is neglected. Prandtl number equality guarantees equivalent rates of momentum and heat transport. Since air is the working fluid in both the atmosphere and the laboratory, Prandtl number equality is always maintained.

The approach flow Richardson number (Ri) and Reynolds number (Re) determine the kinematic and dynamic structure of turbulent flow within a boundary layer. This influence is apparent in the variations that occur in the spectral distribution of turbulent kinetic energies with changing Ri and changing Re.

The Reynolds Number:

Re equality implies $u_m = (L_p/L_m)u_p$. Re equality at a significantly reduced length scale would cause the model's flow velocity to be above sonic; hence, its equality must be distorted. A reduced Re changes only the higher frequency portion of an Eulerian-type description of the spectral energy distribution. Unfortunately, there is no precise definition as to which portion of an Eulerian Spectrum is dominant in flow around structures and over complex terrain.

Most investigators use a minimum Reynolds number requirement based on rough-walled pipe measurements, i.e., $Re = u_* z_o/\nu > 2.5$, where u_*, the friction velocity, and z_o, the roughness length, are derived from a log-linear fit to a measured mean velocity profile. The value 2.5 is an empirically determined constant. At Re below 2.5, it is observed that the mean velocity profiles in turbulent pipe flow lose similarity in shape and deviate from the universal curve of a rough wall turbulent boundary layer. For Re above 2.5, it is observed that the surface drag coefficient (and thus the normalized mean velocity profile) is invariant with respect to increasing Re. For Re between 0.11 and 2.5, the velocity profiles are characteristic of smooth wall turbulent boundary layers, and for values below 0.11, the growth of a laminar sublayer on the wall is observed to increase with decreasing Re.

Extrapolation of results from pipe flow measurement to flat plate boundary layers may cause a shift in the magnitude of the minimum Re requirement, but it is generally felt that this shift is small. Precise similarity in the universal form of mean wind shear may be necessary for invariance with respect to the surface drag coefficient, but this does not necessitate that precise similarity must exist for the invariance of the wind field and dispersion. It is the distribution of turbulent velocities which has the greatest effect on the wind field and dispersion. It is the mean wind shear, however, which generates the turbulent velocities. It is possible that the specification of a minimum Re of 2.5 is overly conservative. The criteria, Re > 2.5, for example, is not applicable for flow over complex terrain or building clusters.

The Richardson Number

Although most wind-tunnel investigations are conducted with neutrally stratified boundary layers, there are circumstances when the stratification of the atmosphere must be considered. In particular, air pollution and dispersion problems are often critical during stratified conditions. Unstable stratification may be expected to mitigate hazards by accelerating plume dilution, whereas stable stratification may permit high concentrations to persist. The stability state of the atmosphere is typically characterized by the Richardson number.

The atmospheric gradient Richardson number can be computed from averaged quantities through the equation

$$\mathrm{Ri} = \frac{g}{T}\,(\Gamma_d - \Gamma)\,\left(1 + \frac{0.07}{B}\right)\,\left[\left(\frac{\partial u}{\partial z}\right)^2 + \left(\frac{\partial v}{\partial z}\right)^2\right] \tag{A-1}$$

where Γ and Γ_d are the actual and dry adiabatic potential temperature lapse rates, and $B = [c_p(T_2-T_1)]/[(z_2-z_1)(q_2-q_1)]$ is the Bowen ratio of sensible to latent heat flux at the surface. The Ri number can be taken to represent the ratio of the relative importance of convective and mechanical turbulence. Negative Ri numbers of large value indicate strong convection and weak mechanical turbulence; zero Ri numbers imply purely mechanical turbulence. Positive Ri numbers less than some critical value, $\mathrm{Ri}_{critical}$, suggest the presence of mechanical turbulence damped by the density-induced buoyancy forces; for larger positive Ri numbers, turbulence essentially disappears, since the stratification overpowers production by wind shear. The critical Richardson number has a value near 0.25.

Other stability parameters which are frequently used are the flux Richardson number, the bulk Richardson number, the Ekman stability parameter, or the Monin-Obukhov similarity length:

The flux Richardson number: $$Ri_f = \frac{g\,\overline{w't'}}{T\,\overline{u'w'}(du/dz)}$$

The bulk Richardson number: $$Ri_b = \frac{gz^2(dT/dz-\Gamma)}{T\,u^2}$$

The Ekman stability parameter: $$f = \frac{ku_*}{f_c L_{mo}}$$

The Monin-Obukhov length: $$L_{mo} = \frac{-T\,u_*^3}{k\,g\,\overline{w't'}}$$

The Richardson Ri, number, is a local parameter rather than a global one since it is based on local flow conditions, but it is inherently related to other parameters such as the Monin-Obukhov stability length. Snyder (1981) calculated typical values for the various stability parameters. Golder (1972) considered the relationships among different stability parameters in the surface layer, and he produced figures to show the relationship between Ri, Ri_b and z/z_o. Ri always approaches zero as z goes to zero at the surface, where mechanical turbulence production due to shear is a maximum.

A few laboratory facilities exist which can control stratification. Wind-tunnel temperatures are generally controlled through upstream heat exchangers, injection of heated air, or the use of a thermal boundary layer permitted to grow over long segments of heated or cooled surfaces (Plate and Cermak, 1963; Teunissen, 1975; Ogawa et al., 1985; Schon and Mery, 1971). Water channels maintain stratification using either heat or, more frequently, layered salt water (Hunt et al., 1978; Snyder et al., 1979).

Arya (1969, 1975) performed velocity, temperature, and turbulence measurements in the lowest 15 percent of a 70 cm deep boundary layer over a smooth surface, where conditions ranged from unstable to moderately stable ($-0.3 < z/L_{mo} < 0.3$). Free stream flow speeds varied from 3 to 9 m/s, and temperature differences were about 40°C across the boundary layer. Cermak, Shrivastava and Poreh (1983) reported mean velocity and turbulence measurements made for a variety of simulated atmospheric boundary layers over different surface roughness. Free stream flow speeds varied from 2.4 to 3.0 m/s and temperature differences were from 150° to -80°C across the boundary layer. Poreh and Cermak (1984) reproduced unstable lapse conditions including mixed layers and elevated inversions. They reproduced the characteristics of convective boundary layer turbulence measured in the atmosphere.

Diffusion studies made by Chaudhry and Meroney (1973) in stable boundary layers investigated previously by Arya have shown agreement of experimental results with Lagrangian similarity theory. Horst (1979) tested Lagrangian similarity predictions of crosswind-integrated ground concentration against the Prairie Grass diffusion experiment (Barad, 1958) and an experiment at Idaho Falls (Islitzer and Dumbauld, 1963). He reported good agreement for all stabilities at distances x/z_o out to 2×10^5. Poreh and Cermak (1984, 1985) released plumes in their modeled mixing layer. Their plumes exhibited the plume lofting typical of ground sources and the descent typical of elevated sources, predicted from water tank experiments by Willis and Deardorff (1974, 1976, 1978) and numerically by Lamb (1982).

Staff at the Fluid Mechanics Laboratory at the Ecole Centrale de Lyon have studied unstable wind-tunnel boundary layers and compared them with the atmospheric boundary layer (Schon and Mery, 1978). Flow speeds were typically 2 to 4 m/s and the floor temperature was maintained 50°C above ambient. Comparisons with the Kansas data (Haugen et al., 1971) were quite satisfactory, but longitudinal turbulence intensities exhibited a slight Reynolds number dependence, and spectral energy was too low in the high frequency portions of the spectra. The most unstable flow they studied had a Monin-Obukhov scale length of about -1 m at model scales, or -500 to -1000 when scaled to the atmosphere.

A.2 Fluid Modeling of Bluff Body Aerodynamics

The interaction of an approach wind field with bluff bodies or structures constructed on the earth's surface is broadly termed "Building Aerodynamics." In a review article on this subject, Meroney (1982) discusses the character of bluff body flow about rectangular buildings and cylindrical cooling towers. Defects in velocity profiles can easily persist to 10 to 15 building heights downwind. Field and laboratory measurements of plume dispersion about the Rancho Seco Nuclear Power Station in Sacramento, California, confirm that cooling tower wake effects persist for significant downwind distances under a variety of stratification conditions (Allwine, Meroney and Peterka, 1979; Kothari, Meroney and Bouwmeester, 1979).

Performance of Prior Fluid Modeling Experiments:

A number of studies have been performed in the CSU Fluid Dynamics and Diffusion Laboratory to establish the effect of buildings and meteorological masts on flow fields. Hatcher et al. (1977) examined flow and dispersion in stratified flow downwind of the Experimental Organic Cooled Reactor, Idaho Falls; Allwine et al. (1979) studied the Rancho Seco Reactor, Sacramento; Kothari et al. (1979) studied the

Duane Arnold Energy Center, Iowa. In each case field measurements were compared to laboratory measurements with good agreement. Specific effects of the structure of a meteorological mast on instrumentation response were reported by Hsi and Cermak (1965).

Simulation Criteria:

Often atmospheric turbulence may cause only weak effects compared to the turbulence generated by buildings, obstacles, and terrain. Yet the magnitude of the perturbations depends upon the incident flow turbulence scale and intensity, details of the obstacle shape and surface roughness, and size of the obstacle compared to the boundary layer depth. Geometrical scaling implies that the ratio of the building height to length scale must be matched and, of course, that all other building length scales be reduced to this same ratio.

Several questions should be considered when modeling flows which include surface obstacles:

a. What size obstacles should be disregarded?

b. What detail or roughness on an obstacle need be included?

c. To what upwind distance should all obstacles be included?

d. At what point does the size of a modeled obstacle become too big for the wind tunnel (i.e., blockage effects)?

e. What is the effect on the flow field of mismatching obstacle and approach flow length scales?

f. What is the minimum allowable model obstruction Reynolds number?

Obstacle sizes to be disregarded:

Boundary layer studies of rough surfaces reveal that if protuberances are of a size k, such that $u_* k/\nu < 5$, they will have little effect on the flow in a turbulent boundary layer. Thus, assuming a laboratory wind speed of 1 m/s and a typical friction coefficient $C_f/2 = (u*/u)^2 = 0.0025$, obstacles of size less than 2 mm would go unnoticed.

Required obstacle surface detail or roughness:

Another question that always arises is "How much detail is required for the building or obstacle model? The answer is, of course, dependent upon the size of the protuberance compared to the plume and the dominant eddies of mixing. If the obstruction is large enough to modify the separated wake over the main obstacle, then it must be included. Often an equivalent obstacle surface roughness suffices. Snyder (1981) concludes a generic surface roughness criterion might be $u_* k/\nu > 20$. For a 1 m/s laboratory flow this results in model roughness elements equal to about 6 mm. But since the exterior flow is usually highly turbulent, the body typically includes a highly unsteady wake, and the u_* value to be used should be that acting on the building surface, rather than that of the approach flow. Hence, even this roughness may be unnecessarily large.

Upstream fetch to be modeled:

Suppose there is another building, tree line, fence, cooling tower, or obstacle some distance, s, upstream of a meteorological measurement location; is it necessary to include this obstacle in the wind-tunnel model? Hunt (1974) showed that the velocity deficit in the wakes of cubes and cylinders is given approximately by:

$$DU_{mx}/U(h) = A\ (s/h)^{-3/2} \qquad \text{(A-2)}$$

downwind of the separation bubble, where DU_{mx} is the maximum mean velocity deficit created by the obstacle, h is the height of the obstacle, S is the distance downstream of the obstacle, and A is a constant dependent upon the obstacle shape, orientation, boundary layer thickness, etc. Typically, A = 2.5, but it may range from 1.5 to 5.0. If we desire that the velocity at the spill site be within 3 percent of its undisturbed value, Snyder (1981) recommends that any upstream obstacle as high as s/20 be included upstream in the model of the spill site. If the obstacle's width is much greater than its height (for example, a fence or ridge), one should include it in the physical model if its height is greater than s/100.

Blockage effects:

Because of the influence of wind-tunnel walls on the behavior of the flow past models, it is desirable to use small models or big tunnels, or both. On the other hand, larger models are not only easier to work with, but they may be needed for similarity reasons to achieve large enough Reynolds numbers. It is possible to identify three different types of effects of wind-tunnel constraints. The first is the simple "solid blockage" effect which arises because the fluid stream is unable to expand laterally as it normally would in unconfined flow. The second effect, called "wake blockage", results because the accelerated flow between an obstacle and the tunnel walls continues to "pinch" the wake flow region and reduce its normal lateral rate of growth. The third effect is produced by the growth of boundary layers on the tunnel walls which produce "wall boundary interference." Tunnel blockage can cause separation and reattachment locations to vary, produce higher velocities, larger wake turbulence, and modify the dispersion patterns in the vicinity of obstructions.

The ratio of the cross-sectional area of a model obstacle to that of the tunnel is called the "blockage ratio," BR. Mass continuity produces an average velocity speed-up of S = BR/(1-BR). Although wind tunnels with adjustable ceilings can compensate to some extent by raising the roof locally, this is not a perfect solution to the problem. Measurements on building and cooling tower models placed in different size wind-tunnel test sections reveal major changes in the character of pressure distributions, separation, and wake growth in the presence of flow restricted by wind-tunnel side walls (Farell et al., 1977).

Blockage corrections, which are conventionally applied in aeronautical tunnels, cannot usually be applied to the typical asymmetric model configuration placed against the wall of a meteorological wind tunnel (Ranga Raju and Singh, 1976). Conventional wisdom now suggests the "rule of thumb" that blockage ratios greater than 5 percent should be avoided.

Simulation of the flow over sharp-edged obstacles

A number of authors have discussed flow studies about simple cubical or rectangular sharp-edged obstacles. An extensive review about such flow fields and the subsequent character of diffusion near obstacles has been provided by Hosker (1984). Peterka, Meroney and Kothari (1985) describe typical flow deviations which result from the presence of a sharp-edged building.

Consider the main features of the flow around a sharp-edged building. Typically, when the approach flow is normal to the building face, the flow separates from the ground upwind of the building and produces a "horseshoe"-shaped vortex which wraps around the base of the building. The surface streamline reattaches on the front of the building, and fluid parcels move up and down the building's forward face. An elevated streamline flows over the obstacle, dips down behind, and stagnates on the surface at the end of the recirculating cavity immediately downwind of the building. Sometimes separation streamlines from the forward building edges reattach to the same face, yet in other cases the streamlines enter the downwind cavity and mingle with the other recirculating fluid. Air which enters the cavity departs through turbulent mixing across the dividing streamlines, mingles with downwind-pointing vortices and is ejected laterally out of the cavity, or leaves suddenly during an exhalation when the entire cavity appears to collapse and then reform.

When a building is oriented obliquely to the wind, flow over the front side walls does not separate, but strong recirculation occurs on the downwind faces. Flow over the roof often produces counter-rotating "delta-wing" vortices which increase mixing over the top and in the wake of the building. These vortices can cause reattachment of the flow in the middle of the roof and serious plume downwash in the near wake. Other features of the flow near the building include vertical vortices produced by the vertical corners of the building.

Golden (1961) measured the concentration patterns above the roof of model cubes in a wind tunnel. Two sizes of cubes were used to vary the Reynolds number from 1000 to 94,000. The concentration isopleths in the fluid above the cube roof showed only slight variations over the entire range of Reynolds numbers studied. The maximum concentration on the roof itself was found to vary strongly with Reynolds numbers less than 11,000, but to be invariant with Reynolds numbers between 11,000 and 94,000. Frequently, modelers quote Golden's experiments as justification for presuming dispersion invariance when obstacle Reynolds numbers exceed 11,000. However, Golden's "11,000 rule" is limited to the measurement of concentrations at only one point on the roof of smooth-walled cubes placed in a uniform approach flow of very low turbulent intensity. It is probably quite conservative because the shear and high turbulence in a simulated atmospheric boundary layer are likely to further reduce the critical Reynolds number. Indeed, Halitsky (1968) observed that for dispersion in the wake region, no change in isoconcentration isopleths from passive gas releases was found to occur for values of Reynolds number as low as 3300.

Flow around sharp-edged obstacles will remain kinematically similar at very low Reynolds numbers. Wake width variation will be minimal, and obstacle generated turbulence scales and intensity will only vary slowly as Reynolds number decreases. Gas clouds dispersing in this environment will remain similar at very low model speeds.

Simulation of flow over rounded obstacles

Flow around a smooth cylinder is Reynolds number dependent. This dependence reflects changes in the nature of the boiundary layer that forms over the cylinder and its behavior in the vicinity of the flow separation. At low Reynolds numbers, the boundary layer is laminar, and separation occurs easily under the influence of even modest positive pressure gradients. At higher Reynolds numbers, the boundary layer becomes turbulent and flow separation is delayed; i.e., the flow can move farther along a curved surface without separation. At prototype scales, obstacles are large enough that only turbulent separation occurs. However, model flows are usually at such low Reynolds numbers that the local boundary layer growing over a curved surface would be laminar. Most modelers attempt the reproduction of full-scale similarity around curved surfaces by artificially roughening the model surface to force transition to turbulence in these laminar boundary layers. This can be done by providing the surface with special (or artificial) roughness elements, for example, sandpaper, thin wires, or grooves. The height of the roughness, k, should be such that $Uk/\nu > 400$ and $k/R < 0.01$, where U is the mean wind speed at obstacle height, and R is the characteristic obstacle radius of curvature. Szechenyi (1975) studied flows about rough circular cylinders and determined that as Reynolds number decreases, roughening the surface becomes less effective. Fage and Warsap (1929) considered the effect of increasing the surface roughness of cylinders on their drag coefficient. Eventually, even ridiculously large roughness is ineffective.

Niemann and Ruhwedel (1980) compared pressures and forces about a 1:333 scale model to a full-scale hyperbolic cooling tower shell. They roughened their model with vertical ribs of height 0.09 mm and width 0.77 mm, producing a roughness coefficient of $k/2R = 0.0006$ and roughness Reynolds number, $Re_k > 270$. They found meridion forces on the cooling tower model and prototype were similar. Model Reynolds numbers were between 4.5×10^5 and 6.0×10^5, and this corresponding to $U_m > 45$ m/s. But again these speeds are much higher than is appropriate for current measurements.

Halitsky et al. (1963) examined dispersion about a smooth-model nuclear-reactor containment building (a hemisphere fitted on a vertical cylinder) and found a critical Reynolds number greater than 79,000. (Yet this critical Reynolds number was for flow very close to the vessel wall. The behavior of concentration isopleths further downwind is likely to be less Reynolds number dependent.)

Although the details of fluid motions around rounded obstacles vary significantly with Reynolds number, the gross features of the flow do not change. Even small models at low wind speeds will produce horseshoe-shaped ground vortices, elevated pairs, and regular vortex shedding. If the internal boundary layer over the obstacle is laminar, then the wake region will be broader and less intense.

REFERENCES

Allwine, K. J., Meroney, R. N. and Peterka, J. A., 1978, "Rancho Seco Building Wake Effects on Atmospheric Diffusion: Simulation in a Meteorological Wind Tunnel," FDDL Report CER77-78KJA-RNM-JAP25, Colorado State University, Fort Collins, Colorado.

Arya, S. D. S. and Plate, E. J., 1969, "Modeling of the Stably Stratified Atmospheric Boundary Layer," Journal of the Atmospheric Sciences, Vol. 26, pp. 656-665.

Barad, M. L., Editor, 1958 Project Prairie Grass, A Field Program in Diffusion (Vols. I and II), Geophysical Research Paper No. 59, Geophysics Research Directorate, Bedford, Massachusetts.

Briatore, L., Elisei, G. and Longhetto, A., 1980, "Local Air Circulations over a Complex Coastal Site: A Comparison among Field Surveys, Hydraulic and Mathematical-Model Data," Il Nuovo Cimento, Vol. 3C, No. 4, Lugiro-Agosto, pp. 365-381.

Cermak, J. E., 1975, "Applications of Fluid Mechanics to Wind Engineering - A Freeman Scholar Lecture," Journal of Fluids Engineering, Trans. of the ASME, Vol. 97, pp. 9-38.

Cermak, J. E., Shrivastava, P. K. and Poreh, M., 1983, "Wind-Tunnel Research on the Mechanics of Plumes in the Atmospheric Surface Layer," FDDL Report No. CER83-84JEC-PKS-MP12.

Chaudhry, F. H. and Cermak, J. E., 1971, "Wind-Tunnel Modeling of Flow and Diffusion over an Urban Complex," Technical Report of Fluid Dynamics and Diffusion Laboratory, CER70-71FHC-JEC24, Colorado State University, Fort Collins, Colorado.

Chaudhry, F. H. and Meroney, R. N., 1973, "A Laboratory Study of Diffusion in Stably Stratified Flow," Atmos. Envir., Vol. 7, pp. 443-454.

Chien, H. C., Meroney, R. N. and Sandborn, V. A., 1979, "Sites for Wind-Power Installations: Physical Modeling of the Wind Field over Kahuku Point, Oahu, Hawaii," FDDL Report No. CER79-80HCC-RNM-VAS25, Colorado State University, Fort Collins, Colorado.

Fage, A. and Warsap, J. H., 1929, "Effects of Turbulence and Surface Roughness on Drag and Circular Cylinders," U.K., ARC R&M 1283.

Farell, C., Carrasquel, Guven and Patel, 1976, "Effect of Wind-Tunnel Walls on the Flow Past Circular Cylinders and Cooling Tower Models," ASME, 76-WA/FE-20, Aug., 12 pp.

Golden, J., 1961, "Scale Model Techniques," M.S. Thesis, New York University, Department of Meteorology and Oceanography.

Golder, D. G., 1972, "Relations among Stability Parameters in the Surface Layer," Boundary Layer Meteorol., Vol. 3, No. 1, pp. 47-58.

Halitsky, J., 1968, "Gas Diffusion Near Buildings," Meteorology and Atomic Energy, pp. 221-231.

Hatcher, R. V. and Meroney, R. N., 1977, "Dispersion in the Wake of a Model Industrial Complex," Joint Conference on Applications of Air Pollution Meteorology, Salt Lake City, Utah, pp. 343-346.

Haugen, D. A., Kaimal, J. C. and Bradley, E. F., 1971, "An Experimental Study of Reynolds Stress and Heat Flux in the Atmospheric Surface Layer," Quart. J. Roy. Meteorol. Soc., Vol. 97, pp. 168-180.

Hinze, J. O., 1975, Turbulence, McGraw-Hill Book Co., New York, NY.

Holmes, J. D., Walker, G. R. and Steen, W. E., 1979, "The Effect of an Isolated Hill on Wind Velocities Near Ground Level-Initial Measurements," Wind Engineering Report 3/79, James Cook University of North Queensland, Queensland, Australia.

Horst, T. W., 1979, "Lagrangian Similarity Modeling of Vertical Diffusion from a Ground Level Source," J. Appl. Meteorol., Vol. 18, pp. 733-740.

Hosker, R. P., Jr., 1984, "Flow and Diffusion Near Obstacles," Atmospheric Science and Power Production, DOE/TIC-27601, pp. 241-326.

Hsi, G. and Cermak, J. E., 1965, "Meteorological-Tower Induced Wind-Field Perturbations," Prepared under U.S. Army Research Grant DA-AMC-28-043-64-G-9, Fluid Mechanics Program Report No. CER65GH-JEC49, Colorado State University, Fort Collins, Colorado.

Hunt, J. C. R., 1974, "Wakes behind Buildings," A paper presented to Environmental Committee of the Aeronautical Research Council, Great Britain, October.

Islitzer, N. F. and Dumbauld, R. K., 1963, "Atmospheric Diffusion-Deposition Studies over Flat Terrain," Int. J. Air Water Pollut., 7C11-127: 999-1022.

Kline, S. J., 1965, Similitude and Approximation Theory, McGraw-Hill, 229 p.

Lamb, R. G., 1981, "Diffusion in the Convective Boundary Layer," from Nieuwstadt, F. T. M. and H. Vandap, Atmospheric Turbulence and Air Pollution Modeling, D. Reidel Publishing Company, 1982.

Meroney, R. N., Cermak, J. E. and Garrison, J. A., 1975a, "Wind-Tunnel Study of Stack Gas Dispersal at Lansing Power Station, Units 1, 2, 3 and 4, FDDL Report No. CER74-75RNM-JEC-JAG28, Colorado State University, Fort Collins, Colorado.

Meroney, R. N., Cermak, J. E. and Garrison, J. A., 1975b, "Wind-Tunnel Study of Stack Gas Dispersal at Lansing Power Station, Units 1, 2, 3 and 4," FDDL Report No. CER74-75RNM-JEC-JAG29, Colorado State University, Fort Collins, Colorado.

Meroney, R. N., Bowen, A. J., Lindley, D. and Pearse, J.R., 1978a, "Wind Characteristics over Complex Terrain: Laboratory Simulation and Field Measurements at Rakaia Gorge, New Zealand," Colorado State University Research Report No. CER77-78RNM29, 219 p.

Meroney, R. N., Sandborn, V. A., Bouwmeester, R. J. B., Chien, H. C. and Rider, M. A., 1978b, "Sites for Wind Power Installations: Physical Modeling of the Influence of Hills, Ridges and Complex Terrain on Wind Speed and Turbulence: Final Report, Part III," Colorado State University Research Report No. CER77-78RNM-VAS50a, p. 91, and CER77-78RNM-VAS50b, p. 197.

Meroney, R. N., Neff, D. E. and Kothari, K. M., 1980, "Behavior of LNG Vapor Clouds: Tests to Define the Size, Shape, and Structure of LNG Vapor Clouds," Annual Report prepared by Colorado State University for Gas Research Institute, GRI Report No. 79/0073.

Neal, D., 1983, "The Influence of Model Scale on a Wind-Tunnel Simulation of Complex Terrain," J. of Wind Engr. and Indus. Aerodynamics, Vol. 12, pp. 125-143.

Niemann, H. J. and Ruhwedel, J., 1980, "Full-scale and Model Tests on Wind-Induced, Static and Dynamic Stresses in Cooling Tower Shells," Eng. Struct., Vol. 2, pp. 81-89.

Ogawa, Y., Diosey, P. G., Uehara, K. and Ueda, H., 1985, "Wind Tunnel Observation of Flow and Diffusion Under Stable Stratification," Atmos. Envir., Vol. 19, pp. 65-74.

Peterka, J. A., Meroney, R. N. and Kothari, K., "Wind-Tunnel Measurements of Dispersion and Turbulence in the Wakes of Nuclear Reactor Power Plants," Ninth Quarterly Progress for 1 January - March 1978 for Contract No. AT(49-24)-0366.

Plate, E. J. and Cermak, J. E., 1963, "Micrometeorological Wind-Tunnel Facility, Description and Characteristics," FDDL Report CER63-EJP-JEC9, Colorado State University, Fort Collins, Colorado.

Poreh, M. and Cermak, J. E., 1984, "Wind-Tunnel Simulation of Diffusion in a Convective Boundary Layer," Boundary-Layer Met., 30, pp. 431-455, Presented at 29th OHOLD Biological Conference, Zichron Ya'Acov, Israel, 1983.

Poreh, M. and Cermak, J. E., 1984, "Criteria for Wind-Tunnel Simulation of Particle Plumes in the Atmospheric Surface Layer," Proceedings of the 1984 CRDC Conference on Obscuration and Aerosol Research, Aberdeen Proving Ground, Maryland, 25-29 June, CEP84-85MP-JEC5.

Ranga Raju, K. G. and Singh, V., 1976, "Blockage Effects on Drag of Sharp Edged Bodies," J. of Industrial Aerodynamics, Vol. 1, pp. 301-309.

Schon, J. P. and Mery, P., 1971, "A Preliminary Study of the Simulation of Neutral Atmospheric Boundary Layer Using Air Injection in a Wind Tunnel," Atmos. Envir., Vol. 5, No. 5, pp. 299-312.

SethuRaman, S. and Cermak, J. E., 1973, "Stratified Shear Flows over a Simulated Three-Dimensional Urban Heat Island," Project THEMIS Technical Report No. 23, CER73-74SS-JEC4, Colorado State University, Fort Collins, Colorado.

Snyder, W. H., Britter, R. E. and Hunt, J. C. R., 1979, "A Fluid Modeling Study of the Flow Structure and Plume Impingement on a Three-Dimensional Hill in Stably Stratified Flow," Proc. Fifth Int. Conf. on Wind Engr., Pergamon Press, NY, Vol. 1, pp. 319-329.

Snyder, W. H., 1981, "Guideline for Fluid Modeling of Atmospheric Diffusion," United States Environment Protection Agency Report EPA-600/8-81-009, 185 p.

Szechenyi, E., 1975, "Supercritical Reynolds Number Simulation for Two-dimensional Flow over Circular Cylinders," J. Fluid Mech., Vol. 70, pp. 529-542.

Teunissen, H. W., 1975, "Simulation of the Planetary Boundary Layer in a Multiple Jet Wind Tunnel," Atmos. Envir., Vol. 9, pp. 145-174.

Willis, G. E. and Deardorff, J. W., 1974, "A Laboratory Model of the Unstable Planetary Boundary Layer," Jour. Atmos. Sci., 31, pp. 1297-1307.

Willis, G. E. and Deardorff, J. W., 1976, "A Laboratory Model of Diffusion into the Convective Boundary Layer," Quart. J. Roy. Meteor. Soc., 102, pp. 427-445.

Willis, G. E. and Deardorff, J. W., 1978, "A Laboratory Study of Dispersion from an Elevated Source within a Modeled Convective Planetary Boundary Layer," Atmos. Environ., 12, pp. 1305-1311.

Yamada, T., 1971, "Numerical and Wind-Tunnel Simulation of Response of Stratified Shear Layers to Nonhomogeneous Surface Features," Ph.D. Dissertation submitted to Colorado State University.

APPENDIX B

Approach Flow Model Data and

Site Wind Frequency Data

APPENDIX B - TABLE OF CONTENTS

Profile Name : Smooth
Flow Condition : Neutral
Configuration : Undisturbed Approach
Ref. Height : 1500.0 ft
Ref. Model Velocity : 9.42 mph

Height (ft)	Velocity (Normalized)	Turb. Int. (%)
15	.544	17.60
28.6	.602	15.60
56.9	.676	13.20
98.3	.718	12.50
148	.779	10.50
197	.794	10.30
248	.816	9.17
374	.838	8.28
749	.916	6.54
1120	.96	5.61
1500	1	5.10

Profile Name : Rough
Flow Condition : Neutral
Configuration : Undisturbed Approach
Ref. Height : 1500.0 ft
Ref. Model Velocity : 19.93 mph

Height (ft)	Velocity (Normalized)	Turb. Int. (%)
15	.356	30.40
28.4	.382	30.00
59.3	.492	27.10
98.1	.555	22.10
147	.631	18.50
196	.655	17.50
248	.698	13.90
375	.763	9.61
747	.875	6.95
1120	.951	5.24
1500	1	

Profile Name : ST-APP-L
Flow Condition : Stable, Low speed
Configuration : Undisturbed Approach
Ref. Height : 1500.0 ft
Ref. Model Velocity : 1.67 mph

Height	Velocity	Turb. Int. (%)		del Theta	Model Temp	Delta Temperature (Deg C)	
(ft)	(Normalized)	u	v	(deg)	(deg C)	4 mph Field	8 mph Field
30.0	.214	4.2	2.8	.00	5.30	.00	.00
57.9	.233	2.7	1.7	.00	8.26	.31	1.25
102.4	.253	1.9	1.4	.00	13.10	.82	3.29
147.3	.253	1.3	2.3	.00	16.51	1.18	4.73
203.1	.270	2.6	3.4	.00	20.83	1.64	6.55
249.2	.270	1.1	1.8	.00	22.71	1.83	7.34
374.7	.322	3.3	2.8	.00	30.20	2.62	10.50
750.8	.458	3.7	2.8	.00	32.85	2.90	11.61
1125.0	.707	5.3	3.6	.00	36.80	3.32	13.28
1501.2	1.000	3.4	3.0	.00	40.67	3.73	14.91

T@100-T@30 = 1.000*T@100-T@30 Undisturbed App. ie Change in del T = .00 .00
T@200-T@30 = 1.000*T@200-T@30 Undisturbed App. ie Change in del T = .00 .00

Profile Name : ST-APP-H
Flow Condition : Stable, High speed
Configuration : Undisturbed Approach
Ref. Height : 1500.0 ft
Ref. Model Velocity : 3.09 mph

Height	Velocity	Turb. Int. (%)		del Theta	Model Temp	Delta Temperature (Deg C)	
(ft)	(Normalized)	u	v	(deg)	(deg C)	4 mph Field	8 mph Field
30.0	.164	14.8	14.4	.00	12.58	.00	.00
60.8	.282	10.6	8.8	.00	18.95	.07	.29
97.9	.360	3.5	2.8	.00	23.69	.12	.50
148.5	.398	3.4	2.3	.00	26.41	.15	.62
198.9	.448	4.6	2.8	.00	28.92	.18	.73
249.0	.511	3.7	3.0	.00	31.36	.21	.84
373.9	.627	2.9	2.9	.00	35.65	.26	1.03
747.6	.878	3.4	4.4	.00	41.27	.32	1.29
1125.4	.964	3.2	3.9	.00	43.73	.35	1.40
1496.7	1.000	1.8	2.6	.00	45.57	.37	1.48

T@100-T@30 = 1.000*T@100-T@30 Undisturbed App. ie Change in del T = .00 .00
T@200-T@30 = 1.000*T@200-T@30 Undisturbed App. ie Change in del T = .00 .00

Profile Name : UN-APP-L
Flow Condition : Unstable, Low speed
Configuration : Undisturbed Approach
Ref. Height : 1500.0 ft
Ref. Model Velocity : 1.09 mph

Height (ft)	Velocity (Normalized)	Turb. Int. (%) u	v	del Theta (deg)	Model Temp (deg C)	Delta Temperature (Deg C) 4 mph Field	8 mph Field
30.0	.723	24.9	19.4	.00	41.72	.00	.00
57.3	.764	20.1	19.3	.00	39.17	-.08	-.30
97.2	.794	15.6	17.5	.00	36.66	-.15	-.60
149.2	.782	13.6	18.2	.00	36.24	-.16	-.65
199.1	.779	13.5	19.8	.00	36.68	-.15	-.60
248.9	.788	13.1	20.4	.00	36.36	-.16	-.64
371.3	.775	13.7	19.6	.00	36.69	-.15	-.60
747.0	.825	8.2	9.2	.00	39.05	-.08	-.32
1121.3	.938	4.5	2.2	.00	44.53	.08	.34
1496.8	1.000	3.3	2.6	.00	45.92	.13	.50

T@100-T@30 = 1.000*T@100-T@30 Undisturbed App. ie Change in del T = .00 .00
T@200-T@30 = 1.001*T@200-T@30 Undisturbed App. ie Change in del T = .00 .00

Profile Name : UN-APP-H
Flow Condition : Unstable, High speed
Configuration : Undisturbed Approach
Ref. Height : 1500.0 ft
Ref. Model Velocity : 2.13 mph

Height (ft)	Velocity (Normalized)	Turb. Int. (%) u	v	del Theta (deg)	Model Temp (deg C)	Delta Temperature (Deg C) 4 mph Field	8 mph Field
30.0	.454	28.3	26.1	.00	42.92	.00	.00
58.5	.503	27.1	22.8	.00	39.99	-.04	-.16
99.8	.549	23.0	18.6	.00	37.41	-.07	-.30
150.7	.577	17.4	15.0	.00	35.23	-.10	-.42
200.4	.590	15.2	15.4	.00	35.40	-.10	-.41
251.0	.593	13.8	13.6	.00	34.51	-.11	-.46
376.2	.612	10.0	12.3	.00	33.62	-.13	-.51
751.8	.671	8.4	11.6	.00	35.16	-.11	-.42
1123.2	.853	5.0	4.2	.00	41.90	-.01	-.06
1497.1	1.000	3.7	3.7	.00	47.90	.07	.27

T@100-T@30 = 1.001*T@100-T@30 Undisturbed App. ie Change in del T = .00 .00
T@200-T@30 = 1.000*T@200-T@30 Undisturbed App. ie Change in del T = .00 .00

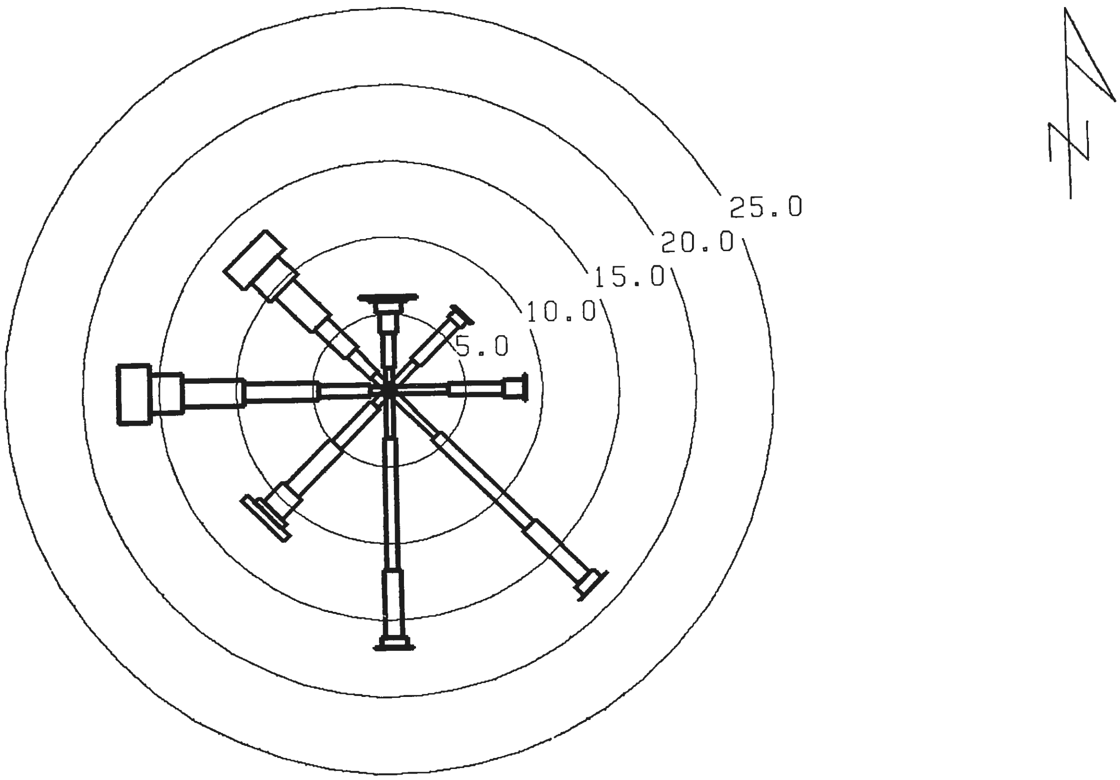

Figure B-1. Wind Rose, 30 ft Elevation, All Wind Categories, Fitzpatrick Tower

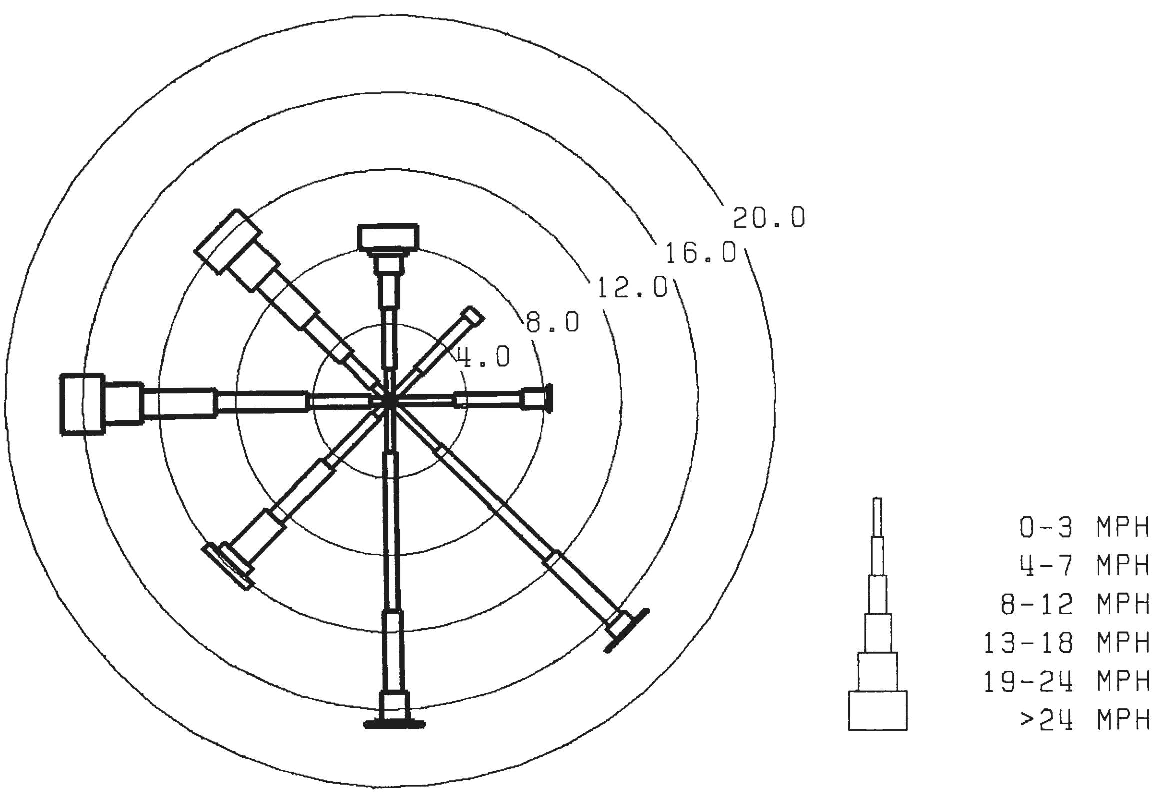

Figure B-2. Wind Rose, 30 ft Elevation, All Wind Categories, Nine Mile Point, Main Tower

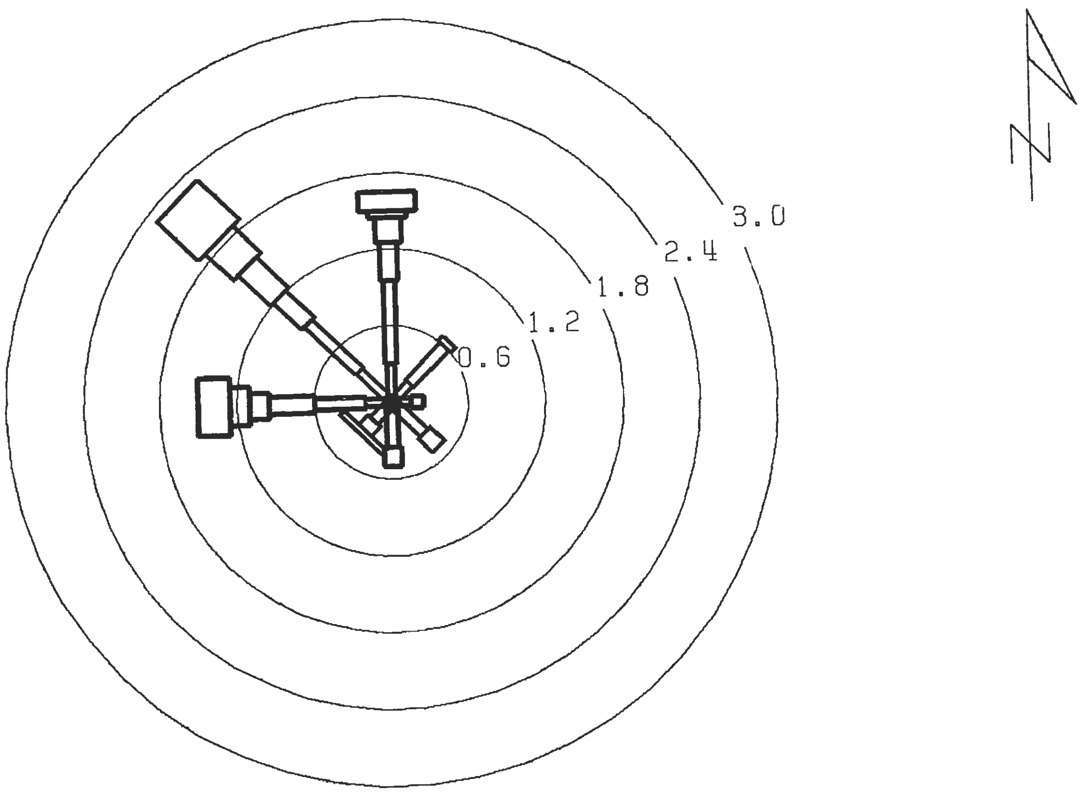

Figure B-3. Wind Rose, 30 ft Elevation, Stability Class A, Nine Mile Point, Main Tower

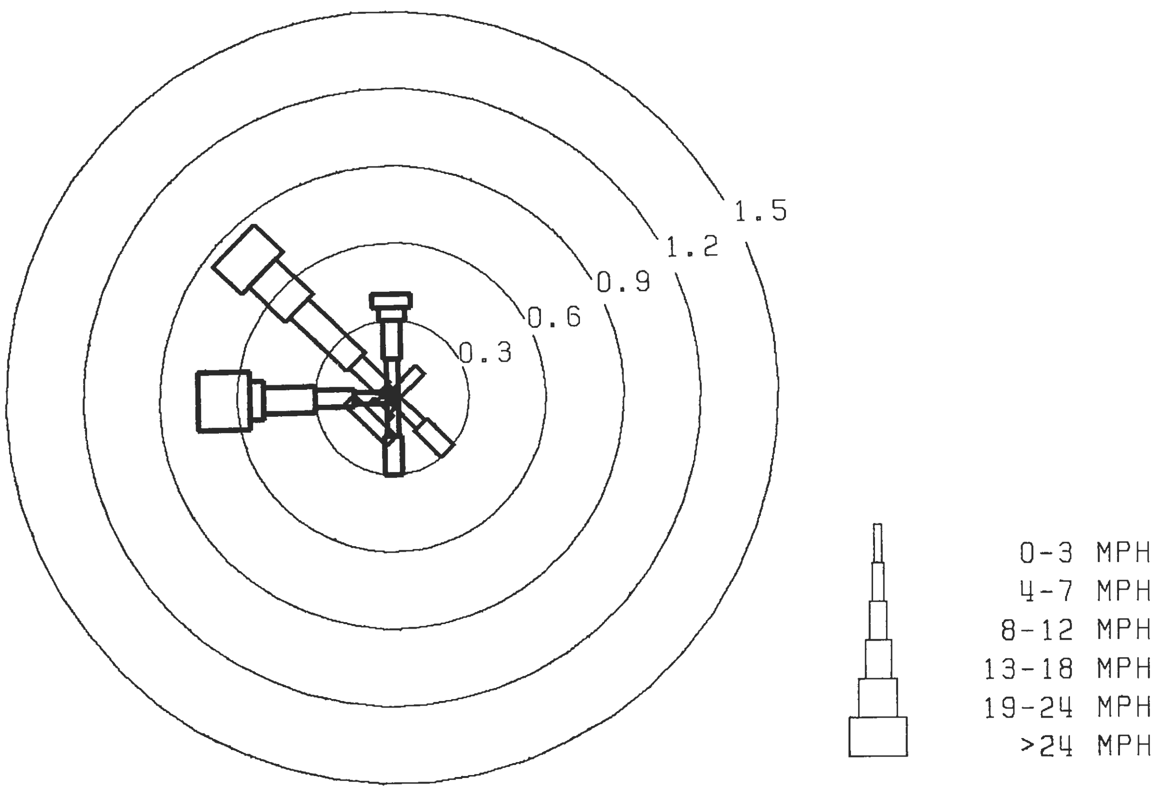

Figure B-4. Wind Rose, 30 ft Elevation, Stability Class B, Nine Mile Point, Main Tower

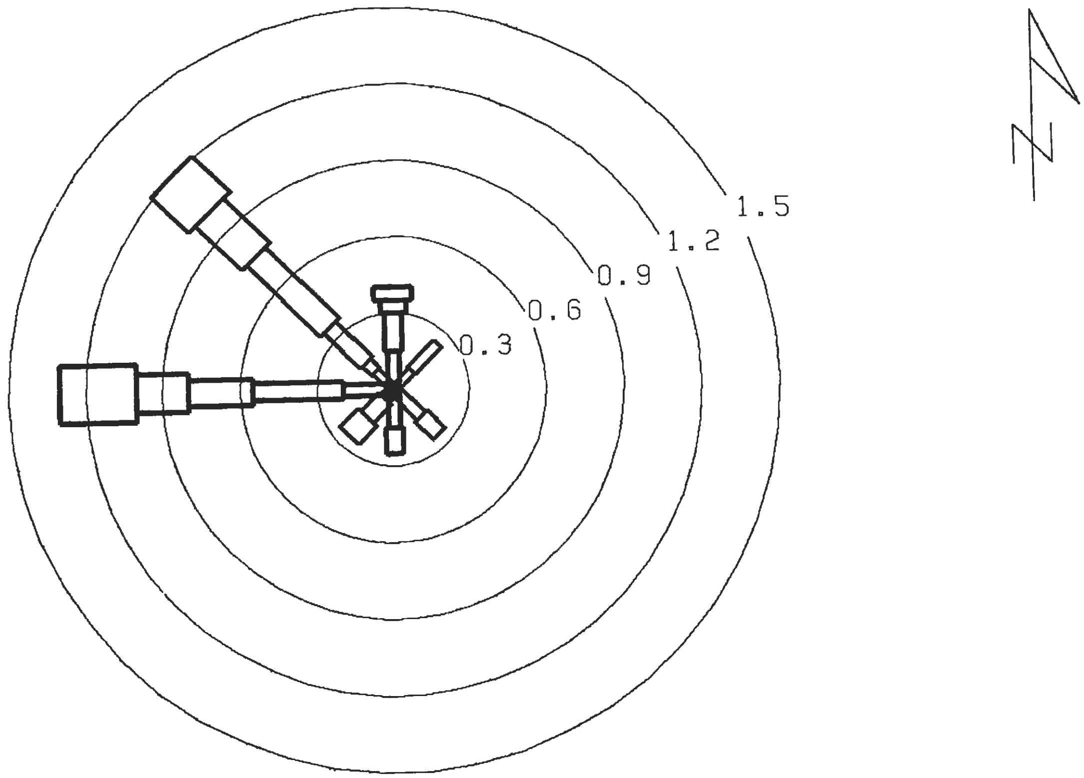

Figure B-5. Wind Rose, 30 ft Elevation, Stability Class C, Nine Mile Point, Main Tower

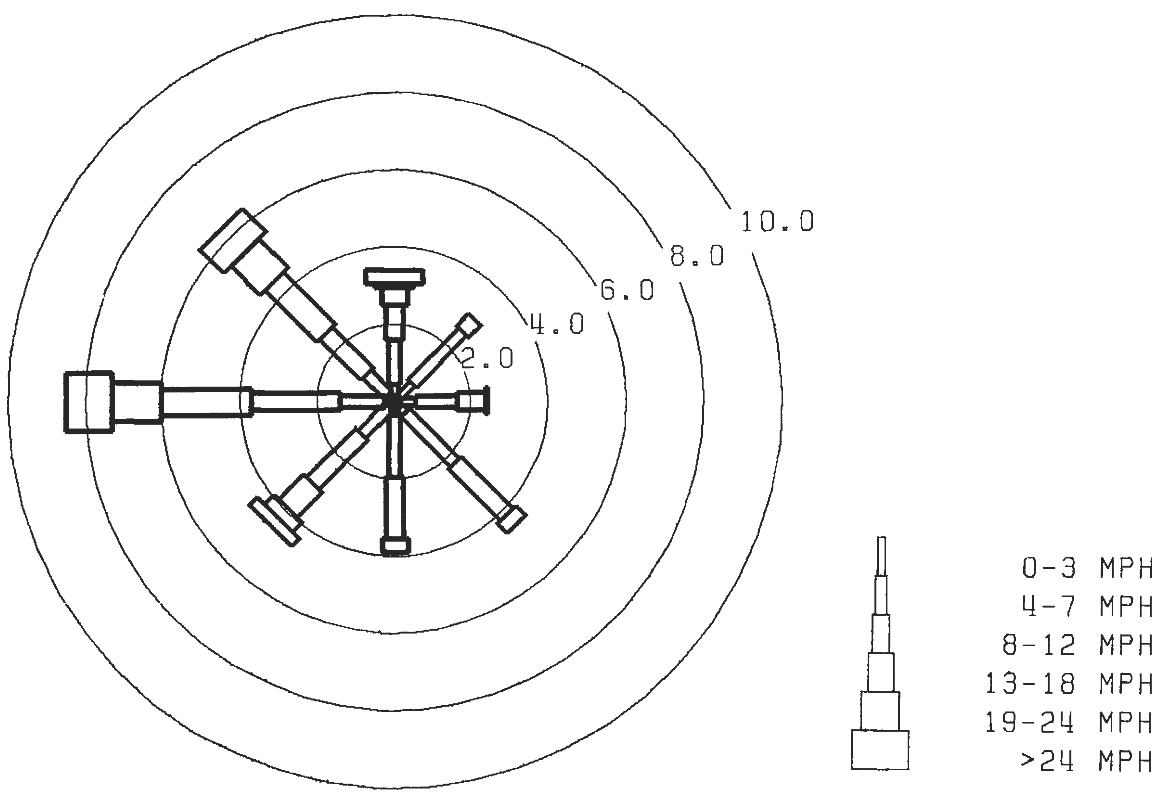

Figure B-6. Wind Rose, 30 ft Elevation, Stability Class D, Nine Mile Point, Main Tower

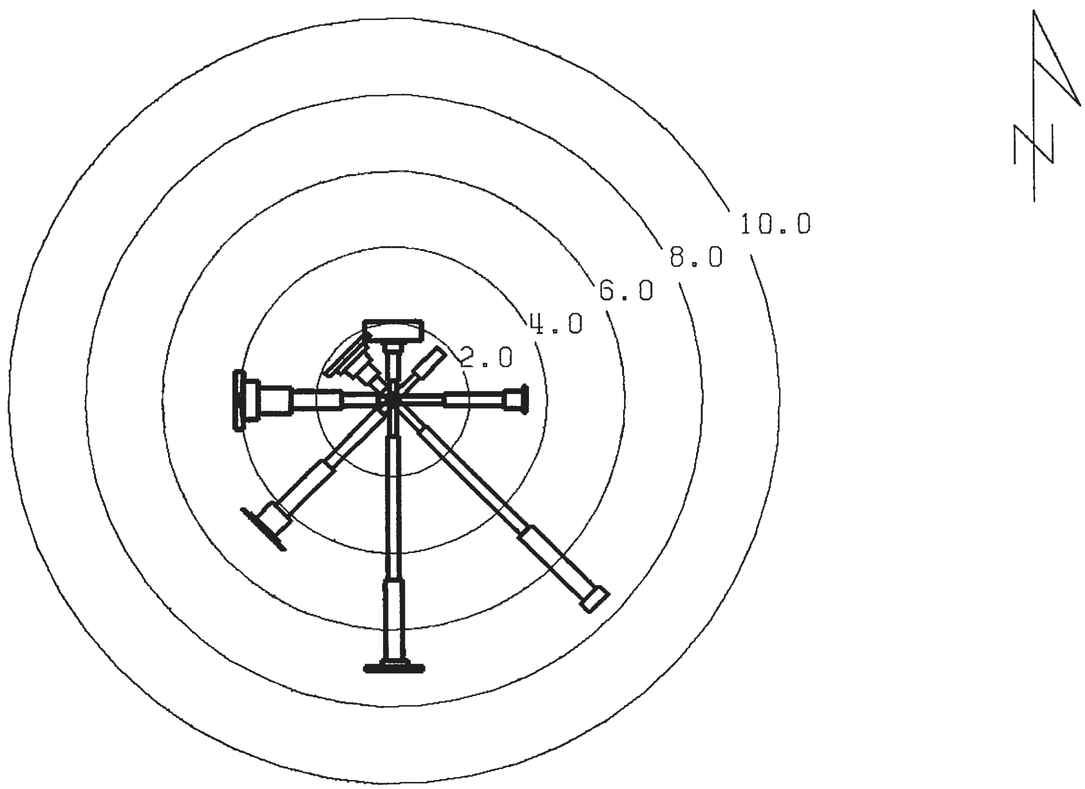

Figure B-7. Wind Rose, 30 ft Elevation, Stability Class E, Nine Mile Point, Main Tower

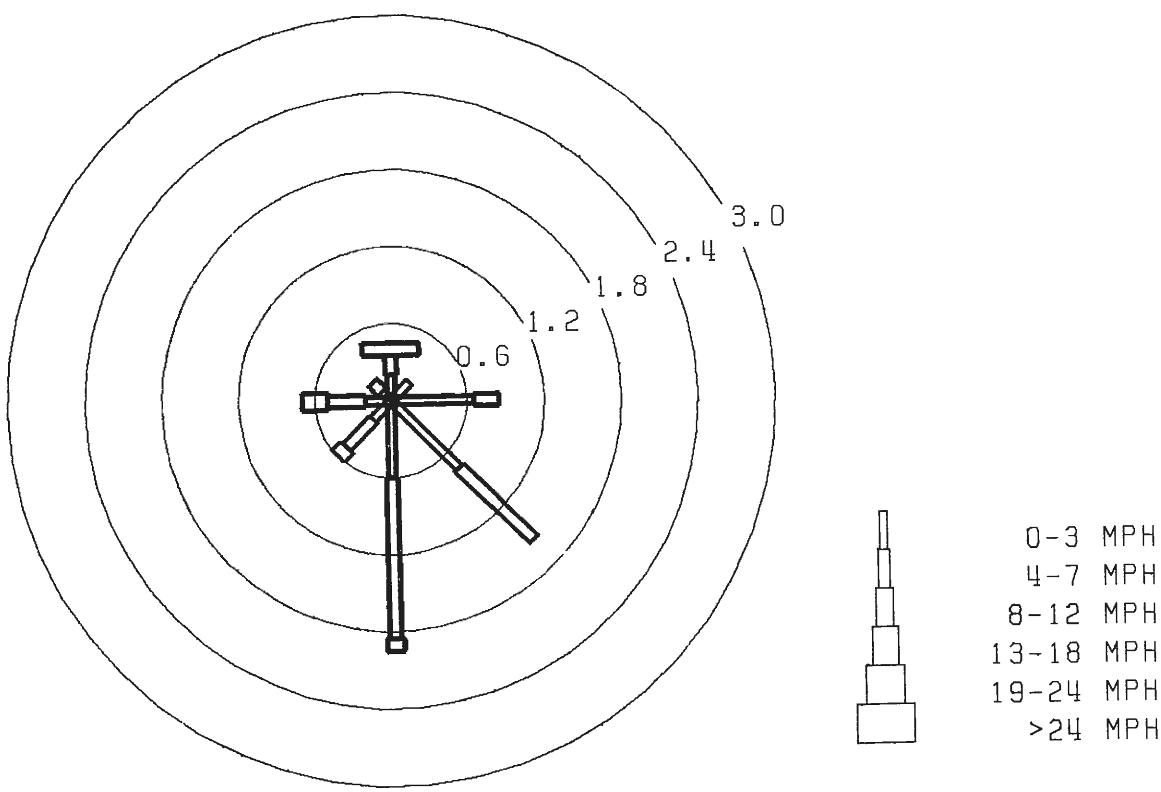

Figure B-8. Wind Rose, 30 ft Elevation, Stability Class F, Nine Mile Point, Main Tower

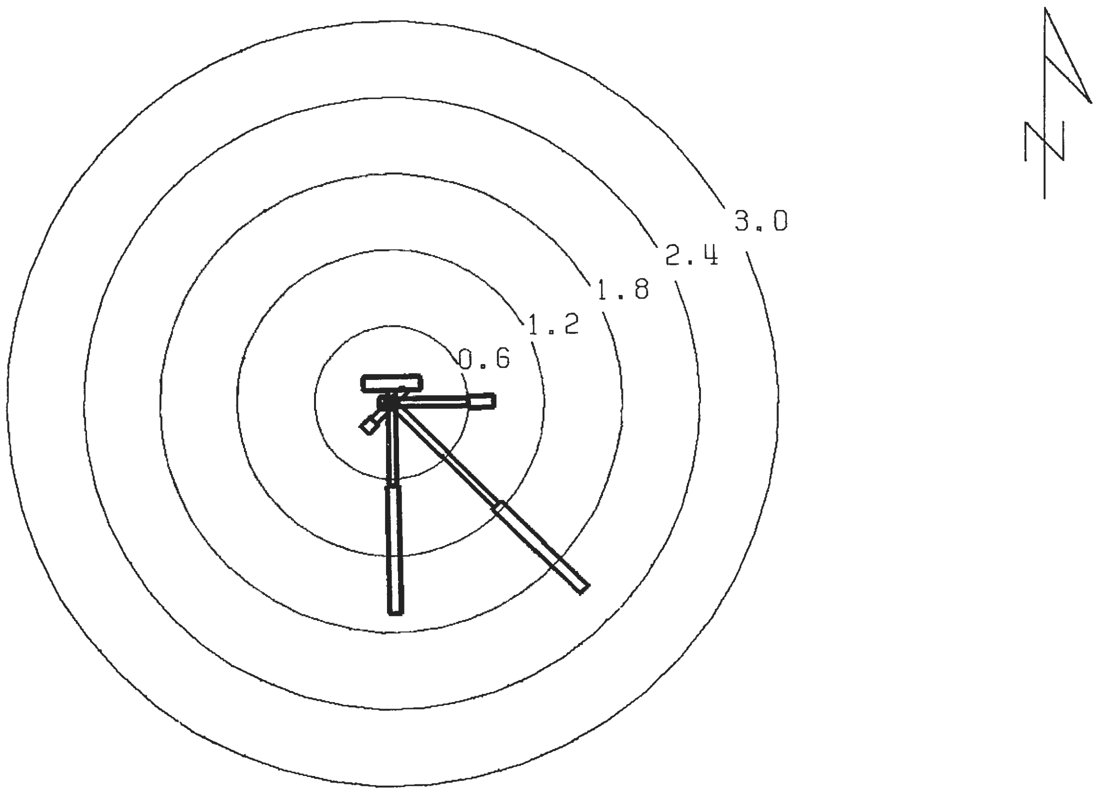

Figure B-9. Wind Rose, 30 ft Elevation, Stability Class G, Nine Mile Point, Main Tower

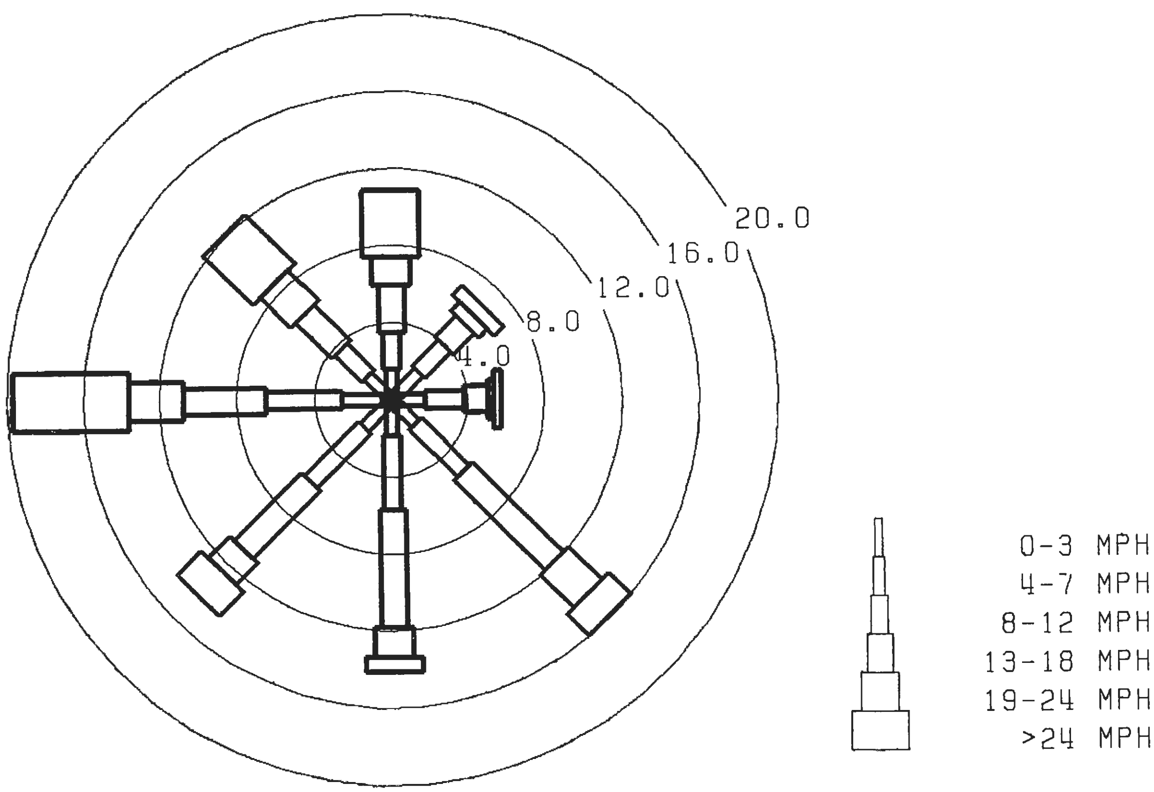

Figure B-10. Wind Rose, 200 ft Elevation, All Wind Categories, Nine Mile Point, Main Tower

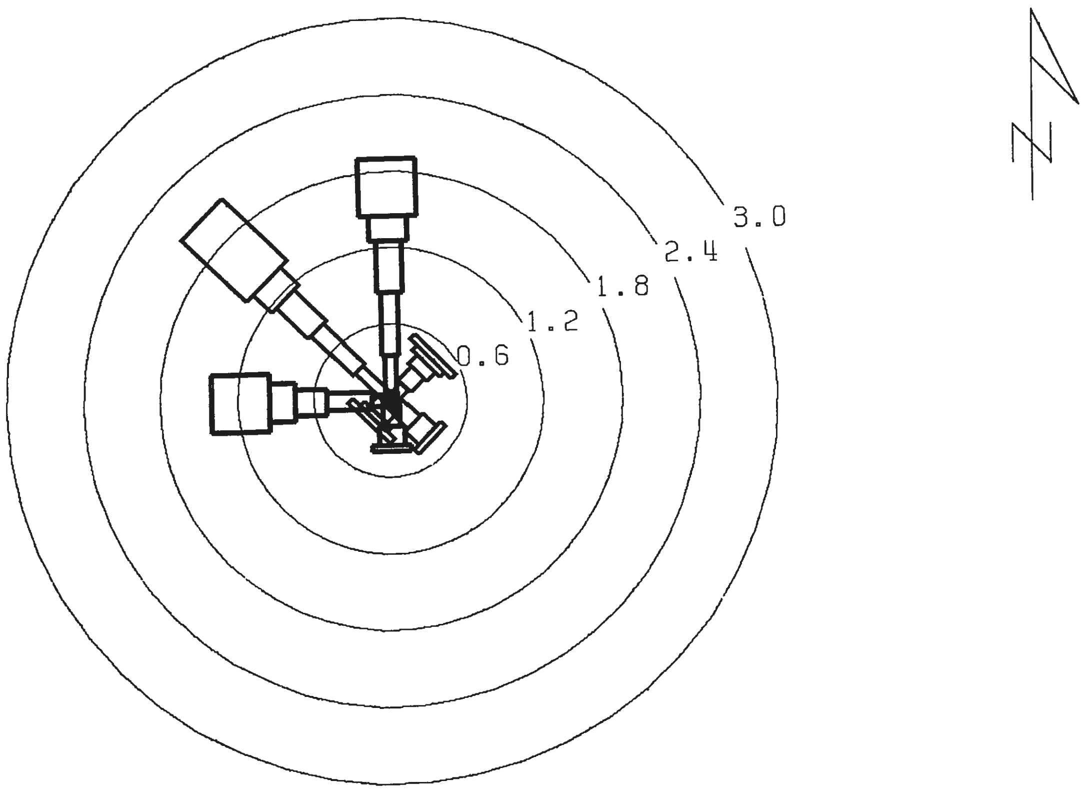

Figure B-11. Wind Rose, 200 ft Elevation, Stability Class A, Nine Mile Point, Main Tower

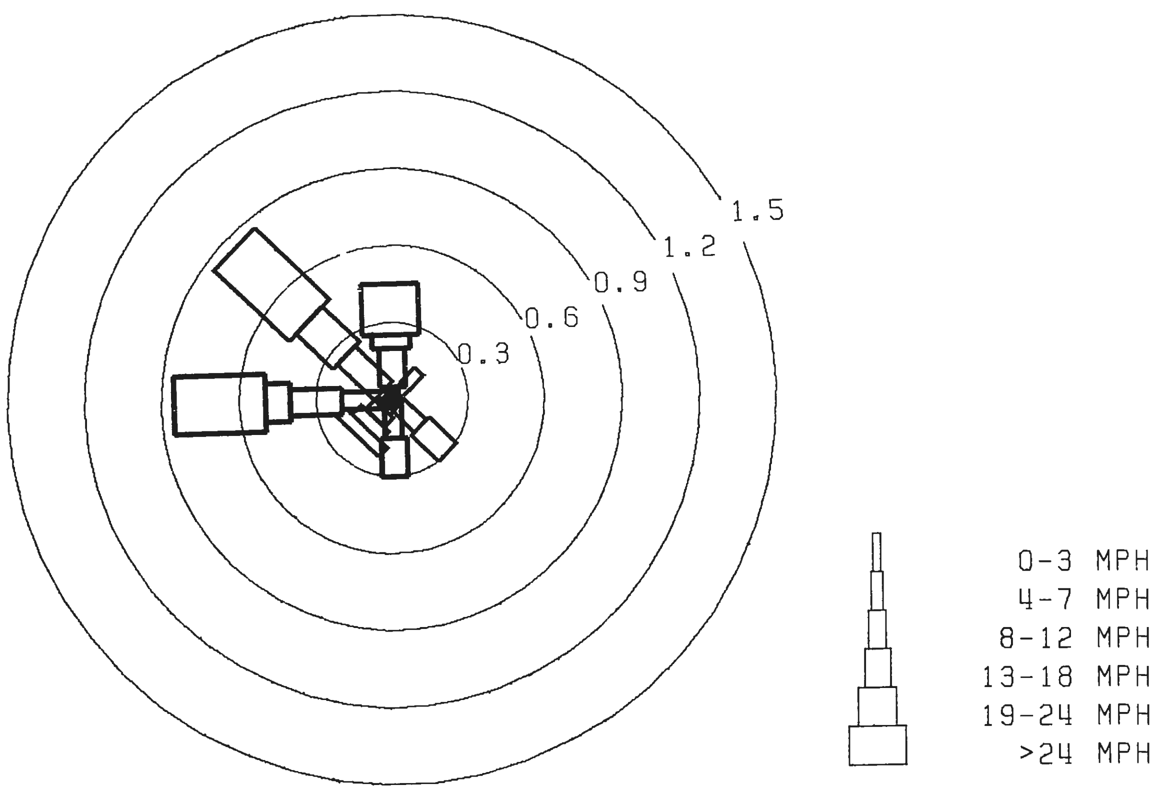

Figure B-12. Wind Rose, 200 ft Elevation, Stability Class B, Nine Mile Point, Main Tower

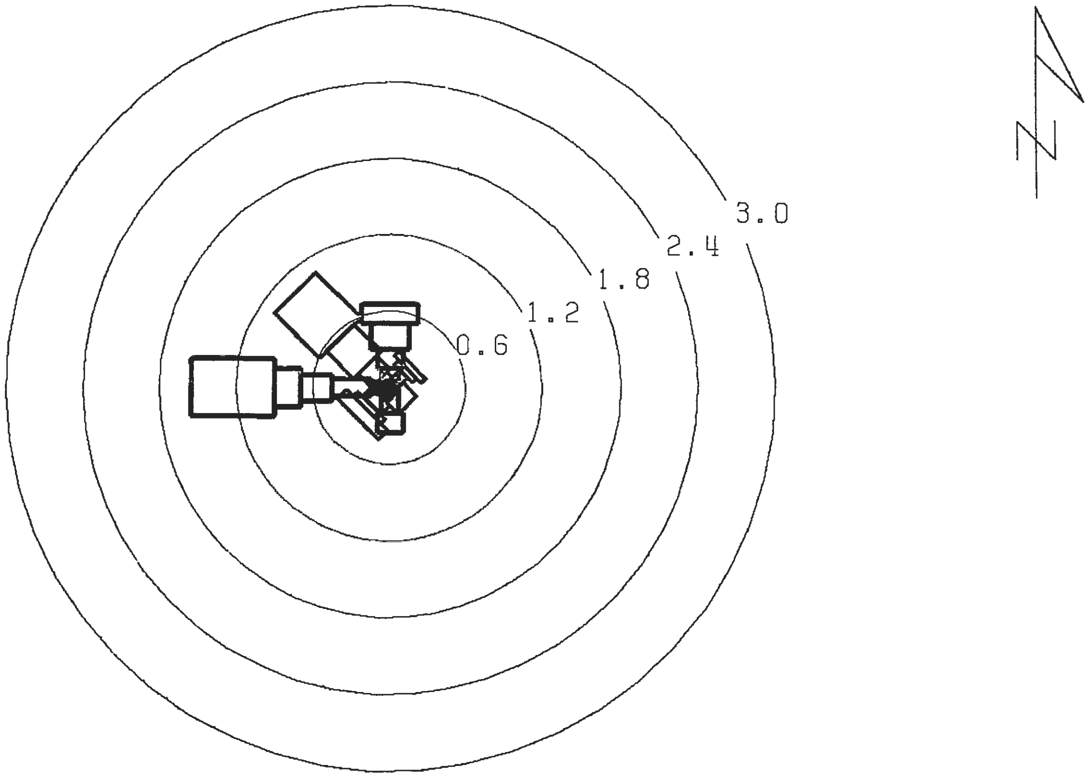

Figure B-13. Wind Rose, 200 ft Elevation, Stability Class C, Nine Mile Point, Main Tower

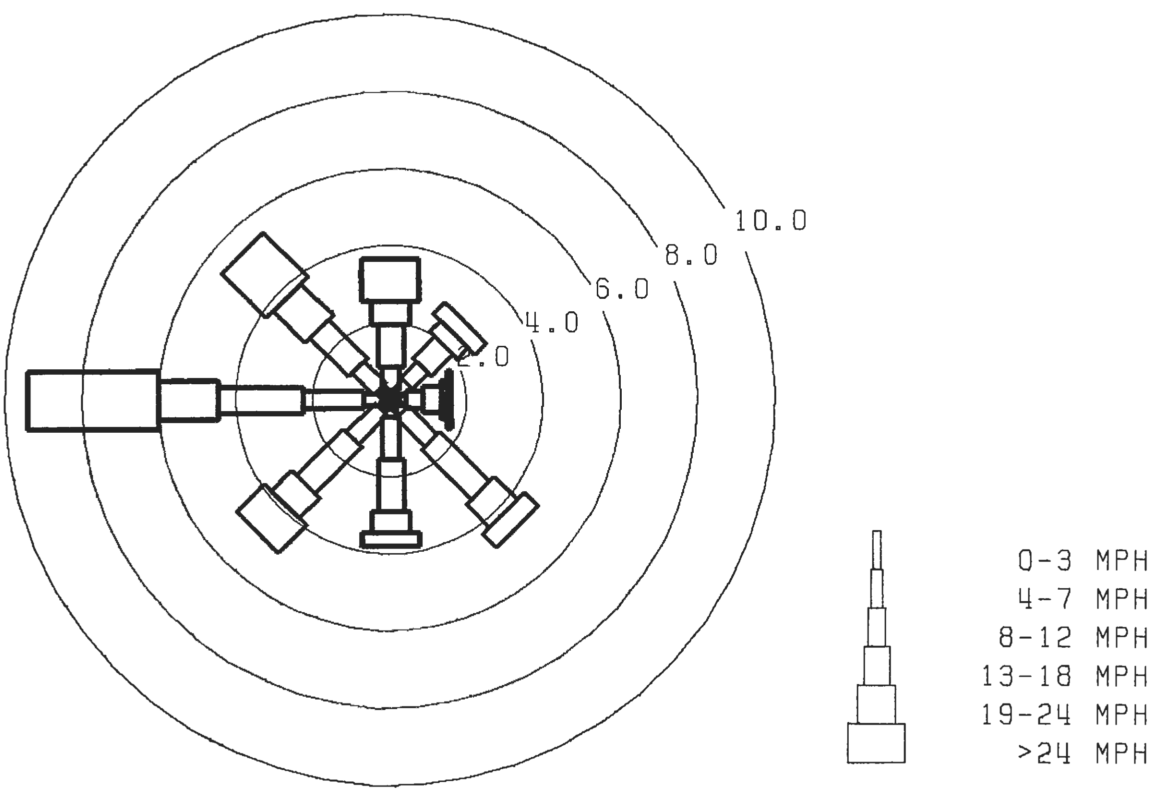

Figure B-14. Wind Rose, 200 ft Elevation, Stability Class D, Nine Mile Point, Main Tower

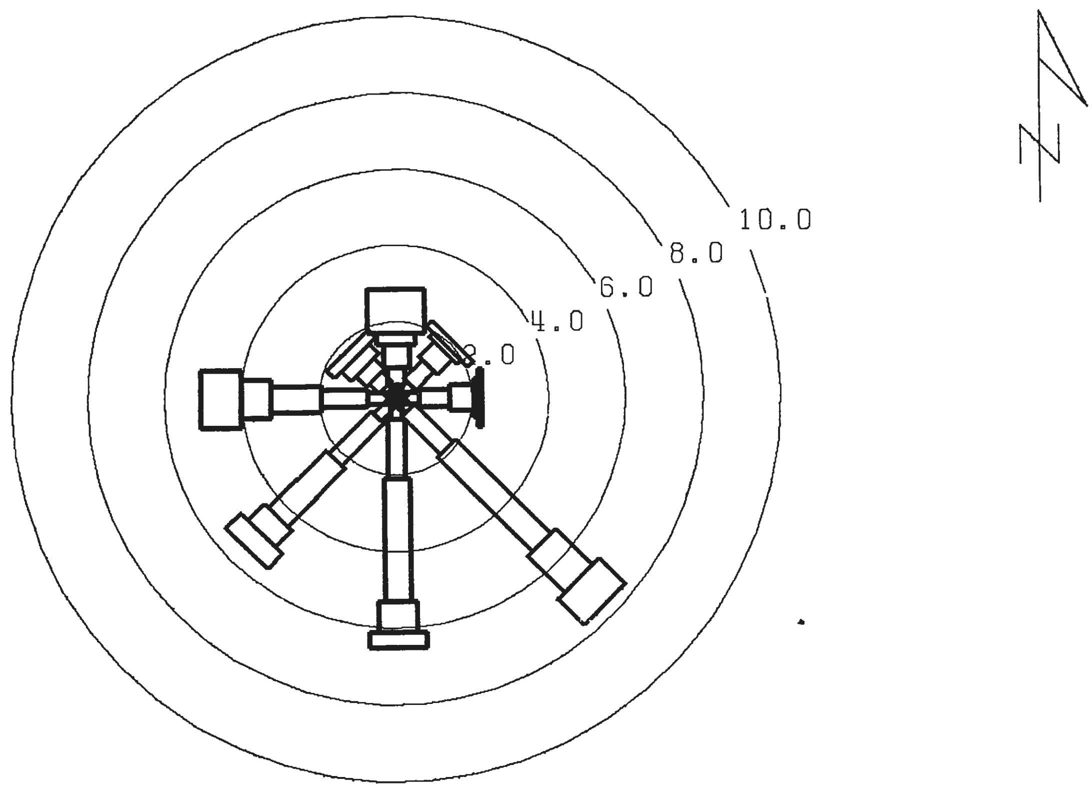

Figure B-15. Wind Rose, 200 ft Elevation, Stability Class E, Nine Mile Point, Main Tower

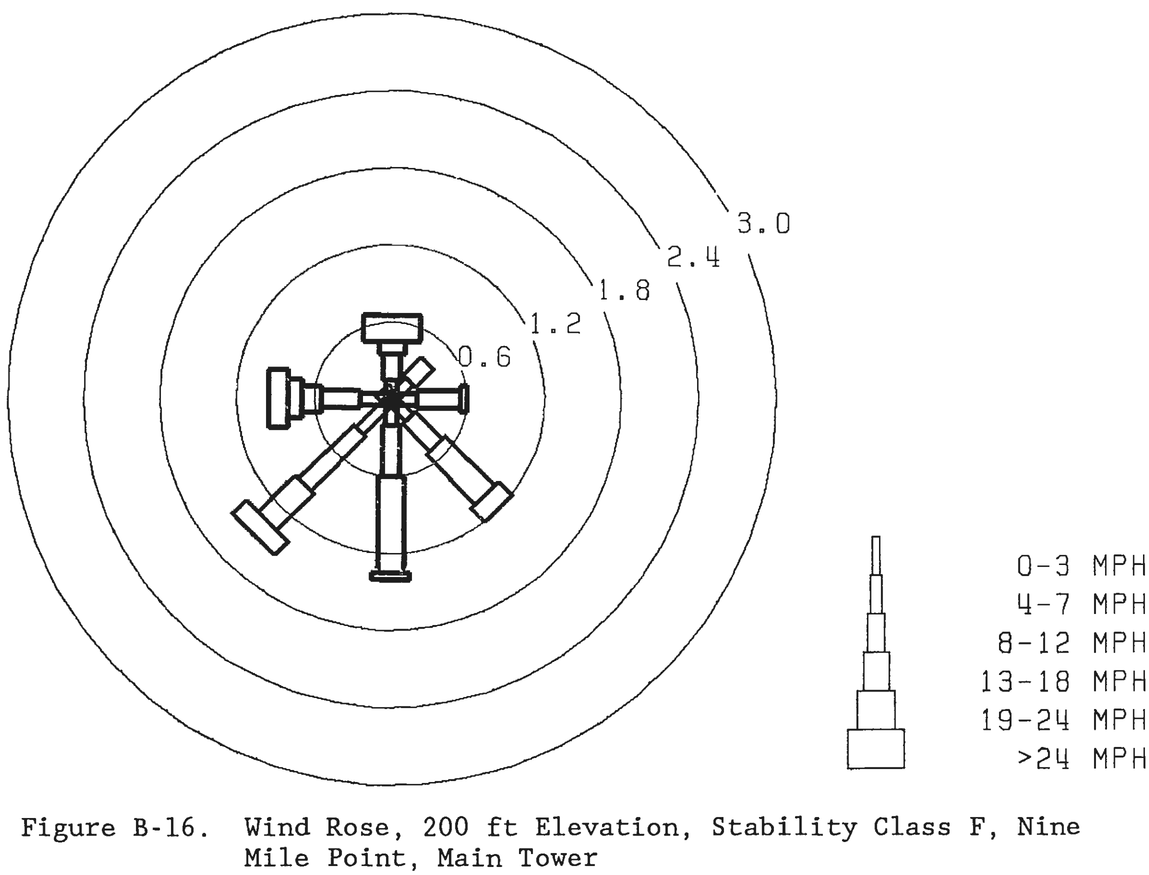

Figure B-16. Wind Rose, 200 ft Elevation, Stability Class F, Nine Mile Point, Main Tower

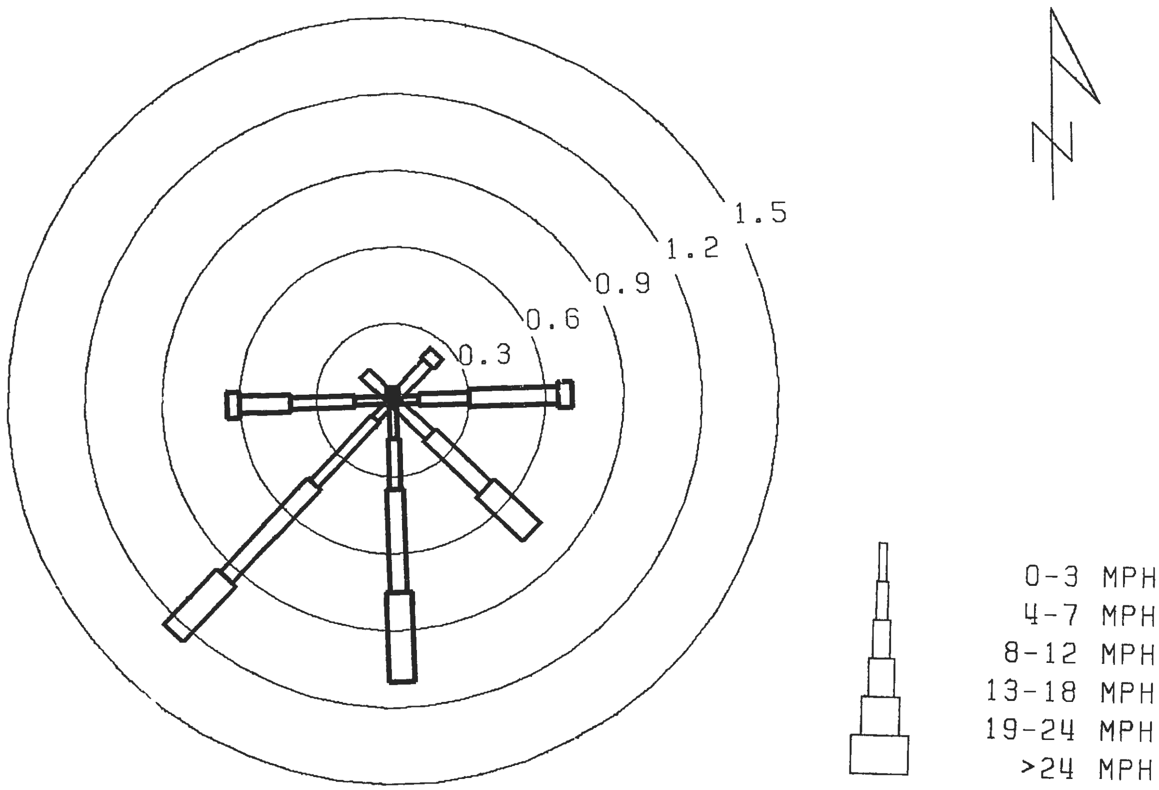

Figure B-17. Wind Rose, 200 ft Elevation, Stability Class G, Nine Mile Point, Main Tower

APPENDIX C

Task I Data: Site Influences on Velocity, Turbulence, Wind Angle, and Temperature Measurements at the Primary Meteorological Tower Location for Neutral, Stable, and Unstable Flow Conditions

APPENDIX C - TABLE OF CONTENTS

Task I: Data File Name Code

Example File Name } NY ___ ___ # - ___ #

Free Stream Velocity Code

Configuration (Letters)

Task #

Flow Condition (Letters)

New York

Flow Condition: PA = Neutral
S- = Stable
U- = Unstable

Task #: 1 = Task 1 ⟵
3 = Task 3
4 = Task 4

Configuration:

A; 3 power plant buildings in place - no cooling tower

B; 3 power plant buildings in place - with cooling tower

C; 3 power plant buildings, cooling tower, and new JAF service building

Free Stream Velocity Code:

1	=	Lower speed	≈	5.6 mph	neutral
				1.6 mph	stable
				1.1 mph	unstable
2	=	Higher speed	≈	11.2 mph	neutral
				3.2 mph	stable
				2.1 mph	unstable

Table Cl. Task I Data Summary and Guide

Data File Name	Flow Condition	Conf.	NMP Units 1 and 2	JAF Bldg.	JAF New Service Bldg.	Cooling Tower	Approx. Free Stream Velocity (mph)
NYPAl-Al	Neutral	A	X	X			5.6
NYPAl-A2	Neutral	A	X	X			11.2
NYPAl-Bl	Neutral	B	X	X		X	5.6
NYPAl-B2	Neutral	B	X	X		X	11.2
NYS-l-Al	Stable	A	X	X			1.6
NYS-l-Bl	Stable	B	X	X		X	1.6
NYS-l-A2	Stable	A	X	X			3.2
NYS-l-B2	Stable	B	X	X		X	3.2
NYU-l-Al	Unstable	A	X	X			1.1
NYU-l-Bl	Unstable	B	X	X		X	1.1
NYU-l-A2	Unstable	A	X	X			2.1
NYU-l-B2	Unstable	B	X	X		X	2.1

Table C2. Task I Velocity Profile Figure Guide

Figure #	1st Profile	2nd Profile	Flow Condition	Comments
C1	NYPA1-B1	NYPA1-B2	Neutral	Velocity independence check
C2	NYPA1-A2	NYPA1-B2	Neutral	Profiles with and without cooling tower
C3	NYS-1-A1	NYS-1-B1	Stable	Profiles with and without cooling tower
C4	NYS-A-A2	NYS-1-B2	Stable	Profiles with and without cooling tower
C5	NYU-1-A1	NYU-1-B1	Unstable	Profiles with and without cooling tower
C6	NYU-1-A2	NYU-1-B2	Unstable	Profiles with and without cooling tower

Profile Name : NYPA-1-A1
Flow Condition : Neutral, Low speed
Task Number : 1
Configuration : A
Ref. Height : 1500.0 ft
Ref. Model Velocity : 4.76 mph

Height (ft)	Velocity (Normalized)	Turb. Int. (%)
15.01	.369	27.9
28.30	.421	27.9
58.57	.493	27.4
97.21	.582	26.1
146.68	.573	21.8
198.11	.629	20.9
248.56	.723	20.1
374.07	.831	15.4
748.14	.87	11.7
1124.68	.93	7.5
1500.00	1	5.4

Profile Name : NYPA-1-A2
Flow Condition : Neutral, High speed
Task Number : 1
Configuration : A
Ref. Height : 1500.0 ft
Ref. Model Velocity : 9.29 mph

Height (ft)	Velocity (Normalized)	Turb. Int. (%)	del Theta
15.01	.345	30.6	
28.30	.386	29.7	.07
58.57	.446	29.6	
99.18	.535	24.4	-.14
148.40	.6	21	
198.60	.636	20.3	.04
248.56	.692	17	
376.53	.793	12.5	
748.14	.896	9	
1124.68	.945	6.9	
1500.00	1	5.6	

Profile Name : NYPA-1-B1
Flow Condition : Neutral, Low speed
Task Number : 1
Configuration : B
Ref. Height : 1500.0 ft
Ref. Model Velocity : 4.97 mph

Height (ft)	Velocity (Normalized)	Turb. Int. (%)
15.01	.352	29.8
28.55	.382	27.9
57.34	.45	23.4
98.19	.514	23.5
147.17	.572	21.7
198.11	.626	21.1
248.56	.649	18.5
376.53	.739	16.8
748.14	.874	10.3
1124.68	.946	7.1
1500.00	1	5.5

Height (ft)	Velocity (Normalized)	Turb. Int. (%)	del Theta
15.01	.367	30.6	
28.06	.394	27.8	.43
58.82	.468	27.1	
97.95	.518	22.7	.4
149.38	.594	19.8	
198.60	.633	18.5	.25
248.56	.686	17.7	
374.07	.741	16.4	
748.14	.885	11.1	
1127.14	.94	7.1	
1500.00	1	5.9	

Profile Name : NYS-1-A1
Flow Condition : Stable, Low speed
Task Number : 1
Configuration : A
Ref. Height : 1500.0 ft
Ref. Model Velocity : 1.62 mph

Height (ft)	Velocity (Normalized)	Turb. Int. (%) u	Turb. Int. (%) v	del Theta (deg)	Model Temp (deg C)	Delta Temperature (Deg C) 4 mph Field	Delta Temperature (Deg C) 8 mph Field
30.0	.217	3.9	2.9	-.30	6.63	.00	.00
59.3	.244	3.2	1.9	-.79	9.92	.35	1.39
101.2	.266	2.6	1.7	-.92	14.47	.83	3.30
152.6	.280	3.2	3.2	.58	18.84	1.29	5.15
202.7	.286	2.4	2.9	-.26	21.99	1.62	6.48
251.1	.311	1.0	1.0	1.84	25.94	2.04	8.14
372.1	.333	3.1	2.2	-1.66	30.28	2.49	9.97
749.0	.443	3.2	2.6	.07	32.88	2.77	11.07
1127.3	.652	5.5	4.0	-.38	36.25	3.12	12.49
1500.6	1.000	3.8	3.2	-.78	40.60	3.58	14.32

T@100-T@30 = 1.005*T@100-T@30 Undisturbed App. ie Change in del T = .00 .02
T@200-T@30 = .989*T@200-T@30 Undisturbed App. ie Change in del T = -.02 -.07

Profile Name : NYS-1-B1
Flow Condition : Stable, Low speed
Task Number : 1
Configuration : B
Ref. Height : 1500.0 ft
Ref. Model Velocity : 1.66 mph

Height (ft)	Velocity (Normalized)	Turb. Int. (%) u	Turb. Int. (%) v	del Theta (deg)	Model Temp (deg C)	Delta Temperature (Deg C) 4 mph Field	Delta Temperature (Deg C) 8 mph Field
30.0	.223	3.6	2.5	-2.14	3.96	.00	.00
59.9	.246	3.3	1.7	-1.60	8.46	.47	1.90
99.7	.270	2.1	1.2	-1.26	14.12	1.07	4.29
151.8	.288	1.6	1.0	1.03	19.05	1.59	6.37
202.9	.275	1.2	1.6	-.84	20.94	1.79	7.16
251.4	.303	2.0	2.0	1.72	25.59	2.28	9.12
371.9	.312	4.7	3.8	-2.56	28.99	2.64	10.56
751.6	.429	3.8	2.6	-.80	32.69	3.03	12.12
1127.9	.660	5.6	4.4	-1.49	36.42	3.42	13.69
1502.7	1.000	3.3	3.0	-.48	40.83	3.89	15.54

T@100-T@30 = 1.304*T@100-T@30 Undisturbed App. ie Change in del T = .25 1.00
T@200-T@30 = 1.094*T@200-T@30 Undisturbed App. ie Change in del T = .15 .62

Profile Name : NYS-1-A2
Flow Condition : Stable, High speed
Task Number : 1
Configuration : A
Ref. Height : 1500.0 ft
Ref. Model Velocity : 3.19 mph

Height (ft)	Velocity (Normalized)	Turb. Int. (%) u	v	del Theta (deg)	Model Temp (deg C)	Delta Temperature (Deg C) 4 mph Field	8 mph Field
30.0	.159	11.9	10.4	.57	12.50	.00	.00
58.7	.278	4.5	4.3	1.00	19.77	.08	.33
97.3	.327	2.9	2.1	.88	23.48	.12	.49
146.7	.379	2.8	2.0	1.42	26.49	.16	.63
199.1	.431	3.5	2.5	1.54	29.24	.19	.75
252.2	.506	3.3	2.4	1.87	32.15	.22	.88
378.1	.625	2.8	2.8	1.62	36.48	.27	1.07
748.5	.864	3.1	4.0	1.44	42.38	.33	1.34
1121.3	.938	3.5	4.2	2.12	44.35	.36	1.43
1500.6	1.000	1.7	2.9	1.54	46.29	.38	1.51

T@100-T@30 = .988*T@100-T@30 Undisturbed App. ie Change in del T = .00 -.01
T@200-T@30 = 1.024*T@200-T@30 Undisturbed App. ie Change in del T = .00 .02

Profile Name : NYS-1-B2
Flow Condition : Stable, High speed
Task Number : 1
Configuration : B
Ref. Height : 1500.0 ft
Ref. Model Velocity : 3.21 mph

Height (ft)	Velocity (Normalized)	Turb. Int. (%) u	v	del Theta (deg)	Model Temp (deg C)	Delta Temperature (Deg C) 4 mph Field	8 mph Field
30.0	.134	10.5	9.6	6.90	14.22	.00	.00
58.7	.182	14.8	11.6	4.72	17.99	.04	.17
100.2	.265	13.7	11.7	4.69	24.16	.11	.45
147.8	.352	14.1	12.5	3.78	29.05	.17	.66
203.7	.435	13.1	12.0	1.41	32.66	.21	.83
250.1	.500	12.3	12.8	-.90	34.38	.23	.90
377.3	.607	10.1	11.4	.19	37.11	.26	1.03
749.4	.870	3.1	4.4	1.90	42.51	.32	1.27
1125.0	.931	3.8	4.3	2.15	44.43	.34	1.35
1503.4	1.000	1.7	2.9	1.94	46.19	.36	1.43

T@100-T@30 = .895*T@100-T@30 Undisturbed App. ie Change in del T = -.01 -.05
T@200-T@30 = 1.128*T@200-T@30 Undisturbed App. ie Change in del T = .02 .09

Profile Name : NYU-1-A1
Flow Condition : Unstable, Low speed
Task Number : 1
Configuration : A
Ref. Height : 1500.0 ft
Ref. Model Velocity : 1.10 mph

Height (ft)	Velocity (Normalized)	Turb. Int. (%) u	Turb. Int. (%) v	del Theta (deg)	Model Temp (deg C)	Delta Temperature (Deg C) 4 mph Field	Delta Temperature (Deg C) 8 mph Field
30.0	.700	23.8	18.0	.54	42.41	.00	.00
57.4	.742	21.7	20.1	1.52	39.76	-.08	-.32
96.3	.774	16.7	18.6	1.38	37.83	-.14	-.55
148.4	.780	14.1	20.0	3.41	37.12	-.16	-.63
197.4	.788	13.9	18.9	1.62	36.70	-.17	-.68
247.7	.783	13.7	21.9	2.00	36.88	-.16	-.66
371.4	.775	14.4	20.9	3.16	36.81	-.17	-.67
746.4	.787	9.1	10.6	1.77	39.08	-.10	-.40
1125.5	.864	4.6	2.4	-.25	44.56	.06	.26
1497.2	1.000	2.1	2.0	-.96	45.98	.11	.42

T@100-T@30 = .905*T@100-T@30 Undisturbed App. ie Change in del T = .01 .06
T@200-T@30 = 1.133*T@200-T@30 Undisturbed App. ie Change in del T = -.02 -.08

Profile Name : NYU-1-B1
Flow Condition : Unstable, Low speed
Task Number : 1
Configuration : B
Ref. Height : 1500.0 ft
Ref. Model Velocity : 1.14 mph

Height (ft)	Velocity (Normalized)	Turb. Int. (%) u	Turb. Int. (%) v	del Theta (deg)	Model Temp (deg C)	Delta Temperature (Deg C) 4 mph Field	Delta Temperature (Deg C) 8 mph Field
30.0	.654	23.2	19.0	3.42	46.37	.00	.00
57.9	.692	22.1	20.1	2.79	43.64	-.08	-.33
96.8	.713	18.4	19.3	2.13	41.25	-.15	-.61
147.2	.752	16.9	19.1	6.82	40.25	-.18	-.73
196.6	.767	15.9	22.5	6.00	39.99	-.19	-.76
248.3	.781	15.5	23.0	9.90	39.68	-.20	-.80
373.1	.771	16.2	27.1	5.88	39.34	-.21	-.84
746.9	.736	13.6	21.6	2.06	39.57	-.20	-.81
1122.9	.924	3.9	4.1	-1.14	44.89	-.04	-.18
1499.8	1.000	2.1	1.8	-.63	46.33	.00	.00

T@100-T@30 = 1.012*T@100-T@30 Undisturbed App. ie Change in del T = .00 -.01
T@200-T@30 = 1.266*T@200-T@30 Undisturbed App. ie Change in del T = -.04 -.16

Profile Name : NYU-1-A2
Flow Condition : Unstable, High speed
Task Number : 1
Configuration : A
Ref. Height : 1500.0 ft
Ref. Model Velocity : 2.11 mph

Height (ft)	Velocity (Normalized)	Turb. Int. (%) u	Turb. Int. (%) v	del Theta (deg)	Model Temp (deg C)	Delta Temperature (Deg C) 4 mph Field	Delta Temperature (Deg C) 8 mph Field
30.0	.448	30.6	25.4	.50	43.48	.00	.00
59.1	.512	27.5	22.1	-4.35	39.84	-.05	-.20
98.2	.552	21.1	18.5	-2.61	37.32	-.08	-.34
150.8	.583	17.1	16.8	-.88	35.96	-.10	-.41
200.3	.591	15.5	15.1	-1.89	34.72	-.12	-.48
250.4	.607	13.6	13.5	-2.75	34.00	-.13	-.52
372.7	.612	10.8	12.4	-3.16	33.47	-.14	-.54
746.7	.671	8.6	11.4	-2.04	34.77	-.12	-.47
1123.4	.851	5.8	4.7	-1.50	41.18	-.03	-.13
1498.7	1.000	3.6	3.3	-.98	47.48	.05	.22

T@100-T@30 = 1.118*T@100-T@30 Undisturbed App. ie Change in del T = -.01 -.04
T@200-T@30 = 1.165*T@200-T@30 Undisturbed App. ie Change in del T = -.02 -.07

Profile Name : NYU-1-B2
Flow Condition : Unstable, High speed
Task Number : 1
Configuration : B
Ref. Height : 1500.0 ft
Ref. Model Velocity : 2.17 mph

Height (ft)	Velocity (Normalized)	Turb. Int. (%) u	Turb. Int. (%) v	del Theta (deg)	Model Temp (deg C)	Delta Temperature (Deg C) 4 mph Field	Delta Temperature (Deg C) 8 mph Field
30.0	.401	30.3	27.4	.87	43.67	.00	.00
57.6	.450	27.3	27.0	-.55	40.64	-.04	-.16
97.5	.485	25.1	24.8	-.81	38.74	-.07	-.27
148.8	.521	20.4	23.7	-.69	36.94	-.09	-.37
197.3	.533	18.8	22.8	-1.98	36.19	-.10	-.41
248.7	.533	18.6	21.4	-2.54	35.93	-.11	-.42
373.7	.577	15.6	18.5	-4.64	34.68	-.12	-.49
746.8	.705	9.8	12.5	-3.11	35.83	-.11	-.43
1121.9	.864	5.0	5.2	-2.86	42.05	-.02	-.09
1498.6	1.000	3.6	3.3	-1.64	47.48	.05	.21

T@100-T@30 = .894*T@100-T@30 Undisturbed App. ie Change in del T = .01 .03
T@200-T@30 = .995*T@200-T@30 Undisturbed App. ie Change in del T = .00 .00

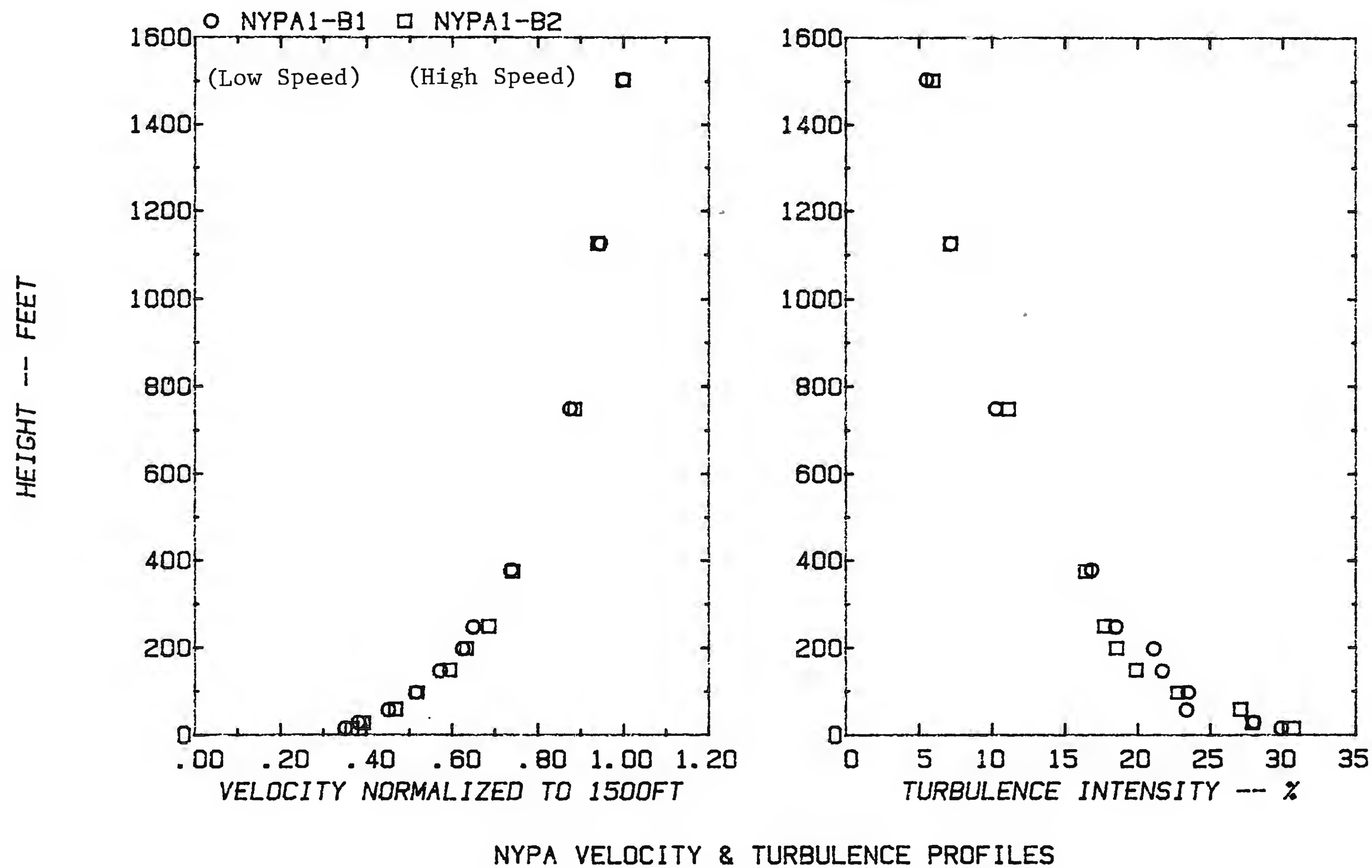

Figure C1. Velocity Independence Check
Neutral Flow

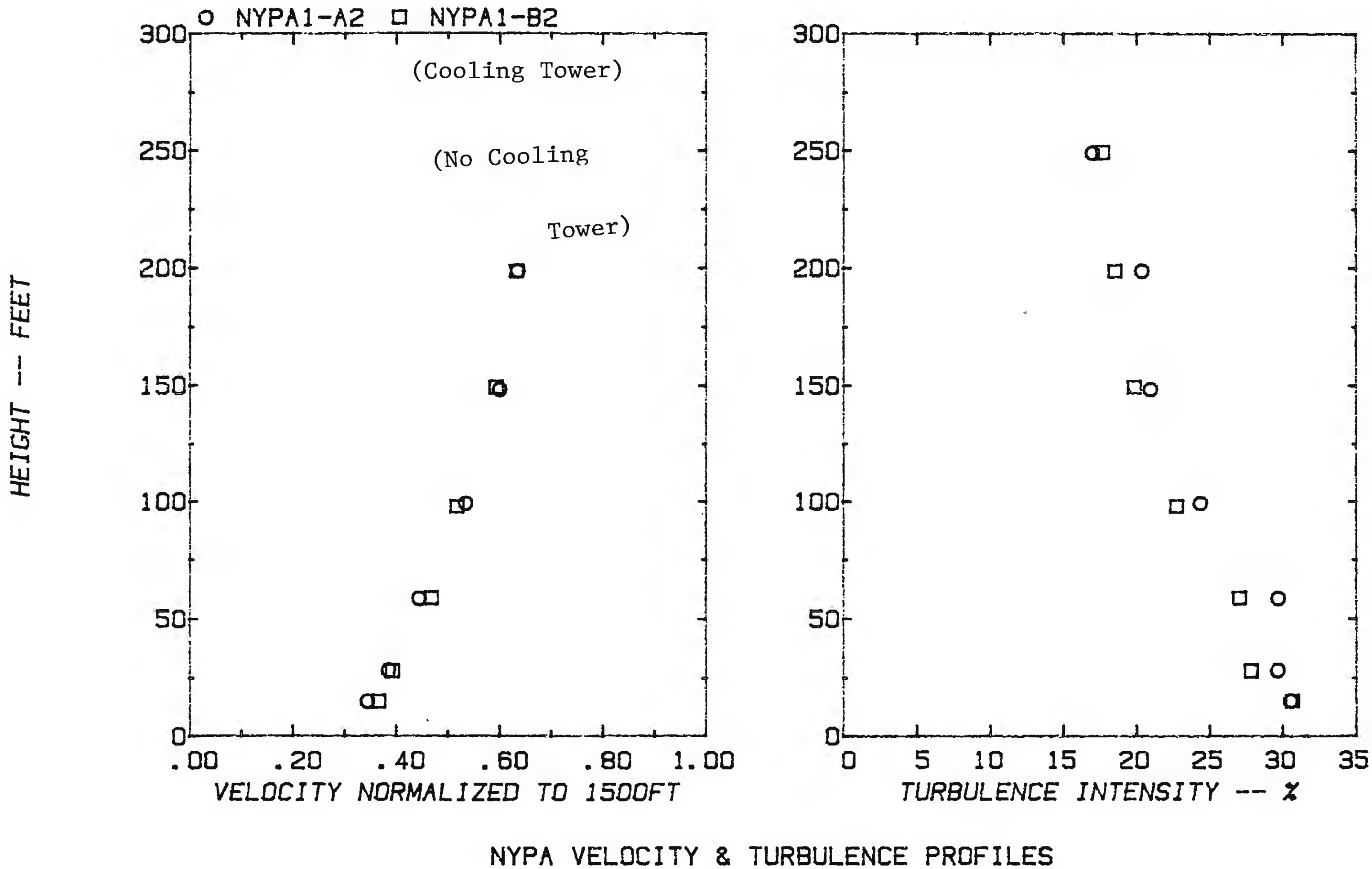

Figure C2. Profiles With and Without Colling Tower
Neutral Flow

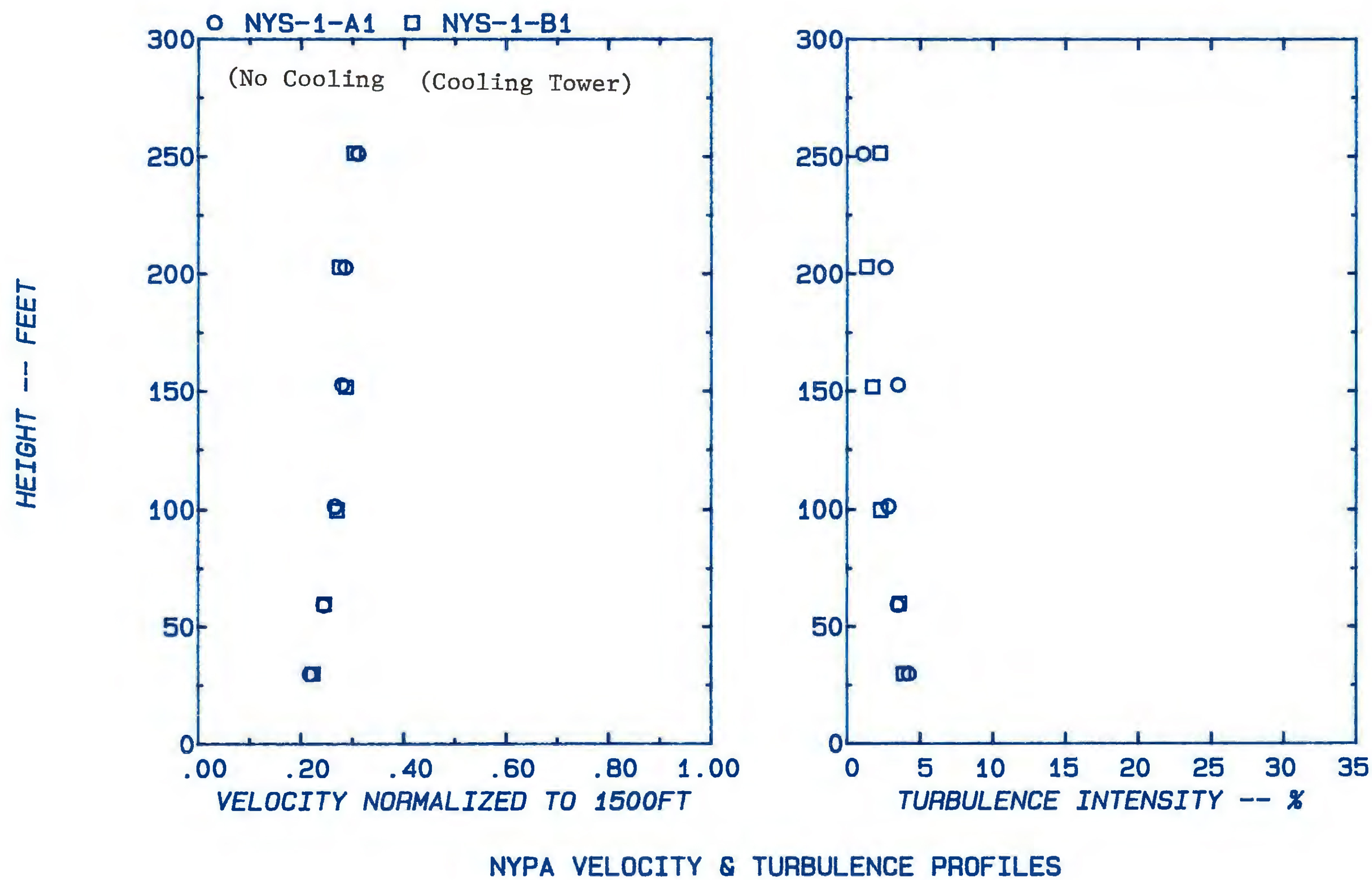

Figure C3. Profiles With and Without Cooling Tower
Stable Flow, Low Speed

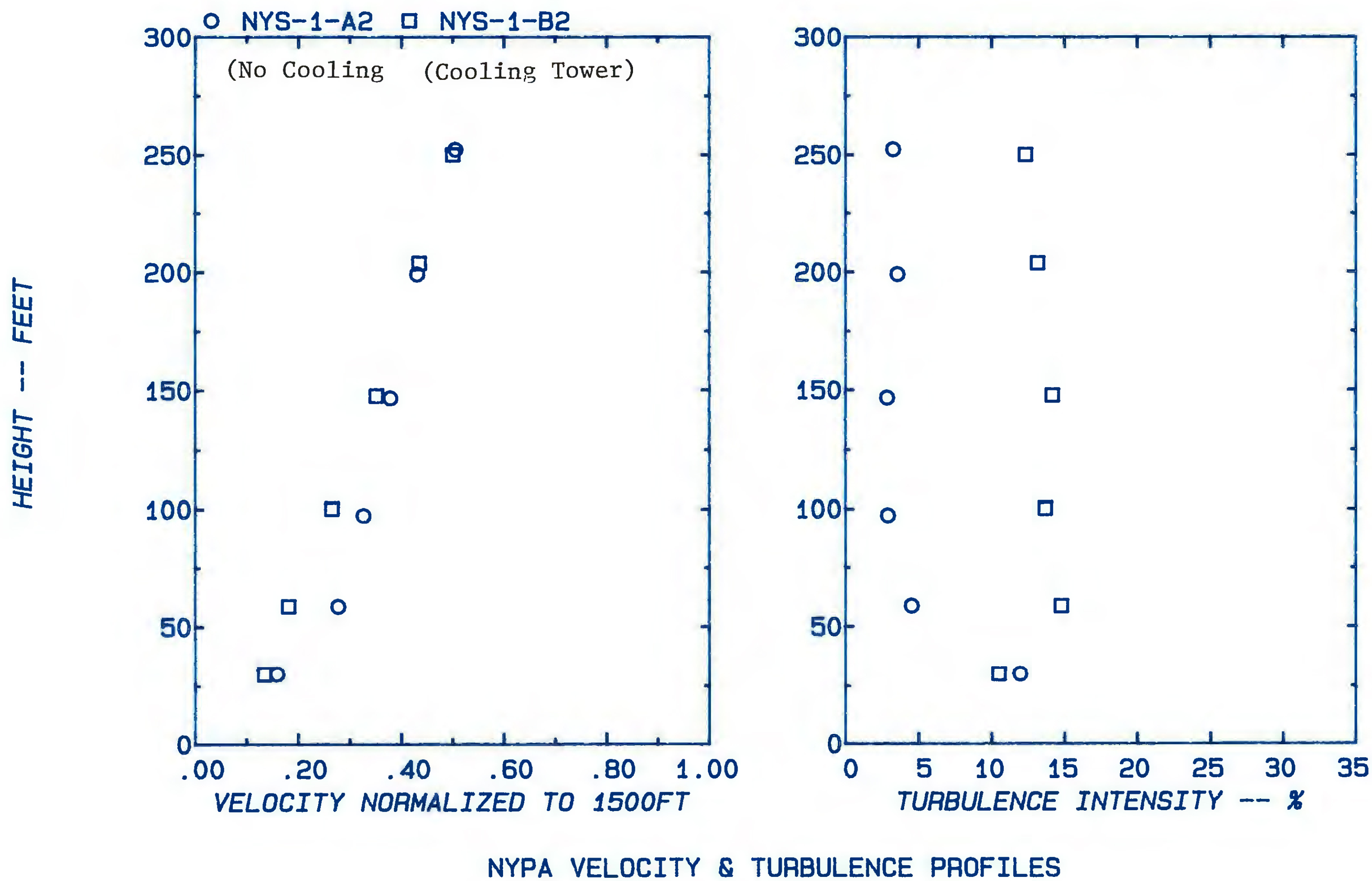

Figure C4. Profiles With and Without Cooling Tower
Stable Flow, High Speed

Tower)

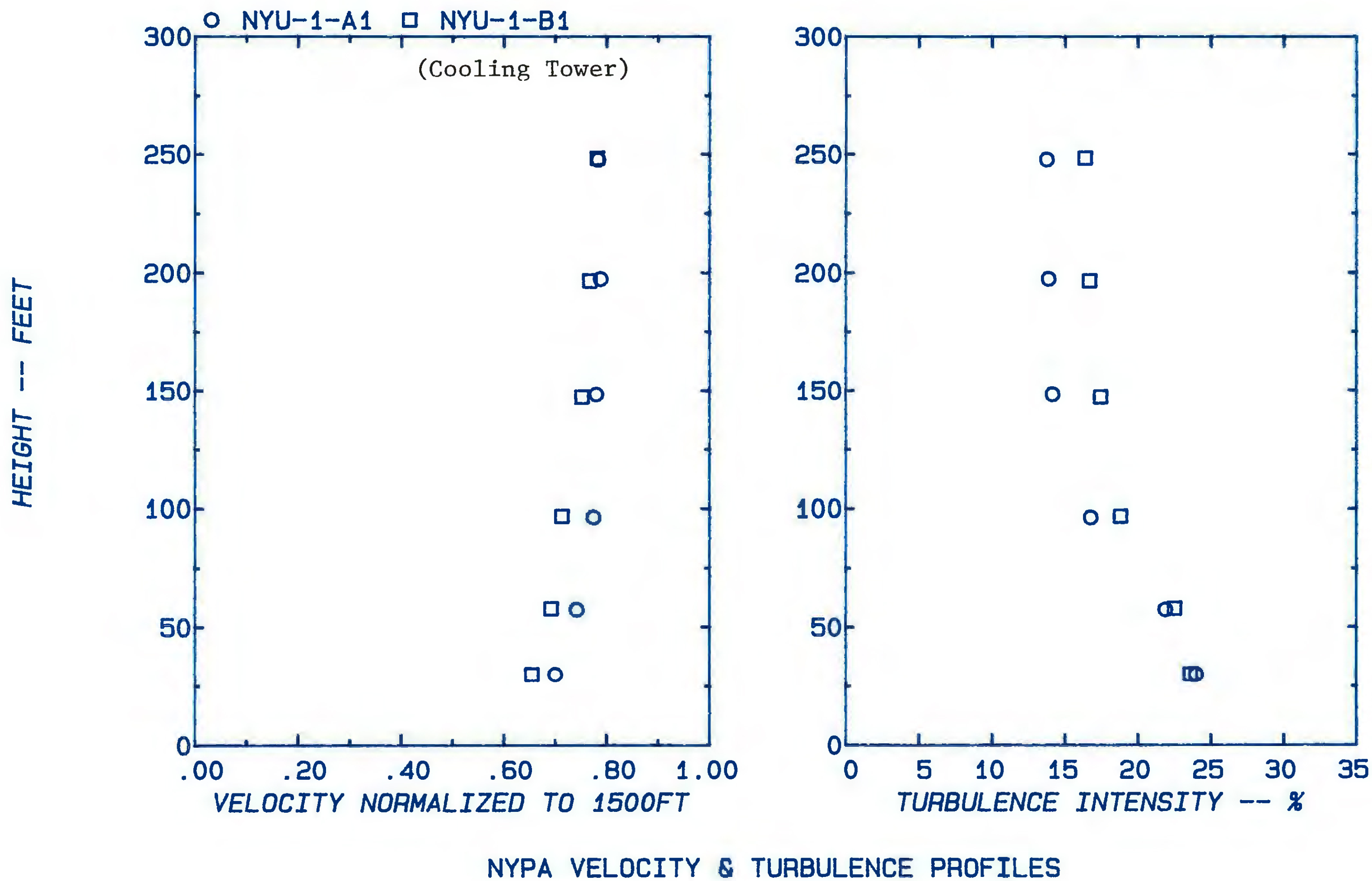

Figure C5. Profiles With and Without Cooling Tower
Unstable Flow, Low Speed

C-16

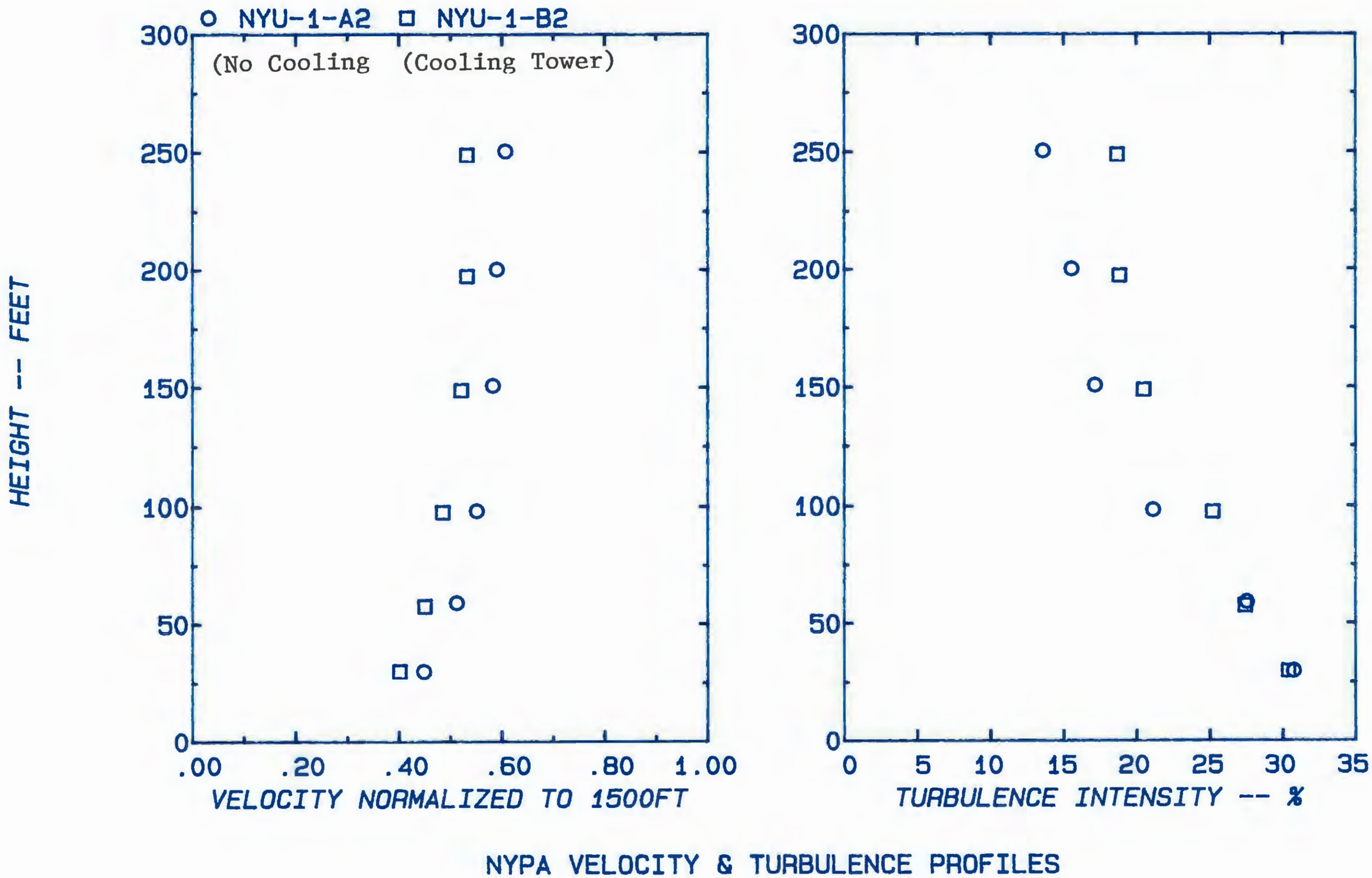

Figure C6. Profiles With and Without Cooling Tower
Unstable Flow, High Speed

Table C3. Task I - $(\bar{U})_c$, $(\Delta T)_c$, and $(TI)_c$

Cooling Tower Caused Changes in $\bar{U}$, ΔT, and TI

Reference (R) Site Condition = Task I, Configuration A

Cooling Tower (CT) Site Condition = Task I, Configuration B

Definition of Terms

$$(\bar{U})_c = \frac{\bar{U}_{CT} - U_R}{U_R} \quad \text{such that} \begin{cases} +(\bar{U})_c & \text{indicates velocity speedup} \\ -(\bar{U})_c & \text{indicates velocity defect} \end{cases}$$

$$(\Delta T)_c = \frac{\Delta T_{CT} - \Delta T_R}{\Delta T_R} \quad \text{such that} \begin{cases} +(\Delta T)_c & \text{indicates increased } \Delta T \\ -(\Delta T)_c & \text{indicates decreased } \Delta T \end{cases}$$

(where $\Delta T = T_h - T_{30'}$)

$$(TI)_c = \frac{TI_{CT} - TI_R}{TI_R} \quad \text{such that} \begin{cases} +(TI)_c & \text{is increased turbulence} \\ -(TI)_c & \text{is decreased turbulence} \end{cases}$$

Parameter	Height (H)	Unstable Low Speed	Unstable High Speed	Neutral Low Speed	Neutral High Speed	Stable Low Speed	Stable High Speed
$(\bar{U})_c$	30	-.066	-.105	.033	.121	.028	-.157
	100	-.079	-.121	.056	.052	.015	-.190
	200	-.027	-.098	-.046	.090	-.038	.009
$(TI)_c$	30	-.025	-.010	-.032	-.051	-.077	-.118
	100	-.102	-.190	-.233	-.083	.192	3.724
	200	.144	.213	.033	-.016	-.500	2.743
$(\Delta T)_c$	100	.109	-.206	X	X	.300	-.095
	200	.118	-.145	X	X	.105	.102

Note: All changes listed are fractional; thus, 0.033 implies a 3.3 percent change.

APPENDIX D

Task II Data: Influence of Primary Meteorological Tower Structure on Wind Speed and Direction Measurement Instrumentation

APPENDIX D - TABLE OF CONTENTS

Table D1. Task II Data - Current Boom Position

Approach Wind Direction	(a) Wind Tunnel Speed, m/sec	Boom Measurements at Current Position (b) Measured Velocity m/sec	Turbulence Intensity % u'/u_∞	Velocity Ratio (b)/(a)	$\Delta\theta$(°)
67 1/2°	15.03	11.93	12.35	0.794	+3.74
67 1/2°	10.00	7.98	12.64	0.798	+4.10
67 1/2°	4.97	4.02	12.47	0.810	+3.74
90°	15.05	9.71	7.90	0.645	-0.83
90°	10.00	6.60	8.40	0.660	-0.83
90°	5.03	3.39	7.97	0.674	-0.25
112 1/2°	15.00	15.10	3.06	1.007	-1.51
112 1/2°	10.01	10.15	2.80	1.014	-1.22
112 1/2°	5.00	5.11	2.42	1.021	-1.22
270°	15.01	13.85	1.33	0.922	+1.12
270°	10.02	9.25	1.13	0.923	+1.48
270°	4.97	4.59	1.07	0.905	+1.48

Table D2. Task II Data - Proposed Boom Location

		Boom Measurements at Proposed Position			
Approach Wind Direction	(a) Wind Tunnel Speed, m/sec	(b) Measured Velocity m/sec	Turbulence Intensity % u'/u_∞	Velocity Ratio (b)/(a)	$\Delta\theta$(°)
67 1/2°	14.98	9.88	7.64	0.660	+2.48
67 1/2°	10.00	6.66	7.67	0.666	+2.70
67 1/2°	5.05	3.30	7.54	0.653	+2.70
90°	15.02	13.66	7.46	0.909	+0.04
90°	10.00	9.44	7.24	0.944	+0.04
90°	5.00	4.71	7.14	0.942	+0.04
112 1/2°	15.03	15.23	1.41	1.013	-0.65
112 1/2°	10.00	10.19	1.19	1.019	-0.11
112 1/2°	5.03	5.14	1.09	1.022	-0.11
270°	15.02	14.43	1.25	0.961	-0.47
270°	10.02	9.62	1.24	0.960	-0.18
270°	5.03	4.81	1.01	0.956	-0.18

Table D3. Task II Addendum Data - Current Boom Position

		Boom Measurements at Current Position			
Approach Wind Direction	(a) Wind Tunnel Speed, m/sec	(b) Measured Velocity m/sec	Turbulence Intensity % u'/u_∞	Velocity Ratio (b)/(a)	$\Delta\theta$(°)
0°	14.96	15.48	1.07	1.035	+1.00
22 1/2°	15.00	15.36	1.73	1.024	-0.08
45°	15.01	9.32	11.70	0.621	-0.22
67 1/2°	15.00	11.91	12.29	0.794	+3.16
90°	15.01	9.78	7.87	0.651	-1.27
112 1/2°	15.02	15.18	2.93	1.011	-2.53
135°	15.01	14.96	1.21	0.997	-1.99
157 1/2°	14.98	14.58	1.17	0.973	-3.75
180°	14.97	14.05	1.15	0.939	-4.11
202 1/2°	15.00	13.68	1.14	0.912	-2.31
225°	15.01	13.56	1.17	0.903	-2.02
247 1/2°	14.98	13.86	1.34	0.925	-1.05
270°	14.96	14.06	1.13	0.940	+0.46
292 1/2°	15.05	14.62	1.46	0.972	+1.72
315°	15.02	14.92	1.09	0.993	+1.68
337 1/2°	15.04	15.23	1.24	1.013	+1.50

Table D4. Task II Addendum Data - Proposed Boom Position

Approach Wind Direction	(a) Wind Tunnel Speed, m/sec	Boom Measurements at Proposed Position: (b) Measured Velocity m/sec	Turbulence Intensity % u'/u_∞	Velocity Ratio (b)/(a)	$\Delta\theta$(°)
0°	15.02	15.75	1.25	1.049	+0.43
22 1/2°	15.02	15.71	1.49	1.046	0
45°	14.98	12.09	12.06	0.807	-0.65
67 1/2°	15.00	9.89	7.59	0.659	+2.84
90°	15.02	14.09	7.34	0.938	+0.04
112 1/2°	15.04	15.46	1.13	1.028	-0.83
135°	14.98	15.09	1.33	1.007	-0.72
157 1/2°	15.05	14.87	1.14	0.988	-2.71
180°	15.02	14.48	1.32	0.964	-2.71
202 1/2°	15.06	14.34	1.31	0.952	-2.67
225°	14.98	14.24	1.16	0.951	-1.92
247 1/2°	15.16	14.81	1.21	0.977	-1.30
270°	15.16	14.93	1.23	0.985	-0.68
292 1/2°	15.17	15.22	1.22	1.003	+0.22
315°	15.19	15.51	1.10	1.021	+0.72
337 1/2°	15.02	15.58	1.07	1.037	+1.12

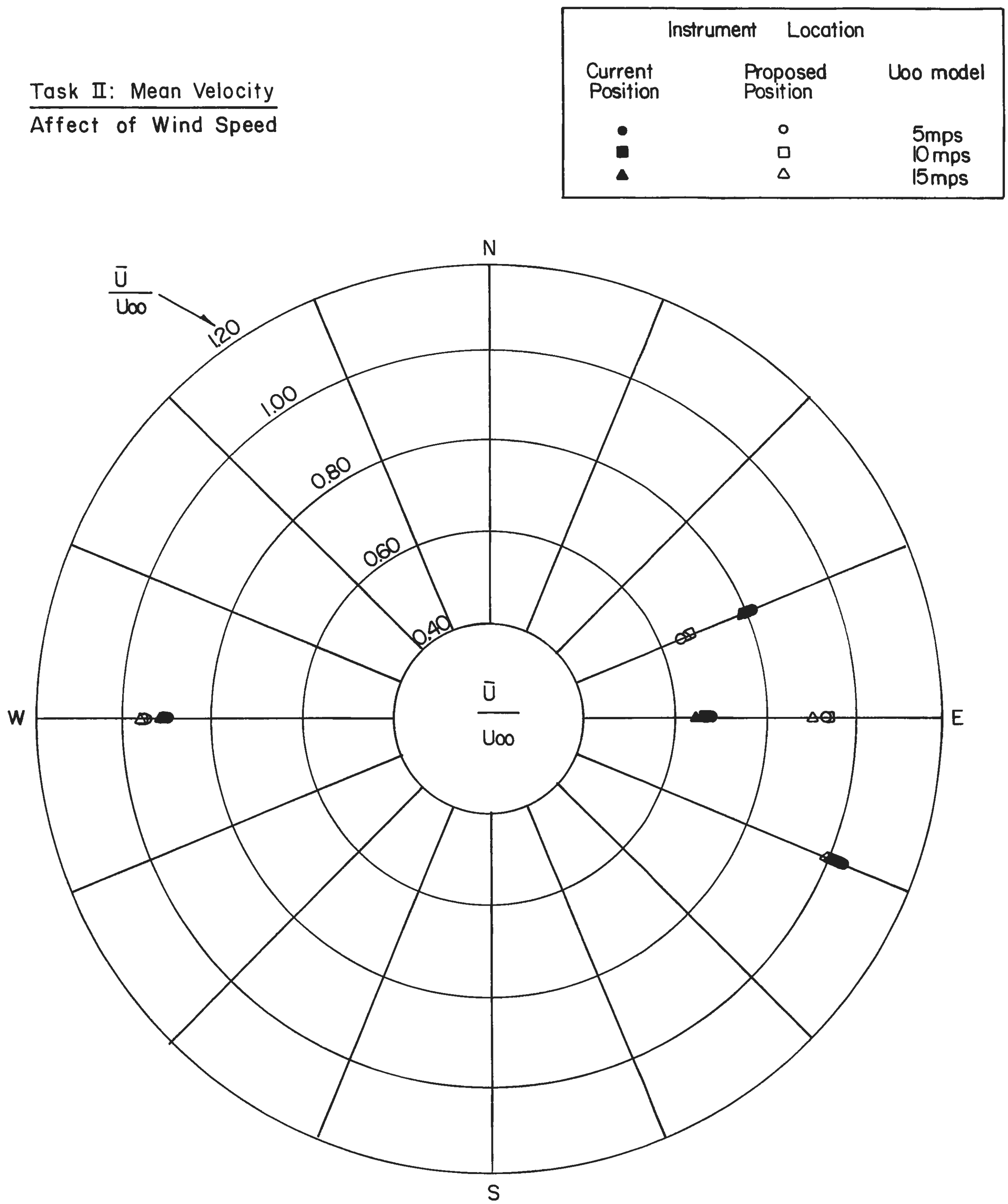

Figure D1. Influence of Wind Speed on Measured Mean Wind Velocity

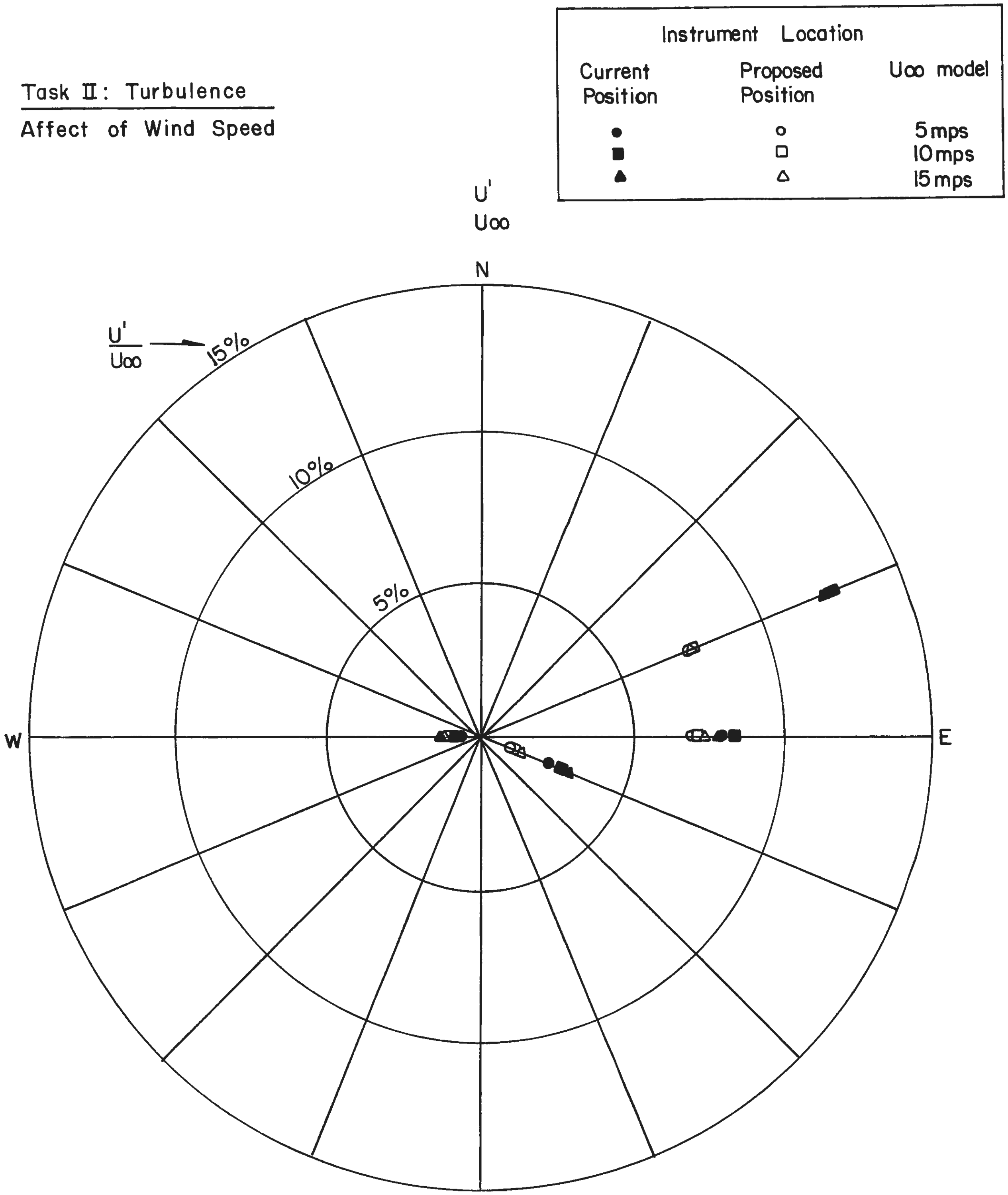

Figure D2. Influence of Wind Speed on Measured Turbulence Intensity

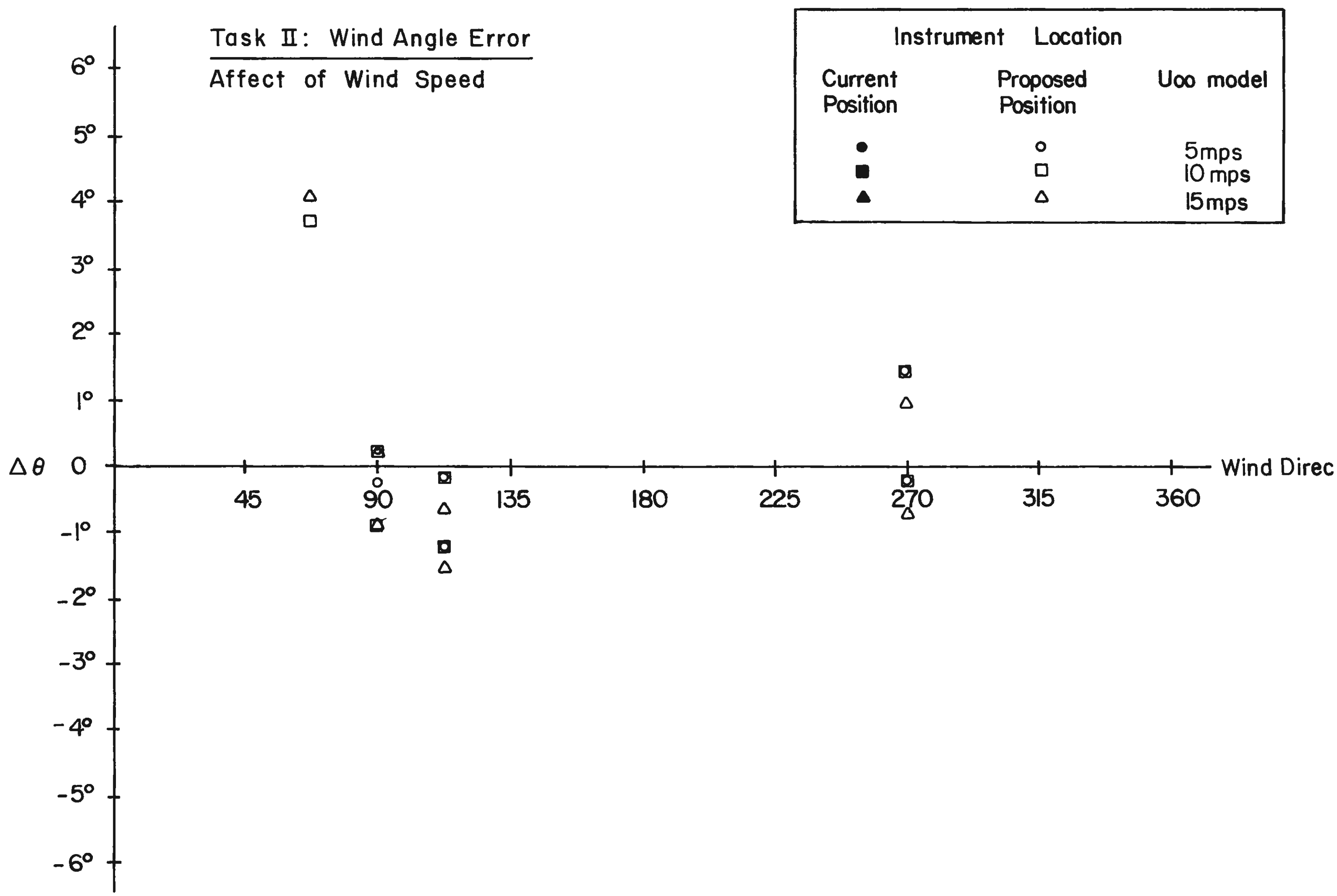

Figure D3. Influence of Wind Speed on Measured Wind Angle

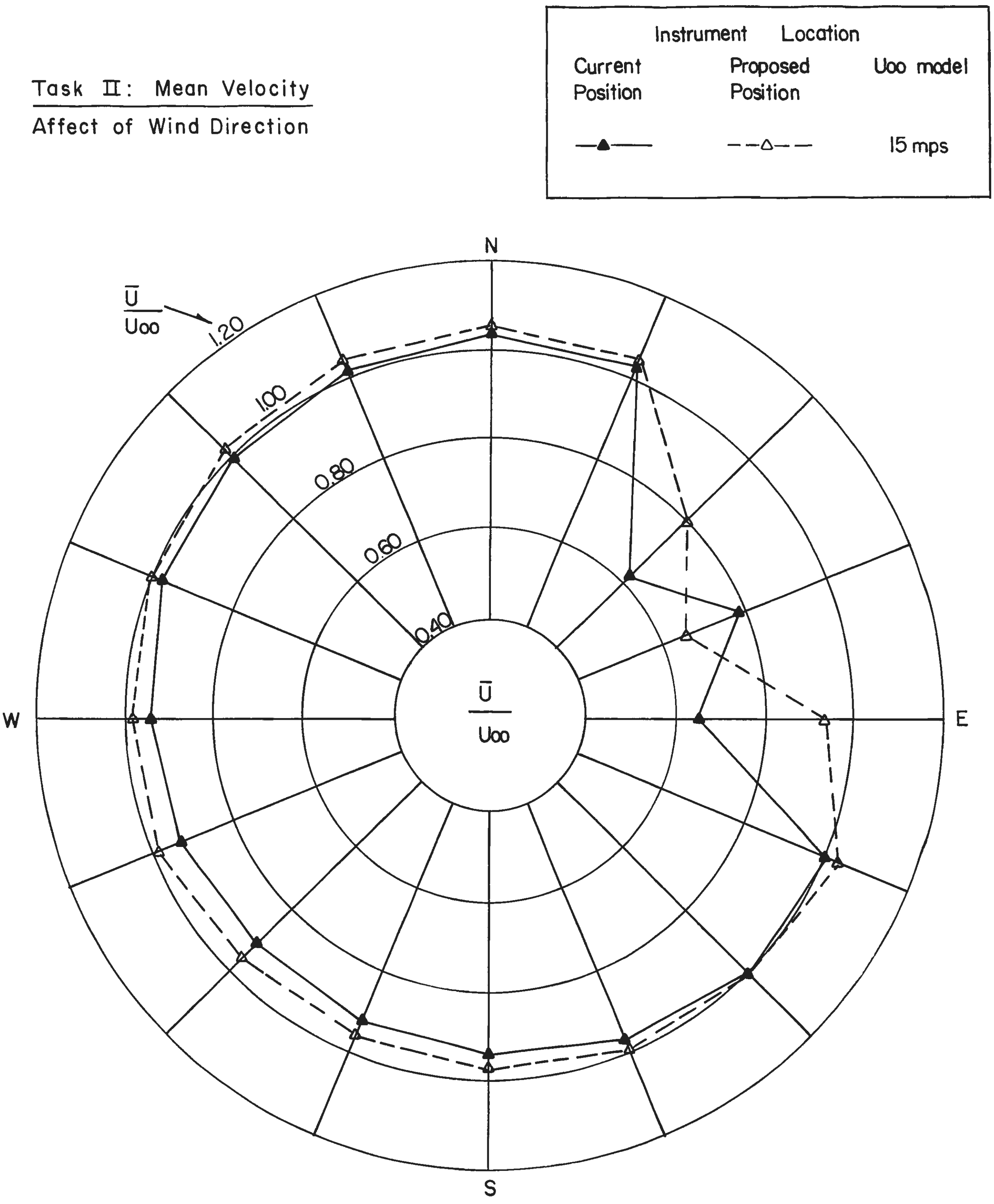

Figure D4. Influence of Wind Direction on Measured Mean Wind Velocity

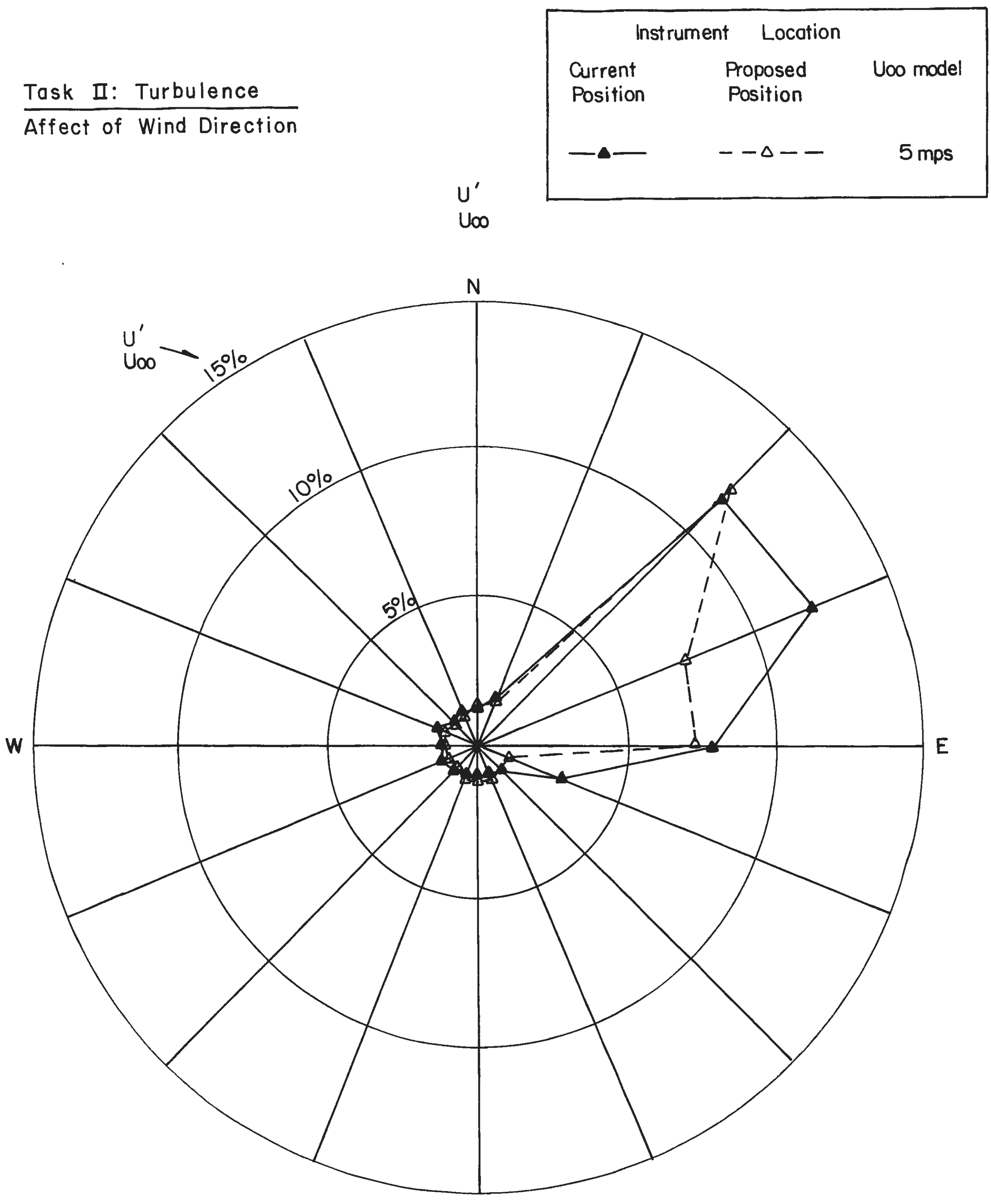

Figure D5. Influence of Wind Direction on Measured Turbulence Intensity

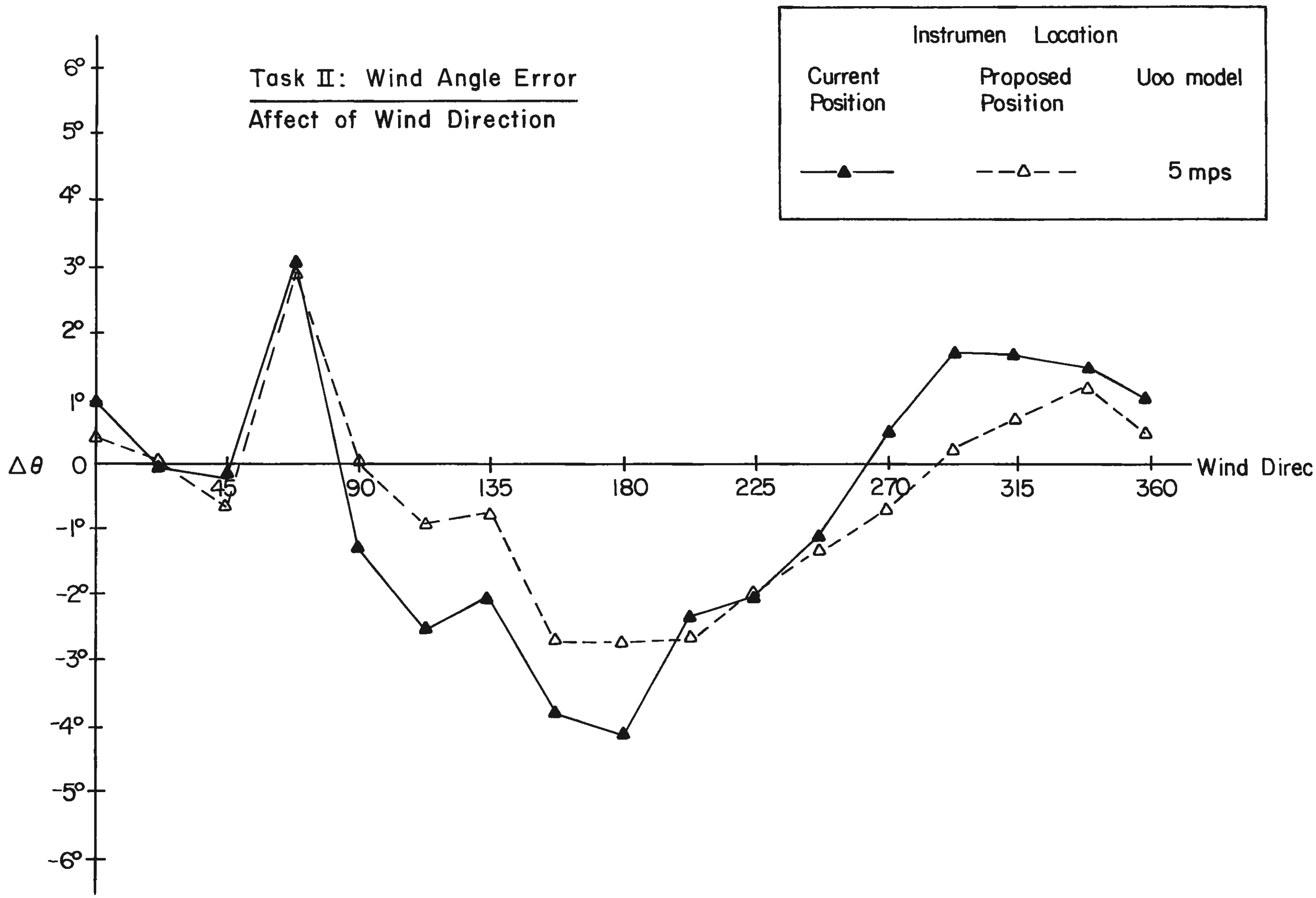

Figure D6. Influence of Wind Direction on Measured Wind Angle

APPENDIX E

Task III Data: Site Influences on Velocity, Turbulence, Wind Angle, and Temperature Measurements at the Backup Meteorological Tower Location for Neutral, Stable, and Unstable Flow Conditions

APPENDIX E - TABLE OF CONTENTS

Task I: Data File Name Code

Example File Name } NY ___ ___ # - ___ #

- NY — New York
- ___ ___ — Flow Condition (Letters)
- # — Task #
- ___ — Configuration (Letters)
- # — Free Stream Velocity Code

Flow Condition:

PA = Neutral
S- = Stable
U- = Unstable

Task #:

1 = Task 1
3 = Task 3 ←
4 = Task 4

Configuration:

A; 3 power plant buildings in place - no cooling tower

B; 3 power plant buildings in place - with cooling tower

C; 3 power plant buildings, cooling tower, and new JAF service building

Free Stream Velocity Code:

1	=	Lower speed	≈	5.6 mph	neutral
				1.6 mph	stable
				1.1 mph	unstable
2	=	Higher speed	≈	11.2 mph	neutral
				3.2 mph	stable
				2.1 mph	unstable

Table E1. Task III Data Summary and Guide

Data File Name	Flow Condition	Conf.	NMP Units 1 and 2	JAF Bldg.	JAF New Service Bldg.	Cooling Tower	Approx. Free Stream Velocity (mph)
NYPA3-A1	Neutral	A	X	X			5.6
NYPA3-A2	Neutral	A	X	X			11.2
NYPA3-B1	Neutral	B	X	X		X	5.6
NYPA3-B2	Neutral	B	X	X		X	11.2
NYPA3-C1	Neutral	C	X	X	X	X	5.6
NYPA3-C2	Neutral	C	X	X	X	X	11.2
NYS-3-A1	Stable	A	X	X			1.6
NYS-3-B1	Stable	B	X	X		X	1.6
NYS-3-A2	Stable	A	X	X			3.2
NYS-3-B2	Stable	B	X	X		X	3.2
NYU-3-A1	Unstable	A	X	X			1.1
NYU-3-B1	Unstable	B	X	X		X	1.1
NYU-3-A2	Unstable	A	X	X			2.1
NYU-3-B2	Unstable	B	X	X		X	2.2

Table E2. Task III Velocity Profile Figure Guide

Figure #	1st Profile	2nd Profile	3rd Profile	Flow Condition	Comments
E1	NYPA3-A2	NYPA3-B2	NYPA3-C2	Neutral	Profiles with and without cooling tower
E2	NYS-3-A1	NYS-3-B1	-	Stable	Profiles with and without cooling tower
E3	NYS-3-A2	NYS-3-B2	-	Stable	Profiles with and without cooling tower
E4	NYU-3-A1	NYU-3-B1	-	Unstable	Profiles with and without cooling tower
E5	NYU-3-A2	NYU-3-B2	-	Unstable	Profiles with and without cooling tower

Profile Name : NYPA-3-A1
Flow Condition : Neutral, Low speed
Task Number : 3
Configuration : A
Ref. Height : 1500.0 ft
Ref. Model Velocity : 4.92 mph

Height (ft)	Velocity (Normalized)	Turb. Int. (%)
15.01	.328	30.1
27.56	.389	26.4
58.33	.418	25.9
97.46	.514	24.2
148.89	.563	22.2
198.11	.631	21.9
248.56	.658	18.1
374.07	.739	13.9
748.14	.86	9.6
1124.68	.959	7
1498.75	1	6.17

Profile Name : NYPA-3-A2
Flow Condition : Neutral, High speed
Task Number : 3
Configuration : A
Ref. Height : 1500.0 ft
Ref. Model Velocity : 10.38 mph

Height (ft)	Velocity (Normalized)	Turb. Int. (%)	del Theta (deg)
15.01	.388	30.2	
28.55	.425	26.8	10.37
59.06	.45	26.6	
97.95	.508	25.3	.07
147.41	.594	22.3	
196.88	.672	19.2	-1.66
248.56	.714	17.6	
374.07	.741	13.1	
748.14	.871	9.7	
1124.68	.954	6.8	
1500.00	1	5.3	

Profile Name : NYPA-3-B1
Flow Condition : Neutral, Low speed
Task Number : 3
Configuration : B
Ref. Height : 1500.0 ft
Ref. Model Velocity : 5.12 mph

Height (ft)	Velocity (Normalized)	Turb. Int. (%)
15.01	.299	29.1
28.55	.392	28.1
59.31	.441	28.9
97.95	.476	23.8
147.91	.576	20.7
198.60	.568	18.9
248.56	.668	17.9
374.07	.747	16.5
748.14	.869	11.4
1124.68	.939	7.5
1500.00	1	5.8

Profile Name : NYPA-3-B2
Flow Condition : Neutral, High speed
Task Number : 3
Configuration : B
Ref. Height : 1500.0 ft
Ref. Model Velocity : 9.60 mph

Height (ft)	Velocity (Normalized)	Turb. Int. (%)	del Theta (deg)
15.01	.352	30.4	
28.79	.387	29	7.56
59.80	.436	27.4	
96.72	.515	23.9	-.29
147.66	.578	19.3	
197.13	.632	18	-1.66
246.10	.683	16.6	
374.07	.713	16.6	
753.07	.872	11.6	
1124.68	.949	6.7	
1500.00	1	5.5	

Profile Name : NYPA-3-C1
Flow Condition : Neutral, Low speed
Task Number : 3
Configuration : C
Ref. Height : 1500.0 ft
Ref. Model Velocity : 4.52 mph

Height (ft)	Velocity (Normalized)	Turb. Int. (%)
15.01	.361	30.6
29.29	.391	26.8
58.33	.428	26.1
98.69	.509	25.1
147.91	.542	22.8
199.83	.636	17.4
251.02	.631	20
374.07	.743	15.3
750.61	.883	12
1127.14	.972	8.7
1500.00	1	6

Profile Name : NYPA-3-C2
Flow Condition : Neutral, High speed
Task Number : 3
Configuration : C
Ref. Height : 1500.0 ft
Ref. Model Velocity : 9.91 mph

Height (ft)	Velocity (Normalized)	Turb. Int. (%)	del Theta (deg)
15.01	.35	29.9	
28.30	.381	29.6	7.74
57.10	.46	27.1	
97.95	.499	24.4	.07
147.17	.551	23.3	
198.60	.634	18.6	-1.44
248.56	.657	18.1	
376.53	.713	16.6	
748.14	.878	10.2	
1124.68	.973	5.7	
1498.75	1	5.3	

Profile Name : NYS-3-A1
Flow Condition : Stable, Low speed
Task Number : 3
Configuration : A
Ref. Height : 1500.0 ft
Ref. Model Velocity : 1.61 mph

Height (ft)	Velocity (Normalized)	Turb. Int. (%) u	Turb. Int. (%) v	del Theta (deg)	Model Temp (deg C)	Delta Temperature (Deg C) 4 mph Field	Delta Temperature (Deg C) 8 mph Field
30.0	.224	3.6	2.7	-1.13	5.56	.00	.00
57.0	.243	2.9	1.8	-1.13	8.41	.30	1.20
101.7	.276	1.9	1.3	-1.18	14.52	.94	3.78
150.9	.285	2.2	1.8	.88	18.38	1.35	5.40
200.1	.279	1.6	1.8	-1.00	20.81	1.61	6.43
251.9	.311	2.3	2.4	1.70	25.41	2.09	8.37
376.4	.329	2.5	1.8	-1.31	29.66	2.54	10.16
747.2	.446	3.7	2.3	-.36	32.92	2.88	11.54
1125.8	.650	5.4	4.3	-.70	36.05	3.21	12.86
1497.3	1.000	5.1	3.5	-.89	40.39	3.67	14.68

T@100-T@30 = 1.149*T@100-T@30 Undisturbed App. ie Change in del T = .12 .49
T@200-T@30 = .982*T@200-T@30 Undisturbed App. ie Change in del T = -.03 -.12

Profile Name : NYS-3-B1
Flow Condition : Stable, Low speed
Task Number : 3
Configuration : B
Ref. Height : 1500.0 ft
Ref. Model Velocity : 1.64 mph

Height (ft)	Velocity (Normalized)	Turb. Int. (%) u	Turb. Int. (%) v	del Theta (deg)	Model Temp (deg C)	Delta Temperature (Deg C) 4 mph Field	Delta Temperature (Deg C) 8 mph Field
30.0	.217	3.7	2.8	-.83	5.55	.00	.00
61.2	.236	2.5	1.8	-.89	8.20	.28	1.12
98.1	.265	2.1	1.3	-1.03	13.72	.86	3.44
150.9	.288	2.2	1.2	.90	19.09	1.43	5.71
201.2	.281	1.6	2.0	-.09	21.44	1.67	6.70
250.4	.304	1.5	1.6	1.83	25.37	2.09	8.36
372.6	.306	1.4	1.6	-1.20	28.25	2.39	9.57
749.5	.452	4.0	2.5	-1.11	32.62	2.85	11.41
1123.8	.695	5.5	3.7	-.05	36.55	3.27	13.07
1500.7	1.000	4.7	3.5	-.97	40.53	3.69	14.75

T@100-T@30 = 1.048*T@100-T@30 Undisturbed App. ie Change in del T = .04 .16
T@200-T@30 = 1.023*T@200-T@30 Undisturbed App. ie Change in del T = .04 .15

Profile Name : NYS-3-A2
Flow Condition : Stable, High speed
Task Number : 3
Configuration : A
Ref. Height : 1500.0 ft
Ref. Model Velocity : 3.19 mph

Height (ft)	Velocity (Normalized)	Turb. Int. (%) u	Turb. Int. (%) v	del Theta (deg)	Model Temp (deg C)	Delta Temperature (Deg C) 4 mph Field	Delta Temperature (Deg C) 8 mph Field
30.0	.224	15.8	17.4	10.12	20.67	.00	.00
60.3	.247	15.5	17.4	4.18	21.53	.01	.04
96.4	.296	13.0	13.0	-1.83	23.04	.03	.11
148.1	.395	6.0	5.7	-1.88	26.38	.06	.26
198.1	.462	4.4	3.2	-1.31	29.55	.10	.40
246.9	.500	3.4	2.8	-1.60	31.66	.12	.49
374.5	.627	2.7	2.7	-.52	35.91	.17	.68
748.0	.867	3.1	4.2	-.03	41.76	.24	.94
1126.0	.952	3.2	3.8	.64	43.78	.26	1.04
1497.2	1.000	1.9	2.9	.48	45.76	.28	1.12

T@100-T@30 = .214*T@100-T@30 Undisturbed App. ie Change in del T = -.10 -.39
T@200-T@30 = .543*T@200-T@30 Undisturbed App. ie Change in del T = -.08 -.33

Profile Name : NYS-3-B2
Flow Condition : Stable, High speed
Task Number : 3
Configuration : B
Ref. Height : 1500.0 ft
Ref. Model Velocity : 3.19 mph

Height (ft)	Velocity (Normalized)	Turb. Int. (%) u	Turb. Int. (%) v	del Theta (deg)	Model Temp (deg C)	Delta Temperature (Deg C) 4 mph Field	Delta Temperature (Deg C) 8 mph Field
30.0	.162	16.5	14.3	9.32	18.36	.00	.00
58.5	.201	19.0	18.7	10.31	21.87	.04	.16
97.7	.252	21.3	19.7	6.16	25.05	.07	.30
148.6	.347	19.3	16.8	1.36	28.95	.12	.47
196.3	.440	14.8	14.7	-1.73	31.92	.15	.61
249.1	.503	12.3	13.2	-3.09	33.92	.17	.70
376.8	.615	9.3	11.3	-2.20	36.86	.21	.83
747.4	.869	3.2	4.4	.06	42.06	.27	1.06
1123.1	.928	3.8	4.8	.63	43.97	.29	1.15
1496.7	1.000	1.8	3.0	.47	45.84	.31	1.23

T@100-T@30 = .602*T@100-T@30 Undisturbed App. ie Change in del T = -.05 -.20
T@200-T@30 = .830*T@200-T@30 Undisturbed App. ie Change in del T = -.03 -.12

Profile Name : NYU-3-A1
Flow Condition : Unstable, Low speed
Task Number : 3
Configuration : A
Ref. Height : 1500.0 ft
Ref. Model Velocity : 1.09 mph

Height (ft)	Velocity (Normalized)	Turb. Int. (%) u	v	del Theta (deg)	Model Temp (deg C)	Delta Temperature (Deg C) 4 mph Field	8 mph Field
30.0	.658	26.4	21.3	-1.33	41.14	.00	.00
57.9	.685	19.1	22.5	-2.91	38.45	-.08	-.32
97.4	.719	15.6	23.2	-5.75	37.30	-.11	-.46
147.7	.730	14.7	19.8	-3.15	36.26	-.15	-.58
198.8	.752	12.2	17.5	-5.35	35.54	-.17	-.67
249.3	.755	11.9	18.3	-4.04	35.60	-.16	-.66
373.8	.777	11.4	16.4	-2.31	36.03	-.15	-.61
750.0	.796	7.3	7.8	-.33	39.52	-.05	-.19
1122.1	.867	4.5	2.5	.19	44.59	.10	.41
1498.7	1.000	2.5	2.1	-.82	46.09	.15	.59

T@100-T@30 = .758*T@100-T@30 Undisturbed App. ie Change in del T = .04 .15
T@200-T@30 = 1.110*T@200-T@30 Undisturbed App. ie Change in del T = -.02 -.07

Profile Name : NYU-3-B1
Flow Condition : Unstable, Low speed
Task Number : 3
Configuration : B
Ref. Height : 1500.0 ft
Ref. Model Velocity : 1.14 mph

Height (ft)	Velocity (Normalized)	Turb. Int. (%) u	v	del Theta (deg)	Model Temp (deg C)	Delta Temperature (Deg C) 4 mph Field	8 mph Field
30.0	.591	26.7	22.4	.55	47.73	.00	.00
57.7	.656	24.7	27.5	-.40	45.67	-.06	-.25
97.5	.673	21.3	28.6	-.62	43.56	-.12	-.50
148.5	.700	19.6	24.0	1.44	41.34	-.19	-.76
201.4	.719	19.3	23.4	3.98	41.86	-.17	-.70
249.4	.698	17.0	25.6	5.38	40.63	-.21	-.85
374.8	.712	15.8	25.2	6.77	39.60	-.24	-.97
748.5	.734	13.3	18.3	.90	39.55	-.24	-.98
1127.8	.934	3.5	3.2	.05	45.05	-.08	-.32
1499.4	1.000	2.6	2.1	.48	46.52	-.04	-.14

T@100-T@30 = .823*T@100-T@30 Undisturbed App. ie Change in del T = .03 .11
T@200-T@30 = 1.165*T@200-T@30 Undisturbed App. ie Change in del T = -.02 -.10

Profile Name : NYU-3-A2
Flow Condition : Unstable, High speed
Task Number : 3
Configuration : A
Ref. Height : 1500.0 ft
Ref. Model Velocity : 2.06 mph

Height (ft)	Velocity (Normalized)	Turb. Int. (%) u	Turb. Int. (%) v	del Theta (deg)	Model Temp (deg C)	Delta Temperature (Deg C) 4 mph Field	Delta Temperature (Deg C) 8 mph Field
30.0	.419	29.3	27.9	1.06	42.69	.00	.00
58.0	.460	27.9	27.6	-.94	40.39	-.03	-.13
96.2	.508	24.6	23.3	-4.51	37.69	-.07	-.27
147.0	.557	20.1	18.2	-4.57	35.68	-.10	-.38
198.9	.602	14.3	15.1	-5.83	34.46	-.11	-.45
247.7	.621	11.8	13.5	-5.71	33.48	-.13	-.50
374.3	.633	10.4	12.2	-4.33	33.30	-.13	-.51
747.9	.689	8.1	11.9	-2.06	34.48	-.11	-.45
1122.1	.866	5.6	5.1	-1.76	40.70	-.03	-.11
1499.1	1.000	3.2	3.3	-.92	47.42	.06	.26

T@100-T@30 = .907*T@100-T@30 Undisturbed App. ie Change in del T = .01 .03
T@200-T@30 = 1.094*T@200-T@30 Undisturbed App. ie Change in del T = -.01 -.04

Profile Name : NYU-3-B2
Flow Condition : Unstable, High speed
Task Number : 3
Configuration : B
Ref. Height : 1500.0 ft
Ref. Model Velocity : 2.14 mph

Height (ft)	Velocity (Normalized)	Turb. Int. (%) u	Turb. Int. (%) v	del Theta (deg)	Model Temp (deg C)	Delta Temperature (Deg C) 4 mph Field	Delta Temperature (Deg C) 8 mph Field
30.0	.392	28.9	27.0	.27	42.78	.00	.00
56.5	.433	26.4	28.5	-1.79	40.98	-.02	-.10
96.4	.460	24.2	25.2	-2.21	38.55	-.06	-.23
147.6	.486	22.6	24.8	-.89	37.39	-.07	-.29
196.7	.509	22.1	22.4	-3.03	36.90	-.08	-.32
249.1	.550	18.3	21.7	-4.71	35.68	-.10	-.39
373.8	.576	16.6	19.7	-5.62	35.27	-.10	-.41
747.2	.726	9.7	12.5	-5.07	36.01	-.09	-.37
1122.0	.874	6.0	5.1	-3.12	42.45	.00	-.02
1496.7	1.000	3.8	3.1	-1.53	47.50	.06	.26

T@100-T@30 = .768*T@100-T@30 Undisturbed App. ie Change in del T = .02 .07
T@200-T@30 = .783*T@200-T@30 Undisturbed App. ie Change in del T = .02 .09

Conf. A - No Cooling Tower, No JAF Service Building
Conf. B - Cooling Tower, No JAF Service Building
Conf. C - Cooling Tower, JAF Service Building

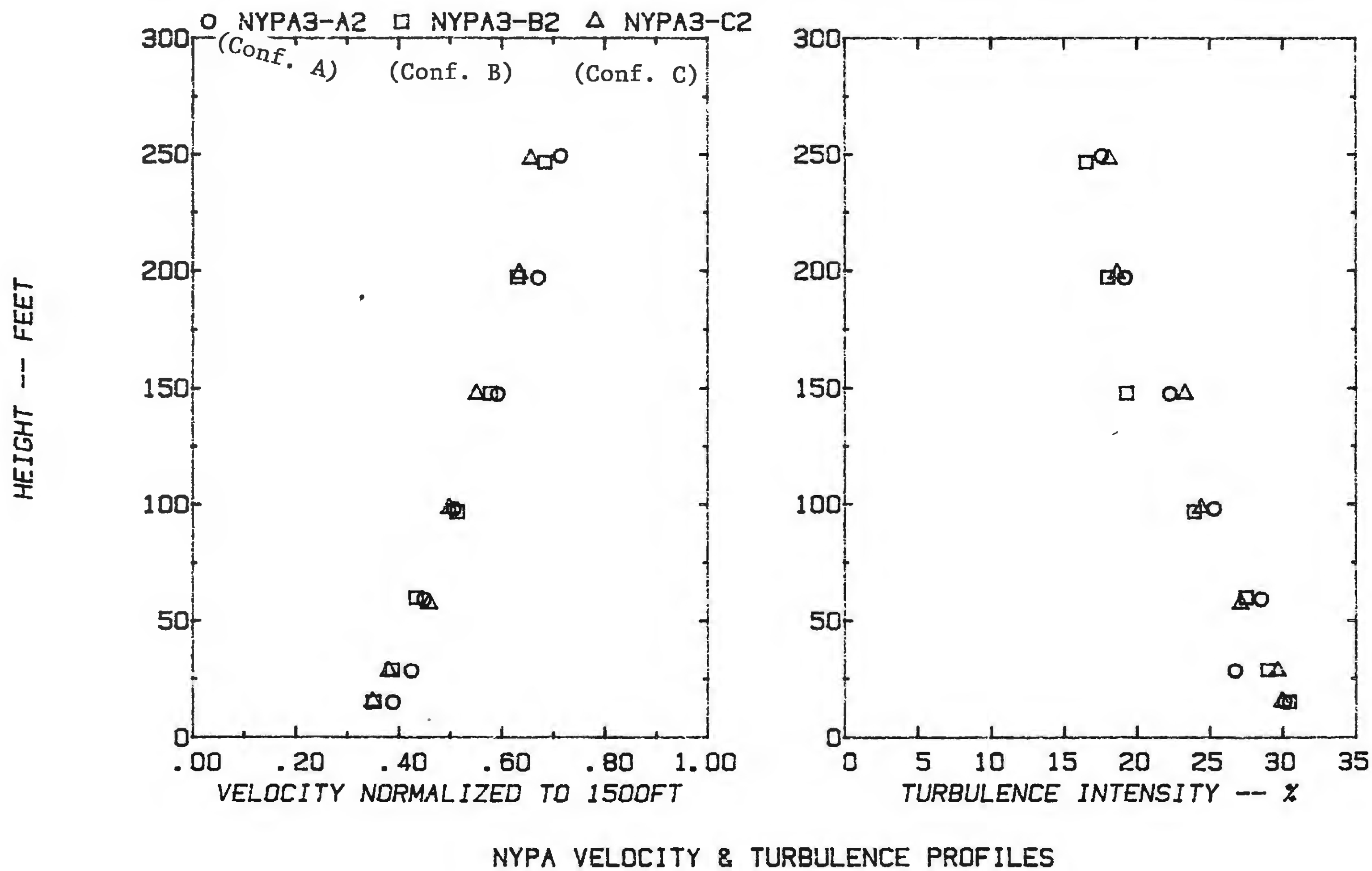

Figure E1. Profiles With and Without Cooling Tower
Neutral Flow, High Speed

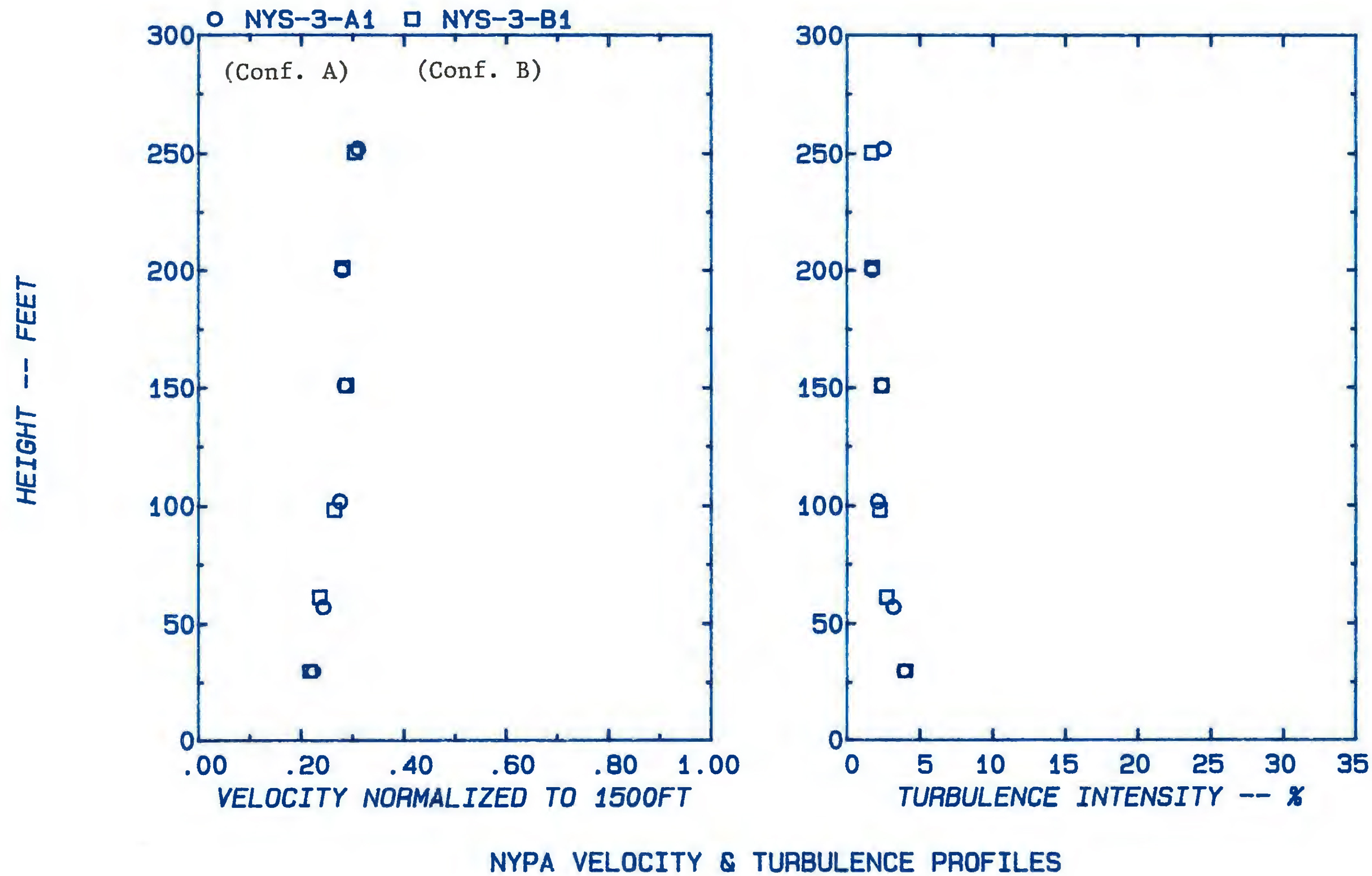

Figure E2. Profiles With and Without Cooling Tower
Stable Flow, Low Speed

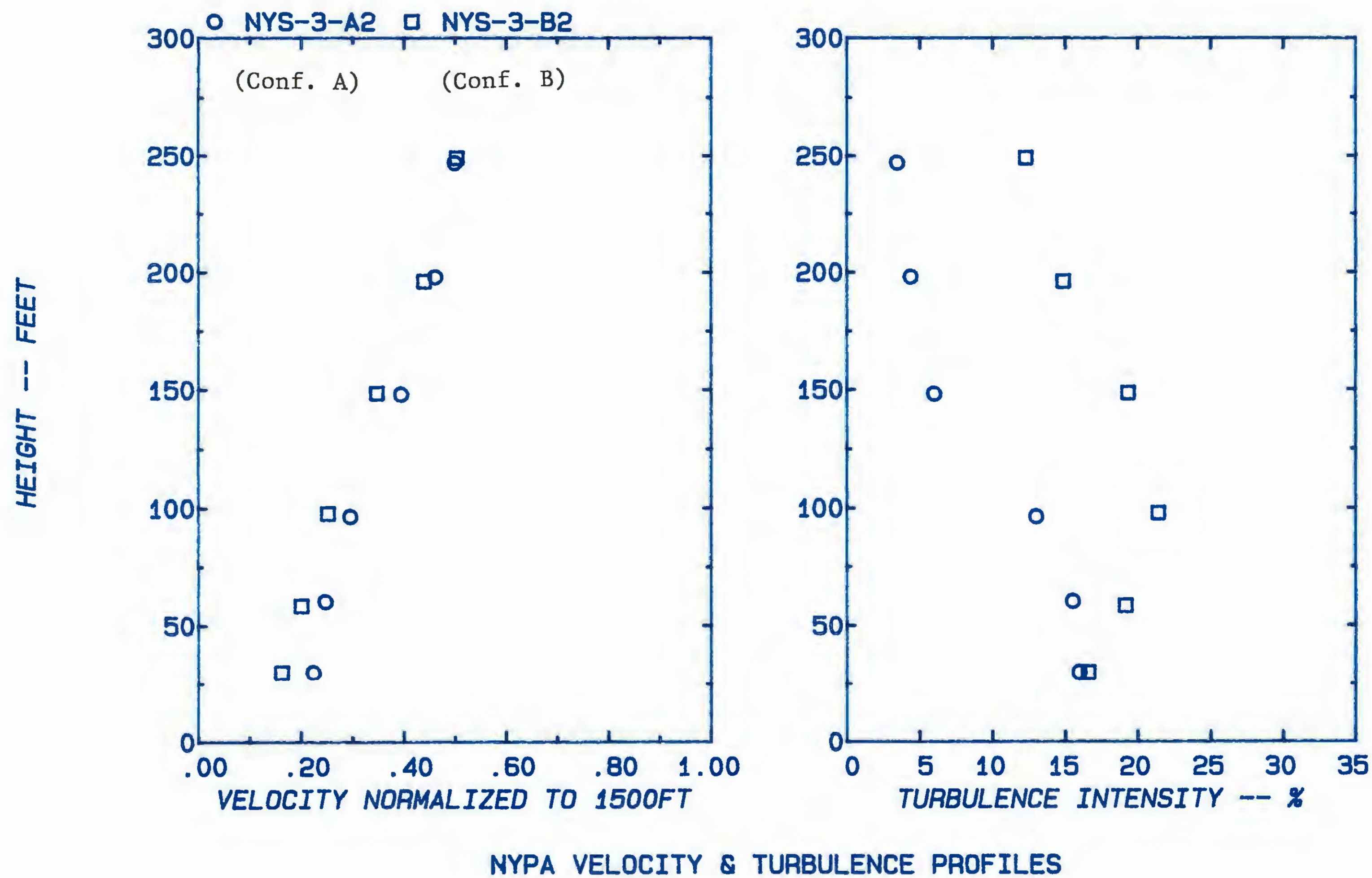

Figure E3. Profiles With and Without Cooling Tower
Stable Flow, High Speed

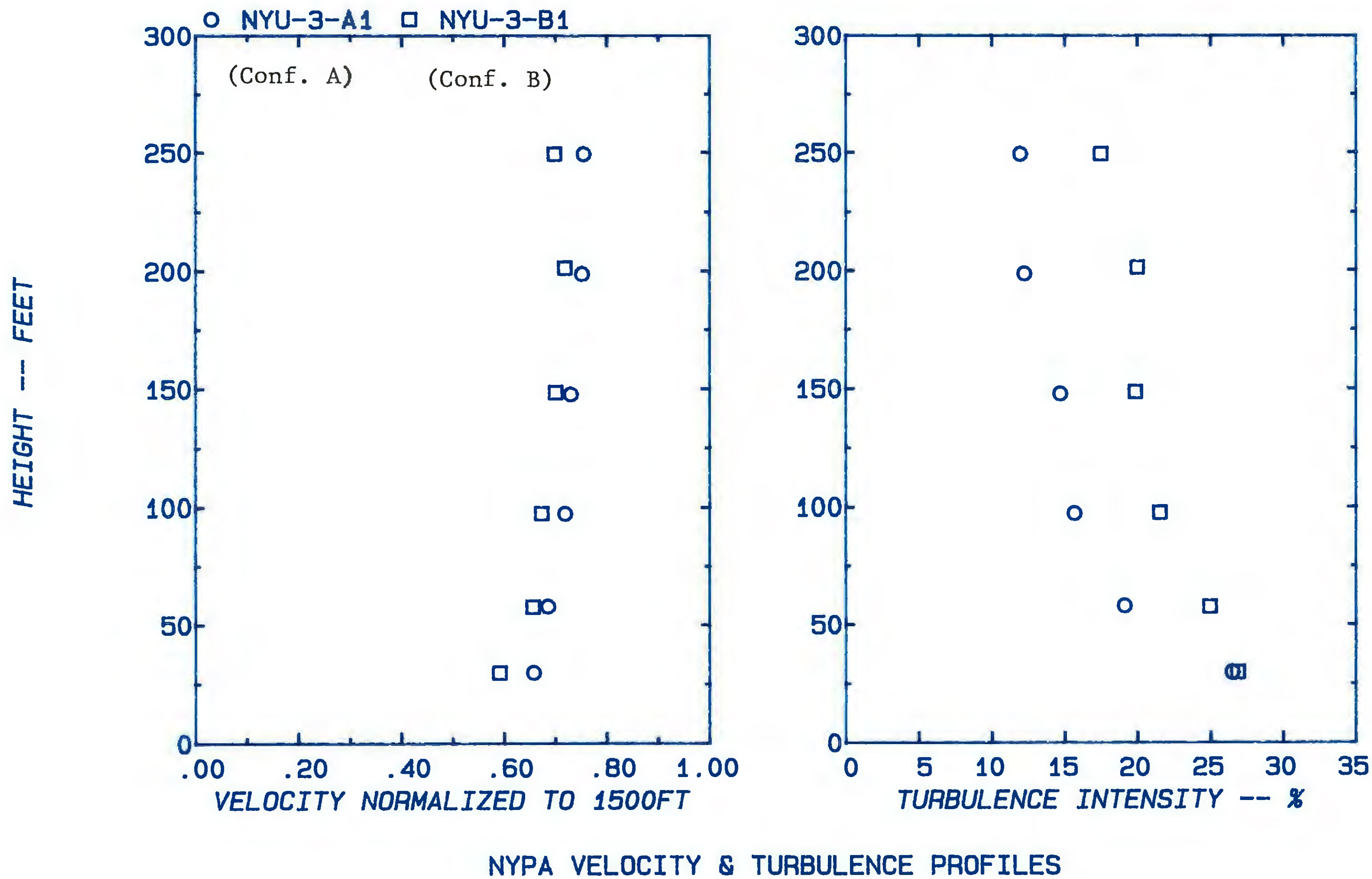

Figure E4. Profiles With and Without Cooling Tower
Unstable Flow, Low Speed

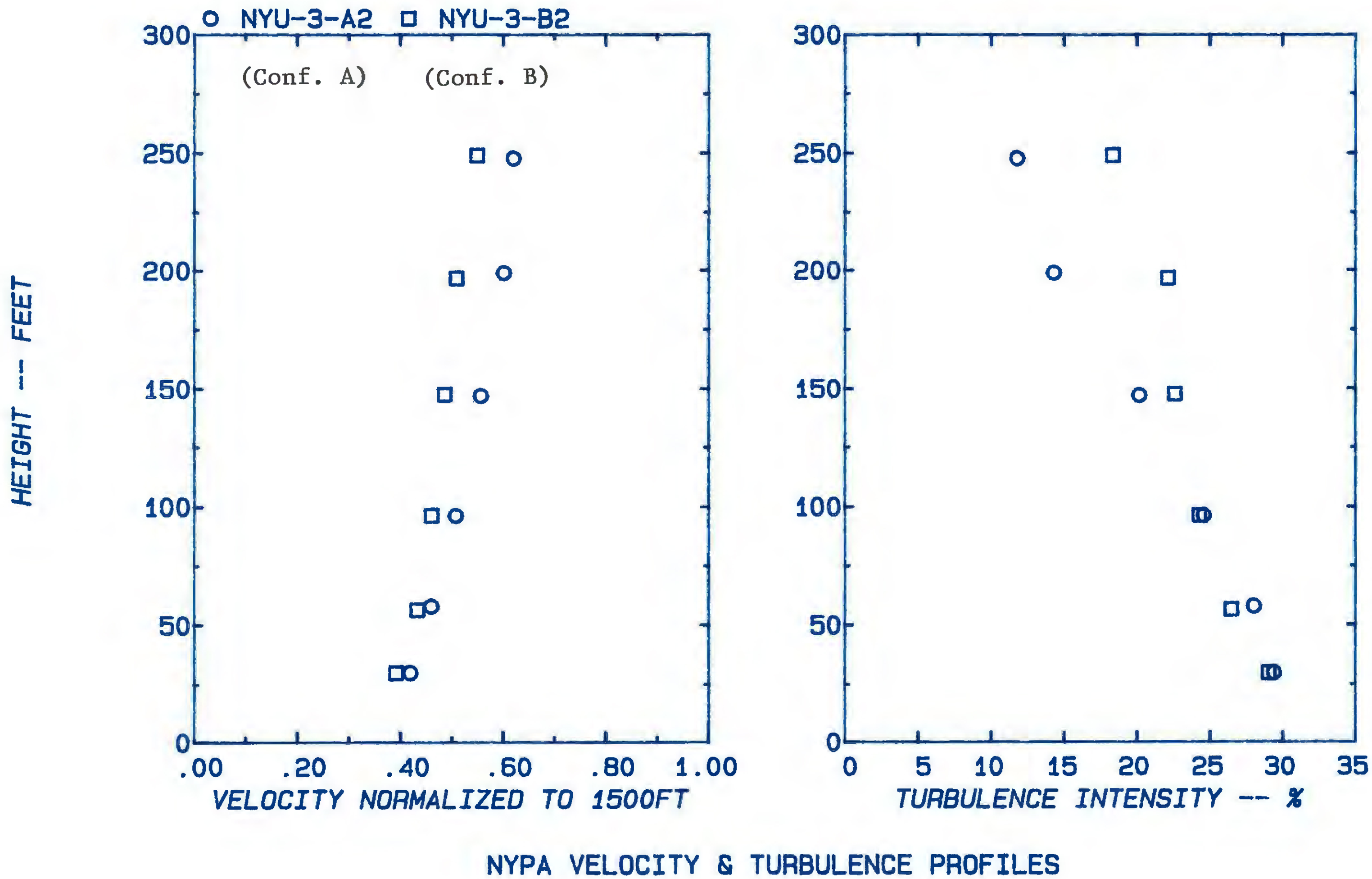

Figure E5. Profiles With and Without Cooling Tower
Unstable Flow, High Speed

Table E3. Task III - $(\bar{U})_c$, $(\Delta T)_c$, and $(TI)_c$

<u>Cooling Tower Caused Changes in $\bar{U}$, ΔT, and TI</u>

Reference (R) Site Condition = Task III, Configuration A

Cooling Tower (CT) Site Condition = Task III, Configuration B

<u>Definition of Terms</u>

$$(\bar{U})_c = \frac{\bar{U}_{CT} - U_R}{U_R} \quad \text{such that} \begin{cases} +(\bar{U})_c & \text{indicates velocity speedup} \\ -(\bar{U})_c & \text{indicates velocity defect} \end{cases}$$

$$(\Delta T)_c = \frac{\Delta T_{CT} - \Delta T_R}{\Delta T_R} \quad \text{such that} \begin{cases} +(\Delta T)_c & \text{indicates increased } \Delta T \\ -(\Delta T)_c & \text{indicates decreased } \Delta T \end{cases}$$

(where $\Delta T = T_h - T_{30}$,)

$$(TI)_c = \frac{TI_{CT} - TI_R}{TI_R} \quad \text{such that} \begin{cases} +(TI)_c & \text{is increased turbulence} \\ -(TI)_c & \text{is decreased turbulence} \end{cases}$$

Parameter	Height (H)	Unstable		Neutral		Stable	
		Low Speed	High Speed	Low Speed	High Speed	Low Speed	High Speed
$(\bar{U})_c$	30	-.102	-.064	-.037	.007	-.031	-.277
	100	-.064	-.094	.068	.002	-.040	-.149
	200	-.044	-.154	.014	-.007	.007	-.048
$(TI)_c$	30	.011	-.014	.000	-.033	.028	.044
	100	.365	-.016	-.168	.022	.105	.638
	200	.582	.545	-.042	.016	.000	2.364
$(\Delta T)_c$	100	.087	-.148	X	X	-.090	1.727
	200	.045	-.289	X	X	.042	.525

Note: All changes listed are fractional; thus -0.037 implies a -3.7 percent change.

APPENDIX F

Task IV Data: Influences of Variable Land Fetch on Velocity, Turbulence, and Wind Angle Measurements at the Main Meteorological Tower Location for Neutral, Stable, and Unstable Flow Conditions

APPENDIX F - TABLE OF CONTENTS

Task IV: Data File Name Code

Example File Name } NY ___ ___ _#_ - ___ _#_

Free Stream Velocity Code

Configuration (Letters)

Task #

Flow Condition (Letters)

New York

Flow Condition: PA = Neutral
S- = Stable
U- = Unstable

Task #: 1 = Task 1
3 = Task 3
4 = Task 4 ←

Configuration:

S: Smooth Floor Approach

T: Land Fetch = 330′

U: Land Fetch = 1625′

V: Land Fetch = 2335′

W: Land Fetch = 4000′

X: Land Fetch = 5500′

see following Figure F1

Free Stream Velocity Code:

1	=	Lower speed	≈	5.6 mph	neutral
				1.6 mph	stable
				1.1 mph	unstable
2	=	Higher speed	≈	11.2 mph	neutral
				3.2 mph	stable
				2.1 mph	unstable

Land/Lake Fetch Configuration for Task IV

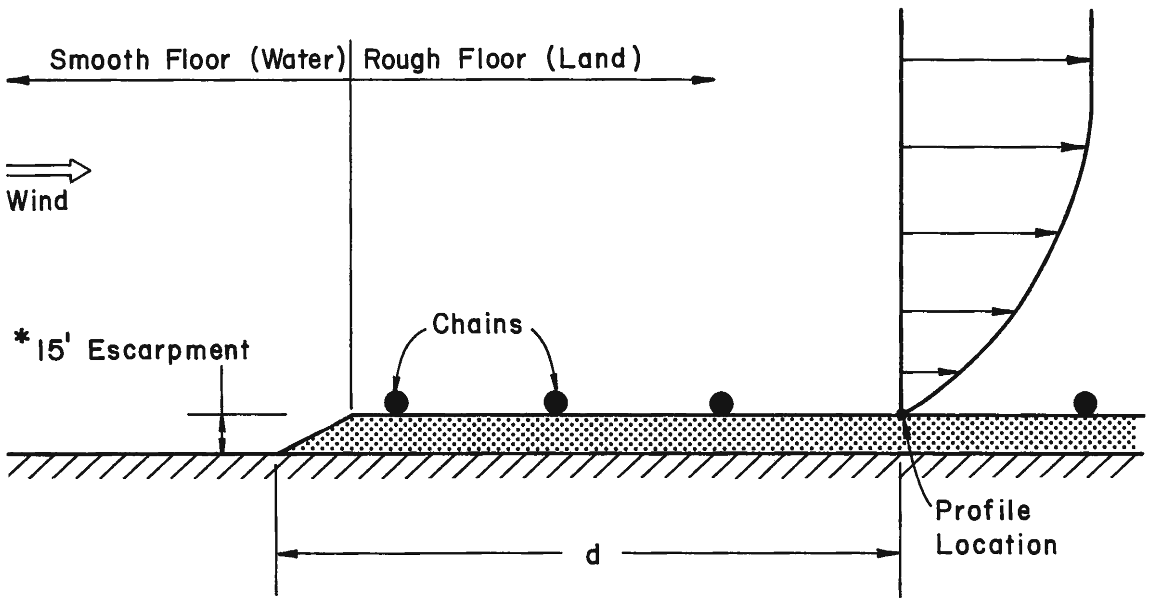

d = Distance Profile Location is Inland from Lake Shore

Configurations: S: Smooth Floor Approach (No Escarpment)

T: d = 330'

U: d = 1625'

V: d = 2335'

W: d = 4000'

X: d = 5500'

* - Neutral Conditions with Escarpment

- Stable and Unstable Conditions without Escarpment

Table F1. Task IV Data Summary and Guide

Data File Name	Flow Condition	Conf.	Length of Land Fetch (ft)	Escarpment	Approx. Free Stream Velocity (mph)
NYPA4-S1	Neutral	S	-	No	5.6
NYPA4-S2	Neutral	S	-	No	11.2
NYPA4-T1	Neutral	T	330	Yes	5.6
NYPA4-T2	Neutral	T	330	Yes	11.2
NYPA4-U1	Neutral	U	1625	Yes	5.6
NYPA4-U2	Neutral	U	1625	Yes	11.2
NYPA4-V1	Neutral	V	2335	Yes	5.6
NYPA4-V2	Neutral	V	2335	Yes	11.2
NYPA4-W1	Neutral	W	4000	Yes	5.6
NYPA4-W2	Neutral	W	4000	Yes	11.2
NYPA4-X1	Neutral	X	5500	Yes	5.6
NYPA4-X2	Neutral	X	5500	Yes	11.2
NYS-4-T1	Stable	T	330	No	1.6
NYS-4-U1	Stable	U	1625	No	1.6
NYS-4-V1	Stable	V	2335	No	1.6
NYS-4-W1	Stable	W	4000	No	1.6
NYS-4-X1	Stable	X	5500	No	1.6
NYS-4-T2	Stable	T	330	No	3.2
NYS-4-U2	Stable	U	1625	No	3.2
NYS-4-V2	Stable	V	2335	No	3.2
NYS-4-W2	Stable	W	4000	No	3.2
NYS-4-X2	Stable	X	5500	No	3.2
NYU-4-T1	Unstable	T	330	No	1.1
NYU-4-U1	Unstable	U	1625	No	1.1
NYU-4-V1	Unstable	V	2335	No	1.1
NYU-4-W1	Unstable	W	4000	No	1.1
NYU-4-X1	Unstable	X	5500	No	1.1
NYU-4-T2	Unstable	T	330	No	2.1
NYU-4-U2	Unstable	U	1625	No	2.1
NYU-4-V2	Unstable	V	2335	No	2.1
NYU-4-W2	Unstable	W	4000	No	2.1
NYU-4-X2	Unstable	X	5500	No	2.1

Table F2. Task IV Velocity Profile Figure Guide

Figure #	1st Profile	2nd Profile	3rd Profile	4th Profile	5th Profile	Comments
F1	NYPA4-S2	NYPA4-T2	Effect of Escarpment at Main Met. Tower: Neutral Cond.			
F2	NYPA4-T2	NYPA4-U2	NYPA4-V2	NYPA4-W2	NYPA4-X2	Fetch Length Comparisons
F3	NYS-4-T1	NYS-4-U1	NYS-4-V1	NYS-4-W1	NYS-4-X1	Fetch Length Comparisons
F4	NYS-4-T2	NYS-4-U2	NYS-4-V2	NYS-4-W2	NYS-4-X2	Fetch Length Comparisons
F5	NYU-4-T1	NYU-4-U1	NYU-4-V1	NYU-4-W1	NYU-4-X1	Fetch Length Comparisons
F6	NYU-4-T2	NYU-4-U2	NYU-4-V2	NYU-4-W2	NYU-4-X2	Fetch Length Comparisons

Table F3. Primary Meteorological Tower and Power Plant Fetch Lengths by Wind Direction

Wind Direction	Main Tower		Nine Mile 1		Nine Mile 2		J.A. Fitzpatrick		Wind Frequency for all Stabilities (%)
	(ft)	Profile	(ft)	Profile	(ft)	Profile	(ft)	Profile	
SW	768	T	-	X	-	X	-	X	5.5
WSW	528	T	3168	W	3984	W	6720	X	10.7
W	384	T	2064	V	2592	V	3600	W	9.9
WNW	326	T	1056	U	1344	U	1344	V	7.4
NW	336	T	864	T	1056	U	768	U	6.9
NNW	384	T	768	T	912	T	624	U	4.3
N	576	T	864	T	912	T	576	U	3.4
NNE	1344	U	1056	U	1152	U	720	U	3.9
NE	1872	U	1536	U	1536	U	1152	U	3.8

TOTAL = 55.8%

Test Profile	T	U	V	W	X
Distance from Shoreline	330′	1625′	2335′	4000′	5500′

Profile Name : NYPA-4-S1
Flow Condition : Neutral, Low speed
Task Number : 4
Configuration : S
Ref. Height : 1500.0 ft
Ref. Model Velocity : 5.03 mph

Height (ft)	Velocity (Normalized)	Turb. Int. (%)
15.00	.509	21.00
28.60	.571	17.00
57.60	.643	13.40
98.10	.684	13.10
148.00	.743	11.10
197.00	.783	9.97
248.00	.806	10.30
374.00	.835	7.43
747.00	.896	6.98
1120.00	.945	5.86
1500.00	1	5.32

Profile Name : NYPA-4-S2
Flow Condition : Neutral, High speed
Task Number : 4
Configuration : S
Ref. Height : 1500.0 ft
Ref. Model Velocity : 9.42 mph

Height (ft)	Velocity (Normalized)	Turb. Int. (%)
15.00	.544	17.60
28.60	.612	15.60
56.90	.676	13.20
98.30	.718	12.50
148.00	.779	10.50
197.00	.794	10.30
248.00	.816	9.17
374.00	.838	8.28
749.00	.916	6.54
1120.00	.96	5.61
1500.00	1	5.10

Profile Name : NYPA-4-T1
Flow Condition : Neutral, Low speed
Task Number : 4
Configuration : T
Ref. Height : 1500.0 ft
Ref. Model Velocity : 5.10 mph

Height (ft)	Velocity (Normalized)	Turb. Int. (%)
15.00	.585	15.20
26.60	.642	13.90
57.40	.692	11.30
98.00	.745	10.20
148.00	.781	8.30
198.00	.81	9.49
248.00	.833	8.29
377.00	.858	7.40
748.00	.924	6.02
1120.00	.972	5.48
1500.00	1	5.53

Profile Name : NYPA-4-T2
Flow Condition : Neutral, High speed
Task Number : 4
Configuration : T
Ref. Height : 1500.0 ft
Ref. Model Velocity : 10.00 mph

Height (ft)	Velocity (Normalized)	Turb. Int. (%)
15.00	.604	14.30
27.50	.65	13.60
56.60	.712	12.00
97.40	.76	10.70
148.00	.789	9.85
198.00	.836	8.31
248.00	.844	9.26
373.00	.871	7.39
750.00	.924	6.24
1130.00	.972	5.68
1500.00	1	5.01

Profile Name : NYPA-4-U1
Flow Condition : Neutral, Low speed
Task Number : 4
Configuration : U
Ref. Height : 1500.0 ft
Ref. Model Velocity : 4.88 mph

Height (ft)	Velocity (Normalized)	Turb. Int. (%)
15.00	.393	25.10
28.30	.445	24.10
56.80	.573	22.80
98.20	.692	15.10
147.00	.775	11.20
197.00	.821	9.32
248.00	.847	8.81
374.00	.854	8.43
749.00	.925	6.56
1130.00	.962	5.29
1500.00	1	5.27

Profile Name : NYPA-4-T2
Flow Condition : Neutral, High speed
Task Number : 4
Configuration : T
Ref. Height : 1500.0 ft
Ref. Model Velocity : 10.00 mph

Height (ft)	Velocity (Normalized)	Turb. Int. (%)
15.00	.604	14.30
27.50	.65	13.60
56.60	.712	12.00
97.40	.76	10.70
148.00	.789	9.85
198.00	.836	8.31
248.00	.844	9.26
373.00	.871	7.39
750.00	.924	6.24
1130.00	.972	5.68
1500.00	1	5.01

Profile Name : NYPA-4-V1
Flow Condition : Neutral, Low speed
Task Number : 4
Configuration : V
Ref. Height : 1500.0 ft
Ref. Model Velocity : 4.94 mph

Height (ft)	Velocity (Normalized)	Turb. Int. (%)
15.00	.39	23.70
28.40	.438	25.30
57.10	.557	21.40
98.80	.68	16.90
148.00	.776	12.80
197.00	.819	10.30
249.00	.821	9.45
375.00	.865	7.62
750.00	.916	6.33
1120.00	.953	5.51
1500.00	1	5.18

Profile Name : NYPA-4-T2
Flow Condition : Neutral, High speed
Task Number : 4
Configuration : T
Ref. Height : 1500.0 ft
Ref. Model Velocity : 10.00 mph

Height (ft)	Velocity (Normalized)	Turb. Int. (%)
15.00	.604	14.30
27.50	.65	13.60
56.60	.712	12.00
97.40	.76	10.70
148.00	.789	9.85
198.00	.836	8.31
248.00	.844	9.26
373.00	.871	7.39
750.00	.924	6.24
1130.00	.972	5.68
1500.00	1	5.01

Profile Name : NYPA-4-W1
Flow Condition : Neutral, Low speed
Task Number : 4
Configuration : W
Ref. Height : 1500.0 ft
Ref. Model Velocity : 4.92 mph

Height (ft)	Velocity (Normalized)	Turb. Int. (%)
15.00	.415	20.60
28.40	.456	20.70
57.10	.534	20.69
98.80	.62	18.50
148.00	.69	14.00
197.00	.779	12.30
249.00	.814	10.60
375.00	.85	7.63
750.00	.907	6.79
1120.00	.961	5.02
1500.00	1	4.57

Profile Name : NYPA-4-W2
Flow Condition : Neutral, High speed
Task Number : 4
Configuration : W
Ref. Height : 1500.0 ft
Ref. Model Velocity : 9.55 mph

Height (ft)	Velocity (Normalized)	Turb. Int. (%)
15.00	.392	25.40
28.40	.424	24.60
59.10	.517	23.00
98.10	.636	20.90
149.00	.715	15.90
199.00	.8	12.90
248.00	.82	10.70
374.00	.868	7.70
747.00	.933	5.84
1130.00	.977	5.68
1500.00	1	5.52

Profile Name : NYPA-4-X1
Flow Condition : Neutral, Low speed
Task Number : 4
Configuration : X
Ref. Height : 1500.0 ft
Ref. Model Velocity : 4.61 mph

Height (ft)	Velocity (Normalized)	Turb. Int. (%)
15.00	.417	20.60
27.90	.477	20.10
58.70	.52	20.00
97.70	.614	16.60
149.00	.693	16.20
198.00	.747	14.90
248.00	.78	11.60
373.00	.888	8.08
748.00	.94	6.18
1130.00	.997	5.00
1500.00	1	5.25

Profile Name : NYPA-4-X2
Flow Condition : Neutral, High speed
Task Number : 4
Configuration : X
Ref. Height : 1500.0 ft
Ref. Model Velocity : 9.44 mph

Height (ft)	Velocity (Normalized)	Turb. Int. (%)
15.00	.383	26.30
29.10	.431	25.60
57.70	.491	23.20
98.60	.593	20.40
148.00	.692	15.90
199.00	.74	16.60
248.00	.787	12.80
374.00	.866	8.50
749749.00	.934	5.59
1120.00	.968	5.77
1500.00	1	5.86

Profile Name : NYS-4-T1
Flow Condition : Stable, Low speed
Task Number : 4
Configuration : T
Ref. Height : 1500.0 ft
Ref. Model Velocity : 1.64 mph

Height (ft)	Velocity (Normalized)	Turb. Int. (%) u	Turb. Int. (%) v	del Theta (deg)	Model Temp (deg C)	Delta Temperature (Deg C) 4 mph Field	Delta Temperature (Deg C) 8 mph Field
30.0	.218	3.9	2.4	-.51	5.99	.00	.00
61.3	.239	2.8	1.7	-.64	9.32	.35	1.40
98.3	.259	1.9	1.3	-.75	13.89	.83	3.33
150.2	.261	1.6	2.3	-.12	17.52	1.22	4.86
196.8	.272	1.4	1.9	-.29	21.02	1.58	6.34
253.1	.275	1.1	1.4	-.08	23.03	1.80	7.18
376.5	.313	4.3	3.9	-1.40	28.90	2.41	9.66
753.2	.458	4.0	2.4	-.81	32.73	2.82	11.27
1127.7	.720	5.2	3.4	-.47	36.63	3.23	12.92
1499.9	1.000	3.2	3.0	-.92	40.59	3.65	14.59

T@100-T@30 = 1.012*T@100-T@30 Undisturbed App. ie Change in del T = .01 .04
T@200-T@30 = .968*T@200-T@30 Undisturbed App. ie Change in del T = -.05 -.21

Profile Name : NYS-4-U1
Flow Condition : Stable, Low speed
Task Number : 4
Configuration : U
Ref. Height : 1500.0 ft
Ref. Model Velocity : 1.64 mph

Height (ft)	Velocity (Normalized)	Turb. Int. (%) u	Turb. Int. (%) v	del Theta (deg)	Model Temp (deg C)	Delta Temperature (Deg C) 4 mph Field	Delta Temperature (Deg C) 8 mph Field
30.0	.216	4.0	2.8	.31	8.08	.00	.00
60.4	.235	2.7	2.3	-.36	10.03	.21	.82
97.1	.264	1.7	1.0	-.60	15.20	.75	3.00
149.6	.259	1.7	2.2	-.23	17.51	.99	3.98
201.9	.283	2.4	2.2	.19	22.29	1.50	5.99
249.3	.279	2.7	3.6	.02	23.93	1.67	6.68
376.7	.329	2.1	1.7	-1.32	30.73	2.39	9.55
746.9	.458	3.3	2.0	-1.17	32.74	2.60	10.40
1121.6	.771	5.3	3.1	-.66	37.19	3.07	12.27
1499.2	1.000	3.2	3.0	-.59	40.67	3.44	13.74

T@100-T@30 = .913*T@100-T@30 Undisturbed App. ie Change in del T = -.07 -.29
T@200-T@30 = .915*T@200-T@30 Undisturbed App. ie Change in del T = -.14 -.56

Profile Name : NYS-4-V1
Flow Condition : Stable, Low speed
Task Number : 4
Configuration : V
Ref. Height : 1500.0 ft
Ref. Model Velocity : 1.59 mph

Height (ft)	Velocity (Normalized)	Turb. Int. (%) u	Turb. Int. (%) v	del Theta (deg)	Model Temp (deg C)	Delta Temperature (Deg C) 4 mph Field	Delta Temperature (Deg C) 8 mph Field
30.0	.219	3.8	2.9	-.64	5.59	.00	.00
58.9	.245	2.7	1.6	-.80	9.21	.38	1.53
99.3	.268	2.1	1.4	-.96	13.97	.88	3.53
151.0	.268	1.5	2.3	-.42	17.26	1.23	4.92
198.5	.282	2.0	2.2	-1.08	21.23	1.65	6.59
249.0	.302	3.8	3.6	.76	24.82	2.03	8.11
374.2	.324	2.3	1.8	-1.20	29.13	2.48	9.92
750.3	.463	3.7	1.8	-1.14	32.58	2.84	11.38
1123.6	.702	5.6	3.6	-1.23	36.27	3.23	12.93
1497.1	1.000	3.9	3.6	-.83	40.33	3.66	14.64

T@100-T@30 = 1.074*T@100-T@30 Undisturbed App. ie Change in del T = .06 .24
T@200-T@30 = 1.007*T@200-T@30 Undisturbed App. ie Change in del T = .01 .04

Profile Name : NYS-4-W1
Flow Condition : Stable, Low speed
Task Number : 4
Configuration : W
Ref. Height : 1500.0 ft
Ref. Model Velocity : 1.61 mph

Height (ft)	Velocity (Normalized)	Turb. Int. (%) u	Turb. Int. (%) v	del Theta (deg)	Model Temp (deg C)	Delta Temperature (Deg C) 4 mph Field	Delta Temperature (Deg C) 8 mph Field
30.0	.221	3.8	2.5	-1.36	4.68	.00	.00
60.7	.241	2.6	1.5	-1.35	8.16	.37	1.47
99.0	.262	2.1	1.2	-1.33	12.86	.86	3.45
147.2	.258	1.1	1.6	-1.11	15.84	1.18	4.71
200.2	.271	1.3	2.2	-1.87	20.04	1.62	6.48
249.6	.272	1.0	1.6	-1.94	21.93	1.82	7.28
371.8	.331	4.1	2.9	-2.24	29.97	2.67	10.67
746.6	.479	3.7	2.1	-1.44	32.69	2.95	11.81
1122.6	.701	5.3	3.5	-1.00	36.33	3.34	13.34
1497.5	1.000	3.6	3.2	-.65	40.38	3.76	15.05

T@100-T@30 = 1.049*T@100-T@30 Undisturbed App. ie Change in del T = .04 .16
T@200-T@30 = .989*T@200-T@30 Undisturbed App. ie Change in del T = -.02 -.07

Profile Name : NYS-4-X1
Flow Condition : Stable, Low speed
Task Number : 4
Configuration : X
Ref. Height : 1500.0 ft
Ref. Model Velocity : 1.64 mph

Height	Velocity	Turb. Int. (%)		del Theta	Model Temp	Delta Temperature (Deg C)	
(ft)	(Normalized)	u	v	(deg)	(deg C)	4 mph Field	8 mph Field
30.0	.224	3.3	2.0	-3.09	2.82	.00	.00
60.7	.246	2.5	1.5	-2.99	7.67	.51	2.04
100.6	.266	2.0	1.2	-2.57	12.90	1.06	4.25
149.4	.282	3.0	2.4	-.65	18.03	1.60	6.41
203.1	.271	1.4	1.9	-2.45	20.05	1.82	7.26
251.5	.278	1.2	1.6	-1.33	22.69	2.09	8.38
375.6	.292	1.3	1.6	-4.84	26.64	2.51	10.04
751.6	.461	3.6	2.1	-2.75	32.64	3.14	12.57
1123.0	.708	5.6	3.7	-2.55	36.32	3.53	14.12
1503.4	1.000	3.6	3.4	-2.34	40.55	3.98	15.91

T@100-T@30 = 1.293*T@100-T@30 Undisturbed App. ie Change in del T = .24 .96
T@200-T@30 = 1.110*T@200-T@30 Undisturbed App. ie Change in del T = .18 .72

Profile Name : NYS-4-T2
Flow Condition : Stable, High speed
Task Number : 4
Configuration : T
Ref. Height : 1500.0 ft
Ref. Model Velocity : 3.07 mph

Height	Velocity	Turb. Int. (%)		del Theta	Model Temp	Delta Temperature (Deg C)	
(ft)	(Normalized)	u	v	(deg)	(deg C)	4 mph Field	8 mph Field
30.0	.221	3.9	1.5	-1.66	13.38	.00	.00
57.9	.316	2.5	1.5	1.02	19.76	.07	.29
96.6	.367	2.6	1.5	-.72	23.62	.11	.46
147.8	.415	3.8	2.3	-.75	26.52	.15	.59
197.2	.478	3.9	2.7	-.55	29.55	.18	.72
250.4	.539	3.7	2.8	-.30	32.33	.21	.85
371.6	.648	2.8	3.0	-.56	36.08	.25	1.02
750.3	.889	3.2	4.5	-.69	41.08	.31	1.24
1124.4	.947	3.5	4.2	-1.05	43.50	.34	1.35
1502.7	1.000	1.8	3.0	-1.24	45.32	.36	1.43

T@100-T@30 = .921*T@100-T@30 Undisturbed App. ie Change in del T = -.01 -.04
T@200-T@30 = .989*T@200-T@30 Undisturbed App. ie Change in del T = .00 -.01

Profile Name : NYS-4-U2
Flow Condition : Stable, High speed
Task Number : 4
Configuration : U
Ref. Height : 1500.0 ft
Ref. Model Velocity : 3.11 mph

Height	Velocity	Turb. Int. (%)		del Theta	Model Temp	Delta Temperature (Deg C)	
(ft)	(Normalized)	u	v	(deg)	(deg C)	4 mph Field	8 mph Field
30.0	.196	10.1	7.7	-3.58	12.30	.00	.00
56.6	.304	3.6	3.7	-.68	19.08	.08	.30
98.3	.361	3.2	2.0	-1.92	23.27	.12	.49
149.8	.412			-1.89	25.51	.15	.59
199.4	.472	4.1	2.5	-1.25	29.36	.19	.76
249.1	.534	3.8	2.8	-.67	31.94	.22	.88
373.0	.652	2.9	3.1	-.79	35.96	.26	1.06
748.7	.891	3.4	4.5	-1.21	40.94	.32	1.28
1124.9	.955	3.6	4.2	-1.03	43.34	.35	1.39
1499.0	1.000	1.7	2.9	-1.28	45.16	.37	1.47

T@100-T@30 = .988*T@100-T@30 Undisturbed App. ie Change in del T = .00 -.01
T@200-T@30 = 1.044*T@200-T@30 Undisturbed App. ie Change in del T = .01 .03

Profile Name : NYS-4-V2
Flow Condition : Stable, High speed
Task Number : 4
Configuration : V
Ref. Height : 1500.0 ft
Ref. Model Velocity : 3.13 mph

Height (ft)	Velocity (Normalized)	Turb. Int. (%) u	v	del Theta (deg)	Model Temp (deg C)	Delta Temperature (Deg C) 4 mph Field	8 mph Field
30.0	.183	12.2	10.4	-1.97	11.91	.00	.00
58.6	.296	5.8	4.8	-.31	18.72	.08	.31
97.7	.357	2.9	2.1	-1.72	23.31	.13	.51
147.7	.401	3.0	2.5	-2.08	26.09	.16	.64
200.5	.453	3.9	2.6	-1.90	28.73	.19	.75
247.0	.518	3.8	2.7	-1.47	31.46	.22	.88
372.8	.643	2.6	3.0	-.91	35.83	.27	1.07
746.2	.881	3.3	4.4	-1.17	40.78	.32	1.29
1122.7	.952	3.4	4.1	-1.19	43.19	.35	1.40
1500.7	1.000	1.7	2.8	-1.55	45.21	.37	1.49

T@100-T@30 = 1.026*T@100-T@30 Undisturbed App. ie Change in del T = .00 .01
T@200-T@30 = 1.029*T@200-T@30 Undisturbed App. ie Change in del T = .01 .02

Profile Name : NYS-4-W2
Flow Condition : Stable, High speed
Task Number : 4
Configuration : W
Ref. Height : 1500.0 ft
Ref. Model Velocity : 3.09 mph

Height (ft)	Velocity (Normalized)	Turb. Int. (%) u	v	del Theta (deg)	Model Temp (deg C)	Delta Temperature (Deg C) 4 mph Field	8 mph Field
30.0	.178	12.5	10.9	-1.99	11.68	.00	.00
59.0	.274	9.5	6.9	-.80	17.24	.06	.25
103.1	.362	3.2	2.1	-1.73	22.89	.13	.50
150.7	.398	2.9	2.3	-2.56	25.31	.15	.61
200.7	.449	4.1	2.7	-2.58	28.06	.18	.73
250.4	.526	3.9	2.8	-1.80	31.20	.22	.87
377.3	.645	2.9	2.9	-1.39	35.52	.27	1.07
748.1	.887	3.1	4.4	-1.67	40.67	.32	1.30
1122.0	.952	3.6	4.2	-1.58	43.06	.35	1.41
1502.8	1.000	1.7	2.8	-1.82	45.12	.37	1.50

T@100-T@30 = 1.009*T@100-T@30 Undisturbed App. ie Change in del T = .00 .00
T@200-T@30 = 1.002*T@200-T@30 Undisturbed App. ie Change in del T = .00 .00

Profile Name : NYS-4-X2
Flow Condition : Stable, High speed
Task Number : 4
Configuration : X
Ref. Height : 1500.0 ft
Ref. Model Velocity : 3.08 mph

Height (ft)	Velocity (Normalized)	Turb. Int. (%) u	Turb. Int. (%) v	del Theta (deg)	Model Temp (deg C)	Delta Temperature (Deg C) 4 mph Field	Delta Temperature (Deg C) 8 mph Field
30.0	.180	13.1	10.6	-2.43	11.84	.00	.00
58.8	.286	8.0	6.3	-.83	17.73	.07	.26
99.6	.358	3.4	2.5	-1.77	22.69	.12	.49
148.7	.392	2.9	2.4	-2.85	24.98	.15	.59
198.0	.437	3.5	3.0	-2.85	26.88	.17	.67
250.9	.503	3.3	2.7	-2.12	30.23	.21	.82
373.9	.636	2.8	2.7	-1.36	35.15	.26	1.04
751.7	.879	3.1	4.2	-1.63	40.54	.32	1.29
1121.9	.933	4.1	4.8	-1.54	42.93	.35	1.39
1497.5	1.000	1.7	2.8	-1.85	45.12	.37	1.49

T@100-T@30 = .977*T@100-T@30 Undisturbed App. ie Change in del T = .00 -.01
T@200-T@30 = .921*T@200-T@30 Undisturbed App. ie Change in del T = -.01 -.06

Profile Name : NYU-4-T1
Flow Condition : Unstable, Low speed
Task Number : 4
Configuration : T
Ref. Height : 1500.0 ft
Ref. Model Velocity : 1.13 mph

Height (ft)	Velocity (Normalized)	Turb. Int. (%) u	v	del Theta (deg)	Model Temp (deg C)	Delta Temperature (Deg C) 4 mph Field	8 mph Field
30.0	.801	26.4	18.8	1.33	37.94	.00	.00
57.8	.855	18.3	17.3	3.68	35.44	-.07	-.30
97.7	.859	14.4	17.5	4.17	33.89	-.12	-.48
148.2	.855	12.8	17.4	5.12	33.99	-.12	-.47
198.6	.835	12.1	15.4	1.98	33.11	-.14	-.58
247.3	.838	12.2	16.7	2.91	33.37	-.14	-.54
377.3	.820	11.9	15.3	3.04	33.75	-.12	-.50
748.9	.906	4.7	4.0	5.43	41.37	.10	.41
1122.9	.883	4.1	2.2	2.12	45.54	.23	.91
1500.3	1.000	2.9	1.9	.37	46.77	.26	1.05

T@100-T@30 = .801*T@100-T@30 Undisturbed App. ie Change in del T = .03 .12
T@200-T@30 = .957*T@200-T@30 Undisturbed App. ie Change in del T = .01 .03

Profile Name : NYU-4-U1
Flow Condition : Unstable, Low speed
Task Number : 4
Configuration : U
Ref. Height : 1500.0 ft
Ref. Model Velocity : 1.13 mph

Height (ft)	Velocity (Normalized)	Turb. Int. (%) u	v	del Theta (deg)	Model Temp (deg C)	Delta Temperature (Deg C) 4 mph Field	8 mph Field
30.0	.706	26.6	20.4	1.12	40.10	.00	.00
57.2	.779	22.6	21.1	1.81	37.08	-.09	-.36
96.4	.801	19.5	20.9	1.77	35.66	-.13	-.53
147.6	.822	15.6	18.9	3.00	34.14	-.18	-.71
196.9	.826	15.1	18.8	2.73	34.20	-.18	-.70
249.3	.836	13.8	17.4	2.56	33.77	-.19	-.76
375.0	.812	12.8	16.4	2.85	33.54	-.20	-.78
750.9	.869	5.3	4.9	4.92	41.04	.03	.11
1124.1	.881	4.0	2.3	1.80	45.43	.16	.63
1497.7	1.000	2.7	2.1	.26	46.66	.20	.78

T@100-T@30 = .879*T@100-T@30 Undisturbed App. ie Change in del T = .02 .07
T@200-T@30 = 1.172*T@200-T@30 Undisturbed App. ie Change in del T = -.03 -.10

Profile Name : NYU-4-V1
Flow Condition : Unstable, Low speed
Task Number : 4
Configuration : V
Ref. Height : 1500.0 ft
Ref. Model Velocity : 1.07 mph

Height (ft)	Velocity (Normalized)	Turb. Int. (%) u	v	del Theta (deg)	Model Temp (deg C)	Delta Temperature (Deg C) 4 mph Field	8 mph Field
30.0	.751	25.2	18.8	1.91	39.90	.00	.00
56.9	.790	21.8	19.6	1.42	36.94	-.09	-.35
97.0	.829	18.3	18.4	2.71	35.40	-.13	-.54
148.6	.842	15.8	17.1	4.19	34.54	-.16	-.64
197.5	.858	13.4	18.5	1.60	34.25	-.17	-.67
249.7	.859	13.2	16.7	1.57	34.47	-.16	-.65
373.4	.871	12.5	16.4	2.11	34.37	-.16	-.66
747.2	.872	6.0	6.1	4.67	40.51	.02	.07
1123.6	.903	3.6	2.3	1.61	45.31	.16	.64
1500.8	1.000	3.7	2.5	.99	46.62	.20	.80

T@100-T@30 = .890*T@100-T@30 Undisturbed App. ie Change in del T = .02 .07
T@200-T@30 = 1.123*T@200-T@30 Undisturbed App. ie Change in del T = -.02 -.07

Profile Name : NYU-4-W1
Flow Condition : Unstable, Low speed
Task Number : 4
Configuration : W
Ref. Height : 1500.0 ft
Ref. Model Velocity : 1.08 mph

Height (ft)	Velocity (Normalized)	Turb. Int. (%) u	v	del Theta (deg)	Model Temp (deg C)	Delta Temperature (Deg C) 4 mph Field	8 mph Field
30.0	.728	25.5	20.0	.98	40.66	.00	.00
58.5	.794	20.1	18.3	2.41	37.18	-.10	-.42
97.4	.819	15.5	17.2	1.95	34.91	-.17	-.69
146.5	.834	15.2	17.3	4.05	34.93	-.17	-.68
196.4	.838	13.9	16.4	2.98	34.60	-.18	-.72
247.7	.825	12.7	17.0	.71	34.60	-.18	-.72
371.2	.837	13.8	18.5	1.96	35.76	-.15	-.58
748.6	.832	6.2	6.6	3.88	40.42	-.01	-.03
1123.3	.883	4.1	2.1	1.40	45.11	.13	.53
1497.7	1.000	3.4	2.3	.45	46.32	.17	.67

T@100-T@30 = 1.138*T@100-T@30 Undisturbed App. ie Change in del T = -.02 -.08
T@200-T@30 = 1.203*T@200-T@30 Undisturbed App. ie Change in del T = -.03 -.12

Profile Name : NYU-4-X1
Flow Condition : Unstable, Low speed
Task Number : 4
Configuration : X
Ref. Height : 1500.0 ft
Ref. Model Velocity : 1.08 mph

Height (ft)	Velocity (Normalized)	Turb. Int. (%) u	v	del Theta (deg)	Model Temp (deg C)	Delta Temperature (Deg C) 4 mph Field	8 mph Field
30.0	.747	24.7	20.2	1.35	41.10	.00	.00
61.4	.777	20.2	18.1	2.49	38.27	-.08	-.34
97.5	.784	16.8	17.4	1.21	36.37	-.14	-.56
152.0	.808	15.3	18.9	6.43	36.07	-.15	-.60
199.3	.794	12.4	17.8	1.08	35.40	-.17	-.68
251.2	.797	13.9	19.4	1.30	35.79	-.16	-.63
373.4	.794	13.3	17.3	1.15	35.98	-.15	-.61
751.1	.813	7.7	8.3	2.37	39.67	-.04	-.17
1122.7	.877	3.6	2.4	1.40	44.86	.11	.45
1496.5	1.000	2.6	2.2	-.21	46.19	.15	.61

T@100-T@30 = .934*T@100-T@30 Undisturbed App. ie Change in del T = .01 .04
T@200-T@30 = 1.131*T@200-T@30 Undisturbed App. ie Change in del T = -.02 -.08

Profile Name : NYU-4-T2
Flow Condition : Unstable, High speed
Task Number : 4
Configuration : T
Ref. Height : 1500.0 ft
Ref. Model Velocity : 2.10 mph

Height (ft)	Velocity (Normalized)	Turb. Int. (%) u	v	del Theta (deg)	Model Temp (deg C)	Delta Temperature (Deg C) 4 mph Field	8 mph Field
30.0	.514	27.1	21.4	1.49	39.96	.00	.00
56.4	.547	21.7	18.8	1.30	38.03	-.03	-.10
97.6	.573	17.2	17.6	3.02	36.09	-.05	-.21
148.5	.588	14.8	16.4	4.51	35.49	-.06	-.24
197.3	.599	13.5	14.8	3.66	34.66	-.07	-.29
247.2	.601	11.9	14.1	2.65	34.05	-.08	-.32
372.2	.602	10.1	12.6	2.47	33.34	-.09	-.36
748.5	.654	8.0	10.0	2.14	34.55	-.07	-.29
1122.7	.901	4.9	3.7	1.59	44.30	.06	.24
1496.7	1.000	3.2	3.3	2.19	48.41	.11	.46

T@100-T@30 = .703*T@100-T@30 Undisturbed App. ie Change in del T = .02 .09
T@200-T@30 = .705*T@200-T@30 Undisturbed App. ie Change in del T = .03 .12

Profile Name : NYU-4-U2
Flow Condition : Unstable, High speed
Task Number : 4
Configuration : U
Ref. Height : 1500.0 ft
Ref. Model Velocity : 2.12 mph

Height (ft)	Velocity (Normalized)	Turb. Int. (%) u	v	del Theta (deg)	Model Temp (deg C)	Delta Temperature (Deg C) 4 mph Field	8 mph Field
30.0	.437	30.7	26.2	2.99	44.64	.00	.00
56.3	.484	28.0	23.5	-.41	40.28	-.06	-.24
98.6	.546	24.2	20.2	2.12	38.22	-.09	-.35
148.5	.578	18.0	17.1	2.06	35.75	-.12	-.48
198.0	.595	14.8	15.4	1.35	34.89	-.13	-.53
249.2	.595	13.5	14.6	.79	34.25	-.14	-.57
373.5	.607	10.1	12.9	1.82	33.29	-.15	-.62
748.8	.640	7.8	10.1	2.29	34.14	-.14	-.57
1121.8	.876	5.2	3.8	.81	43.97	-.01	-.04
1499.3	1.000	3.5	3.5	1.30	48.30	.05	.20

T@100-T@30 = 1.166*T@100-T@30 Undisturbed App. ie Change in del T = -.01 -.05
T@200-T@30 = 1.297*T@200-T@30 Undisturbed App. ie Change in del T = -.03 -.12

Profile Name : NYU-4-V2
Flow Condition : Unstable, High speed
Task Number : 4
Configuration : V
Ref. Height : 1500.0 ft
Ref. Model Velocity : 2.11 mph

Height (ft)	Velocity (Normalized)	Turb. Int. (%) u	Turb. Int. (%) v	del Theta (deg)	Model Temp (deg C)	Delta Temperature (Deg C) 4 mph Field	Delta Temperature (Deg C) 8 mph Field
30.0	.443	31.1	26.7	.63	43.41	.00	.00
56.8	.493	28.2	23.0	.18	40.42	-.04	-.16
97.7	.540	22.1	19.4	.90	37.46	-.08	-.32
148.9	.575	18.3	16.8	1.94	35.98	-.10	-.40
197.7	.593	14.5	16.1	1.81	35.01	-.11	-.46
248.8	.602	13.2	14.5	1.15	34.07	-.13	-.51
372.5	.606	9.9	13.2	2.52	33.12	-.14	-.56
746.6	.649	7.7	10.0	1.81	34.18	-.13	-.50
1121.2	.883	5.0	3.8	.71	43.61	.00	.01
1499.7	1.000	3.4	3.4	1.01	48.22	.07	.26

T@100-T@30 = 1.080*T@100-T@30 Undisturbed App. ie Change in del T = -.01 -.02
T@200-T@30 = 1.117*T@200-T@30 Undisturbed App. ie Change in del T = -.01 -.05

Profile Name : NYU-4-W2
Flow Condition : Unstable, High speed
Task Number : 4
Configuration : W
Ref. Height : 1500.0 ft
Ref. Model Velocity : 2.11 mph

Height (ft)	Velocity (Normalized)	Turb. Int. (%) u	Turb. Int. (%) v	del Theta (deg)	Model Temp (deg C)	Delta Temperature (Deg C) 4 mph Field	Delta Temperature (Deg C) 8 mph Field
30.0	.441	31.2	25.4	-.83	42.44	.00	.00
57.7	.482	27.5	26.0	-.25	40.33	-.03	-.11
100.8	.540	22.3	20.8	-.22	37.03	-.07	-.29
150.4	.565	17.6	17.5	.87	35.64	-.09	-.37
202.5	.574	17.2	17.2	1.32	35.33	-.10	-.39
250.9	.592	14.9	16.6	.42	34.84	-.10	-.41
377.9	.599	11.0	13.0	.78	33.14	-.13	-.51
753.3	.647	7.7	10.1	1.25	33.96	-.12	-.46
1126.1	.883	5.2	3.8	-.13	43.45	.01	.05
1498.9	1.000	3.2	3.6	.49	48.08	.08	.31

T@100-T@30 = .981*T@100-T@30 Undisturbed App. ie Change in del T = .00 .01
T@200-T@30 = .945*T@200-T@30 Undisturbed App. ie Change in del T = .01 .02

Profile Name : NYU-4-X2
Flow Condition : Unstable, High speed
Task Number : 4
Configuration : X
Ref. Height : 1500.0 ft
Ref. Model Velocity : 2.03 mph

Height (ft)	Velocity (Normalized)	Turb. Int. (%) u	Turb. Int. (%) v	del Theta (deg)	Model Temp (deg C)	Delta Temperature (Deg C) 4 mph Field	Delta Temperature (Deg C) 8 mph Field
30.0	.451	31.3	28.1	.45	42.91	.00	.00
63.7	.517	26.2	25.8	-.42	39.40	-.05	-.19
99.3	.553	22.0	22.7	.23	37.15	-.08	-.31
147.9	.568	20.1	18.4	1.69	36.39	-.09	-.35
199.2	.596	15.6	17.8	.90	34.90	-.11	-.44
253.5	.596	16.0	17.1	1.07	34.73	-.11	-.45
372.8	.620	12.3	13.4	1.35	33.28	-.13	-.52
747.7	.678	8.0	10.3	.73	33.95	-.12	-.49
1125.4	.917	5.1	3.9	-.48	43.35	.01	.02
1499.4	1.000	3.2	3.3	.97	47.93	.07	.27

T@100-T@30 = 1.047*T@100-T@30 Undisturbed App. ie Change in del T = .00 -.01
T@200-T@30 = 1.065*T@200-T@30 Undisturbed App. ie Change in del T = -.01 -.03

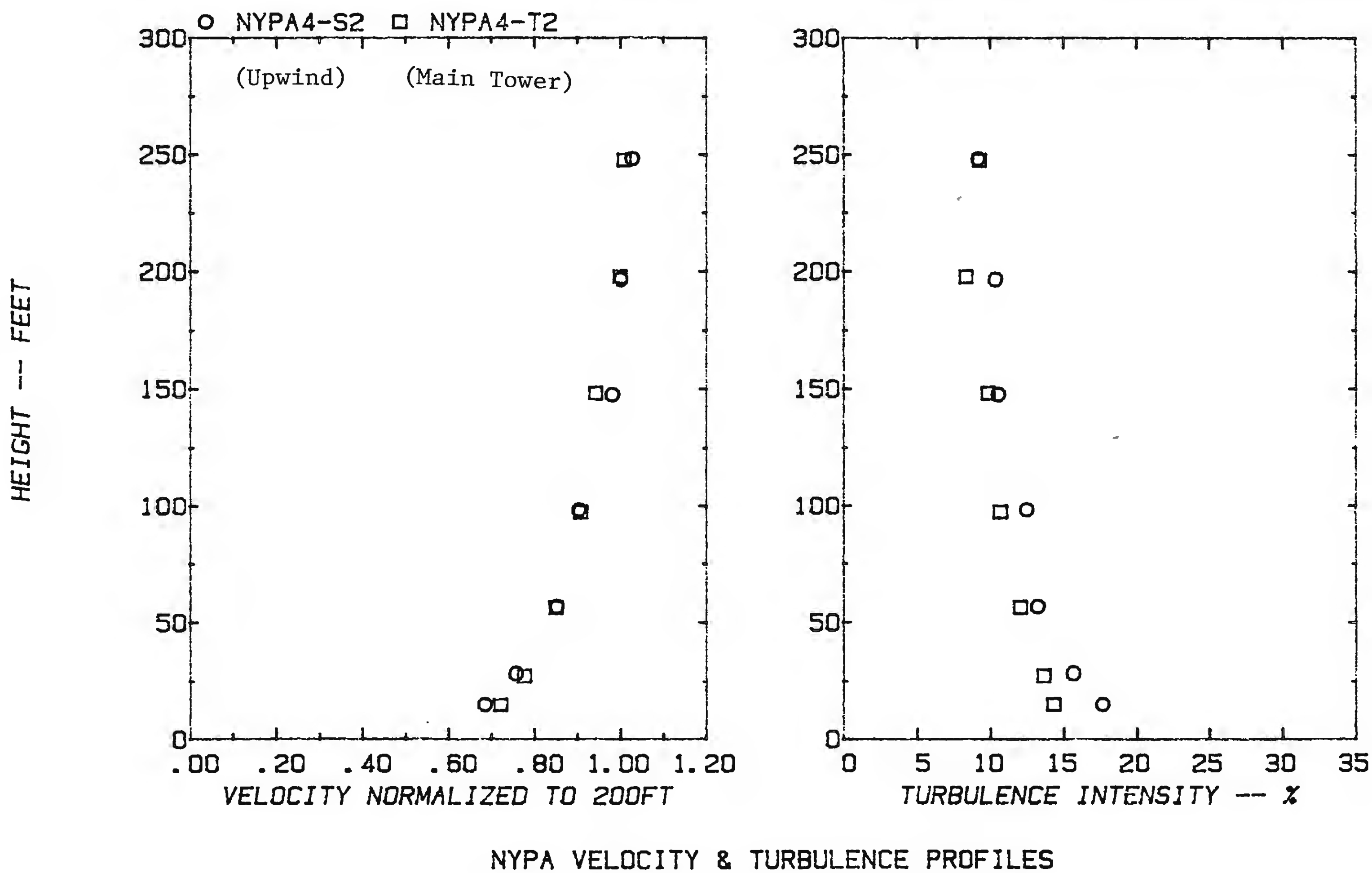

Figure F1. Effect of Escarpment at Main Meteorological Tower, Neutral Flow

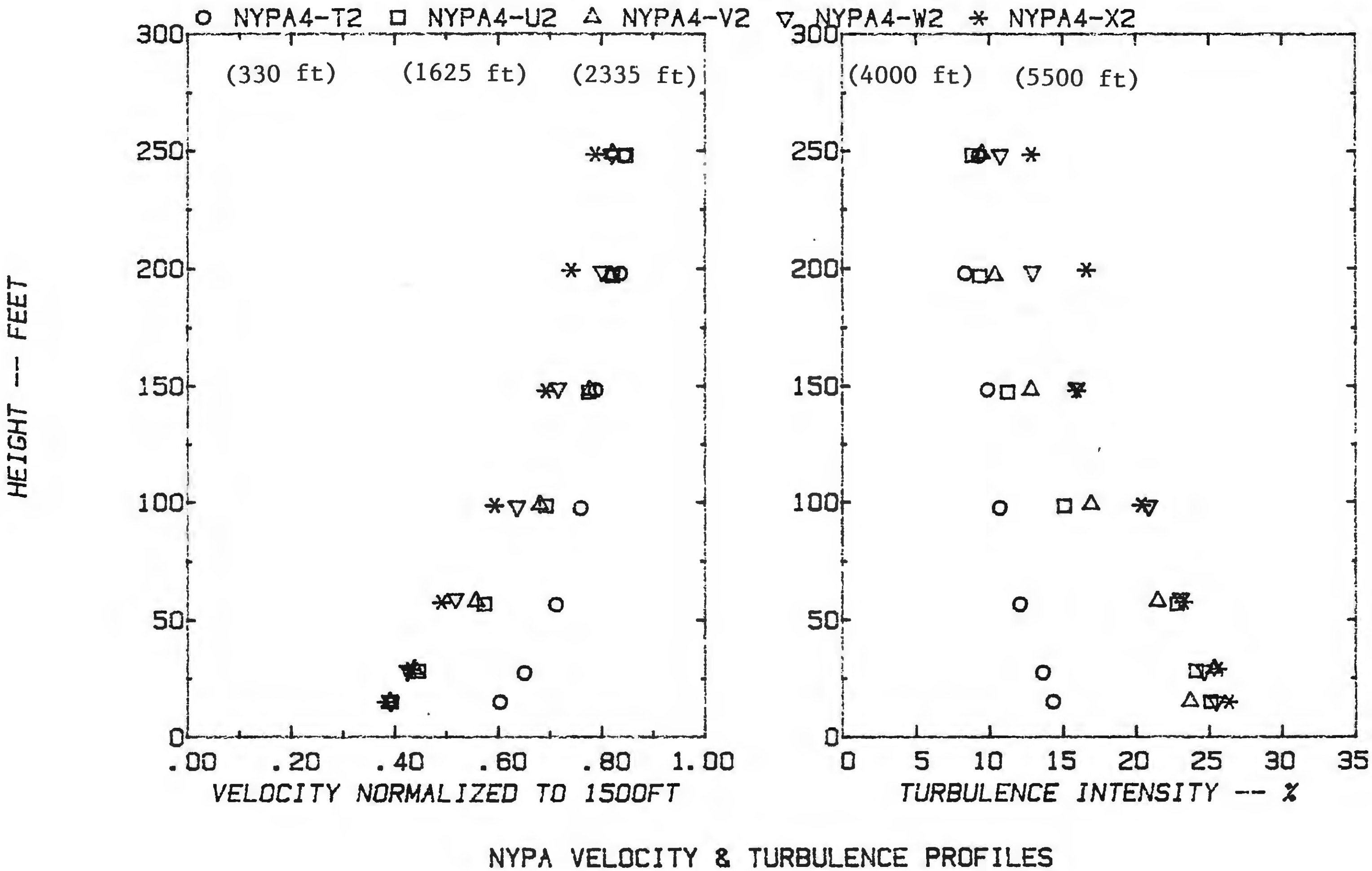

Figure F2. Fetch Length Comparisons of Profiles, Neutral Flow, High Speed

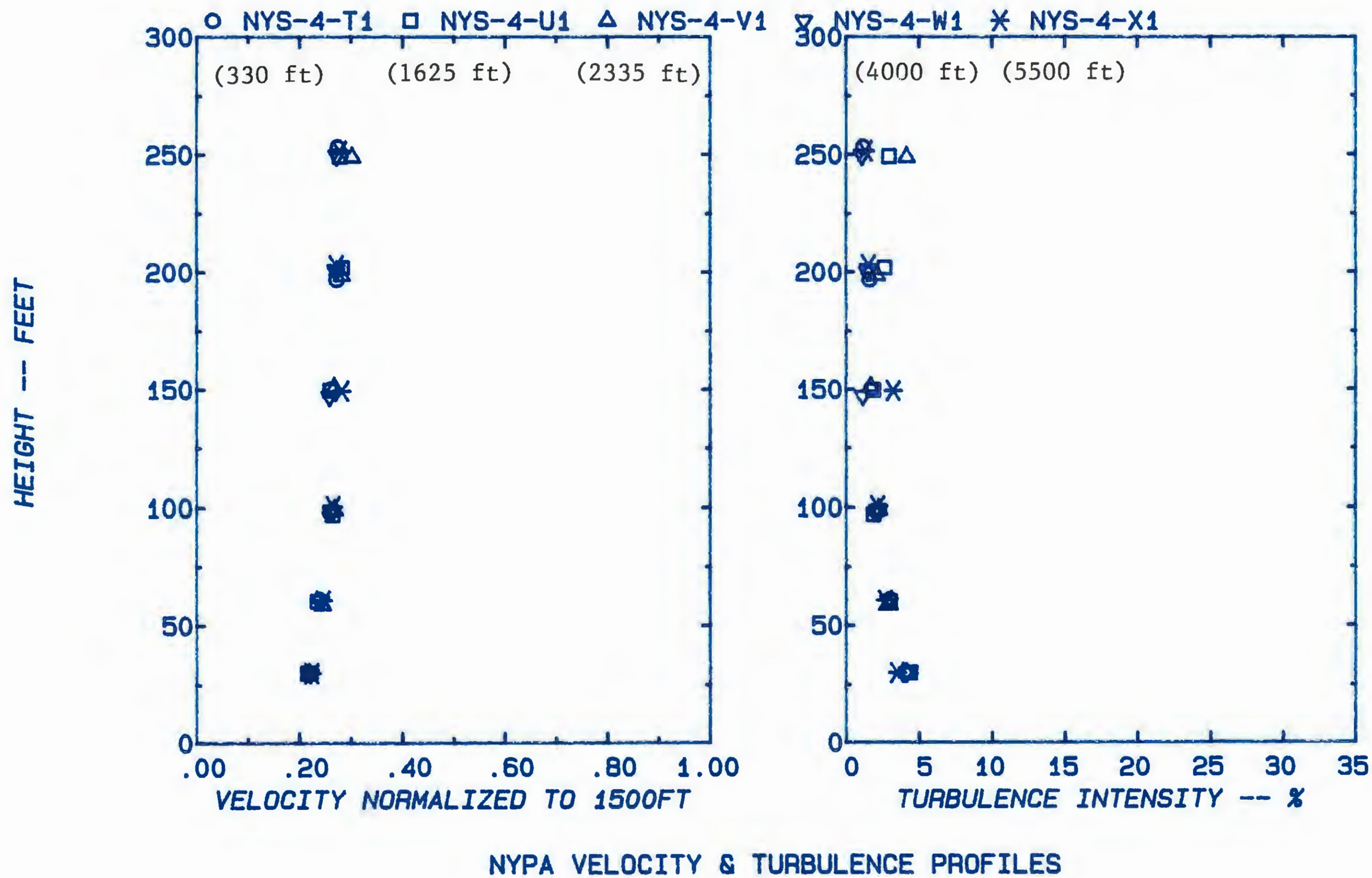

Figure F3. Fetch Length Comparisons of Profiles, Stable Flow, Low Speed

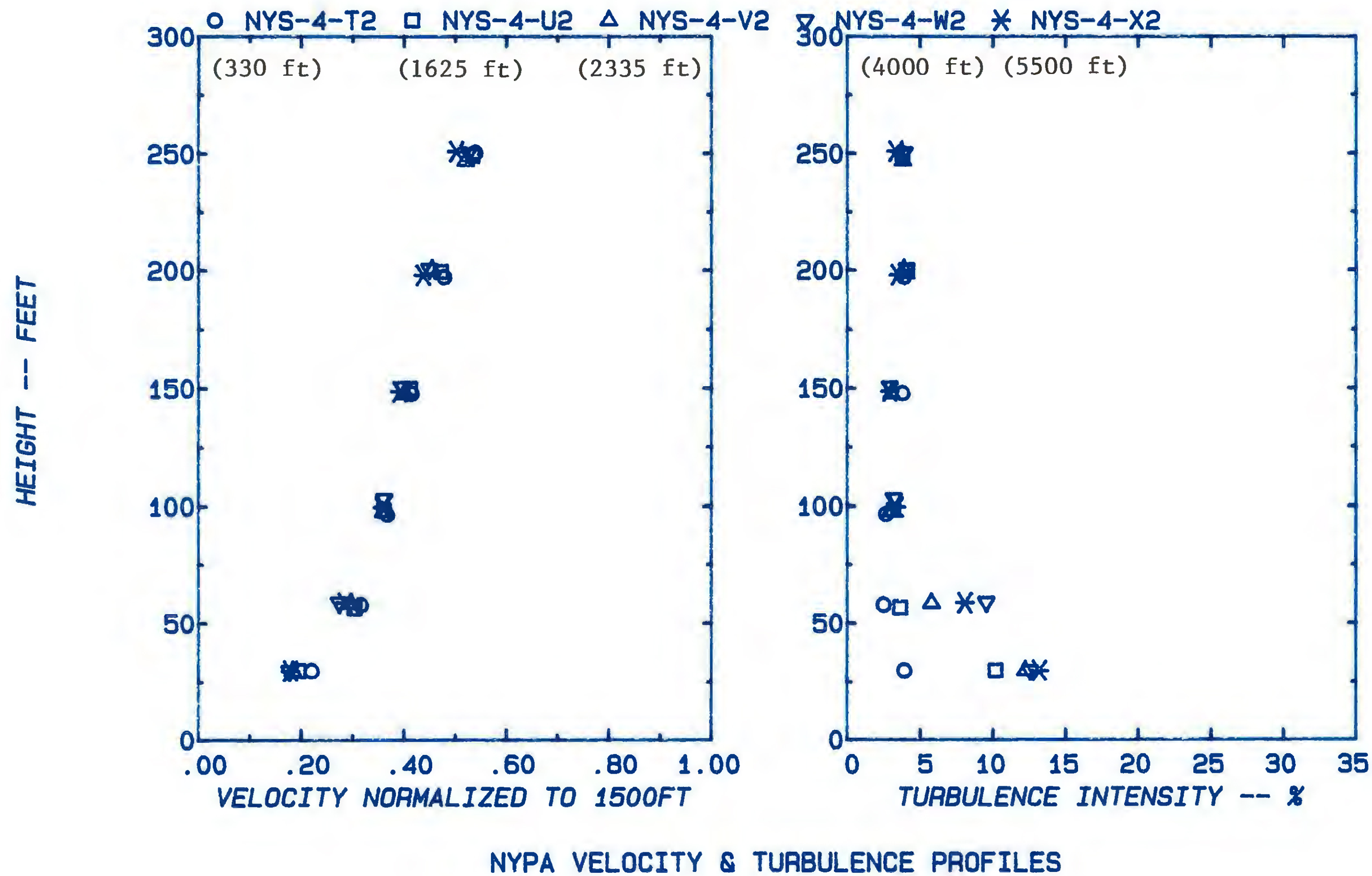

Figure F4. Fetch Length Comparisons of Profiles, Stable Flow, High Speed

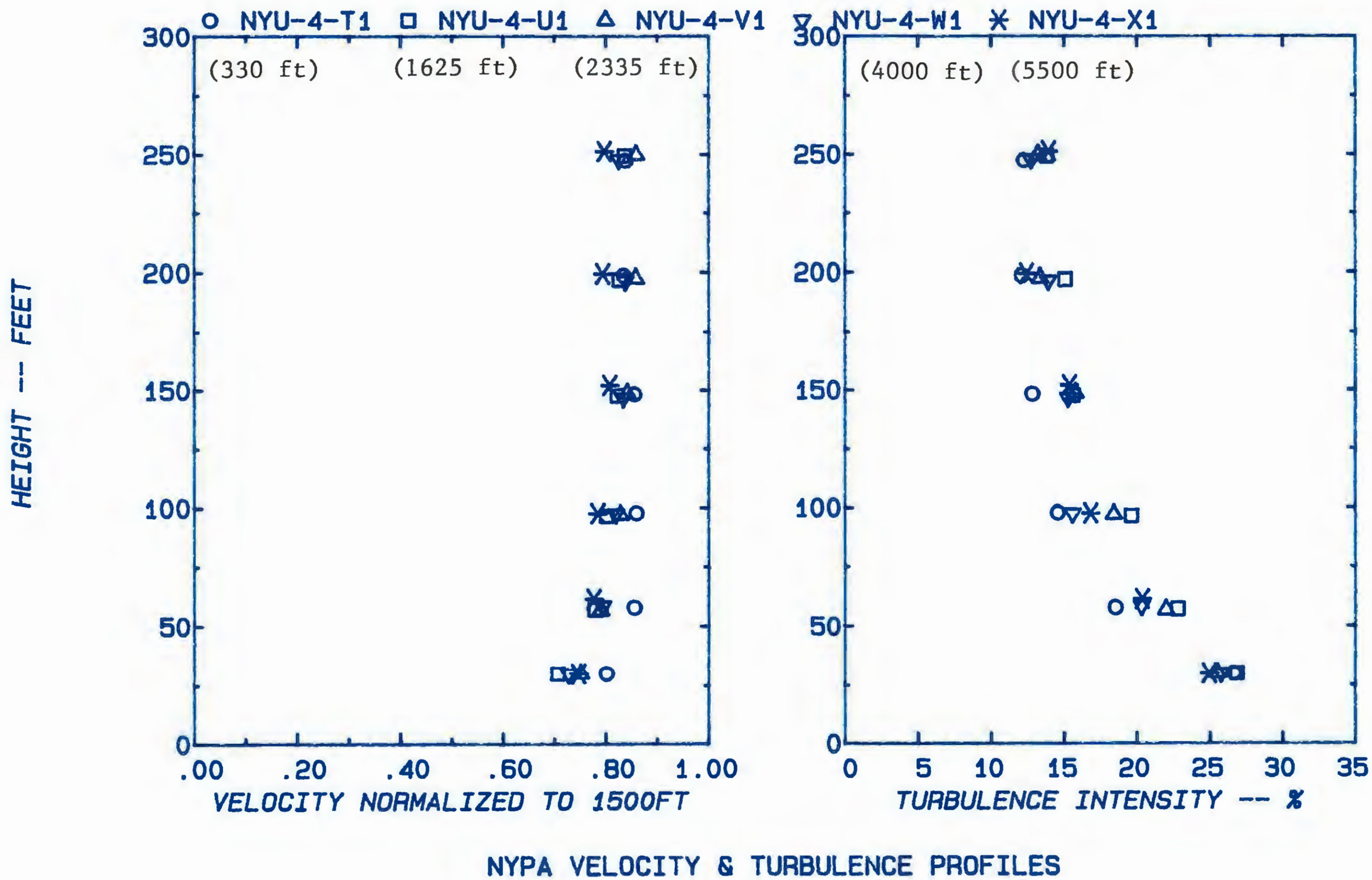

Figure F5. Fetch Length Comparison of Profiles, Unstable Flow, Low Speed

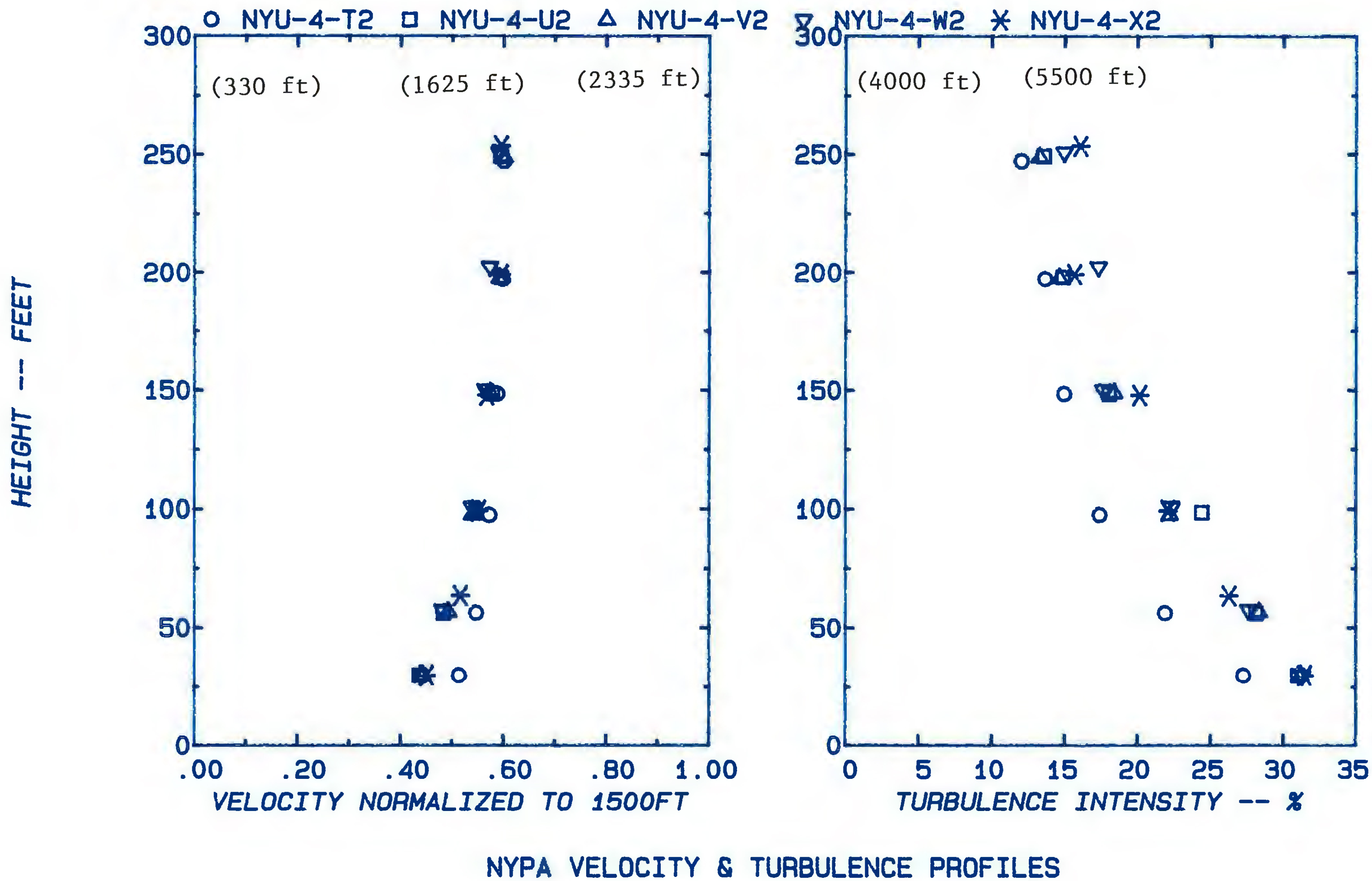

Figure F6. Fetch Length Comparison of Profiles, Unstable Flow, High Speed